Synthesis, Characterization, Critical Micelle Concentration and Antimicrobial Activity of Two-headed Amphiphiles

Bhadreshkumar Maisuria

Thesis submitted to the Faculty of Virginia Polytechnic Institute and State University in partial fulfillment of the requirements for the degree of

MASTER OF SCIENCE

In

Chemistry

Richard D. Gandour, Chairman

David G. I. Kingston

Webster L. Santos

August 12, 2009

Blacksburg, VA 24061

Keyword: homologous, two-headed, di-carboxylato, amphiphile, critical micelle concentration, minimal inhibitory concentration, *S. aureus*, MRSA

Synthesis, Characterization, Critical Micelle Concentration and Antimicrobial Activity of two-headed Amphiphiles

Bhadreshkumar Maisuria

ABSTRACT

This project is about the synthesis of homologous series of two-headed, long-chain amphiphiles (the **2CCbn** series, where **n** = 16, 18, 20, 22, 30, 5α-cholestan-3ß-ol). The **2CCbn** series was synthesized in five steps. The first step involves a reaction of nitroethane and two equivalents of *tert*-butyl acrylate to form nitrodiester by successive Michael addition reaction. The second step is the reduction of nitrodiester with Raney nickel to form aminodiester. The third step involves a reaction of aminodiester with di-*tert*-butyl dicarbonate [$(Boc)_2O$] to form isocyanatediester. The fourth step is addition of iscocyanatediester with aliphatic alcohol to give alkyl carbamate diester (**2ECbn**) series. The fifth step is the removal of the *tert*-butyl protecting group to give the **2CCbn** series.

The critical micelle concentrations (CMC) were measured by the pyrene-based fluorescent probe method. The pyrene excited at 345 nm and fluoresces with maxima at 374 nm (I_1) and 385 nm (I_3). The stock solution and the dilution series for each amphiphiles were made in 0.9% triethanolamine solution. The CMCs were measured at two pH ~9.2 and 7.4. The CMCs were determined by plotting I_1/I_3 vs. concentrations. The CMCs were decreasing with increasing chain length. The CMCs for the **2CCbn** series are lower than the **3CCbn** series but higher than the fatty acids.

The minimal inhibitory concentrations were measured against *Staphylococcus aureus* and methicillin-resistant *Staphylococcus aureus*. These strains were grown on

BHIB+S with 5% triethanolamine. The MICs of the **2CCbn** series amphiphiles were measured by using microtiter plate reader and by looking turbidity. The cutoff effect was found for the **2CCbn** series. The MIC decreased up to C_{20} chain length and started rising for C_{22}. The **2CCb18** (MIC–2.2 μg/mL) of the **2CCbn** series was the most effective amphiphile against *S. aureus* and MRSA.

The CMC/MIC ratio was used to determine the safety of an amphiphile as a drug use. The amphiphile **2CCb18** has given the largest safety ratio (CMC/MIC = 273) against *S. aureus* and MRSA. It suggests that micelle formation is not a mechanism of action for anti-*Staphylococcal* activity.

Acknowledgements

I would like to thank my wife, Trupti Maisuria, without whose motivation and encouragement I would not have considered a graduate career in Chemistry. She is the one who truly made a difference in my life. She provided me with direction, support, and became more of a mentor and a friend, than a wife. It was through her persistence, understanding, and kindness that encouraged me to do my best and work my hardest. I doubt that I will ever be able to convey my appreciation fully, but I owe her my eternal gratitude. I would also like to thank her family for the support they provided me throughout my studies. I must acknowledge my father-in-law, Babu Maisuria, for giving me his encouragement and persistence.

I would like to express my gratitude to my advisor, Dr. Richard Gandour, whose expertise, understanding, and patience, added considerably to my graduate experience. I appreciate his vast knowledge and skill in many areas and his assistance in writing reports, especially my thesis. I would like to thank him for the assistance he provided at all levels of my research. Thank you for taking the time out from your busy schedule to serve as my external reader, I am extremely grateful for all his efforts.

I would like to thank my lab partners, Dr. André Williams, Richard Macri, Shauntrece Hardrict, and Marcelo Actis for providing practical information and advise.

I would like to thank my collaborator, Dr. Joseph Falkinham III, for doing bioassay work and for allowing the use of lab and instruments. I would like to thank Myra Williams for doing bioassay. I would like to thank Lilit Stepanyan, for her kindness, expertise, and taking the time out from her busy schedule to do thesis correction.

Finally, I would like to thank my masters committee, Dr. David G. Kingston, and Dr. Webster Santos, for teaching and their guidance.

Table of Contents

List of Figures

List of Tables

Lists of Schemes

Chapter 1: Background, Critical Micelle Concentration, and Antimicrobial Activity of Amphiphiles

1.1 Goals

The aim of this research project is to synthesize a new homologous series of two-headed long chain amphiphiles, to measure the critical micelle concentrations (CMCs), and to measure their antimicrobial activity. These amphiphiles are the **2CCbn** series (Figure 1.1), which is bioisosteric with the **2CAmn** series synthesized by Marcelo Actis.[1] The CMCs will be measured for this **2CCbn** series to determine if detergency is a key factor on the biological activity. Finally, others will measure the antimicrobial activity for this **2CCbn** series against *Staphylococcus aureus* and several strains of methicillin-resistant *S. aureus* (MRSA).

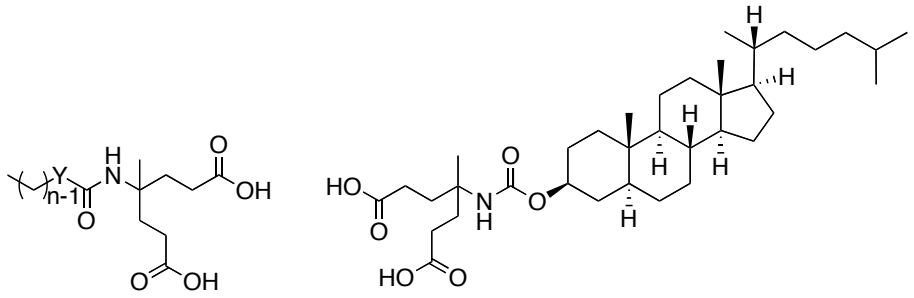

Figure 1.1 Structures of the **2CCbn** and **2CAmn** series.

Where **2C**= two carboxyl groups, **Cb**= carbamato linker, **Am**= amido linker, and **n**= number of carbons in the alkyl chain

1.2. Introduction

Amphiphiles are commonly referred to as surfactants (surface-active-agents), which exhibit interfacial activity. Ionic and nonionic surfactants find uses in a variety of applications[2] — detergents, shampoos, crude oil, recovery enhancers, cosmetics, chelating agents,[3] and antimicrobial agents.[2, 4, 5] In our project, we prefer to use the term amphiphiles rather than surfactants, which act as detergents and cause cytotoxicity, inflammation, and irritation. For this reason, our goal is to make amphiphiles that do not act as detergents. Amphiphiles become detergents at or near the CMC.[6, 7] So our target is to make amphiphiles with high CMCs and good antimicrobial activity (MIC_{99}, minimal inhibitory concentration) at very low concentration. Having a high CMC/MIC_{99} ratio, will reduce the likelihood that detergency is the mechanism of inhibition for our amphiphiles. Consequently, the amphiphile will have low cytotoxicity, inflammation, irritation and other side effects.

Antimicrobial activity of a series of amphiphiles or fatty acids tends to increase with increasing the length of the alkyl chain (hydrophobic part).[8, 9] But in order to achieve high antimicrobial activity, one must sacrifice solubility.[10] Antimicrobial activity does not have a linear relationship with chain length; a "cutoff effect"[8] (Section 1.3) (Figure 1.2) is often observed. For example, the activity of the homologous **3CCbn** (Figure 1.3) series amphiphile against *Mycobacterium smegmatis* shows a cutoff at C_{18}. In this phenomenon, antimicrobial activity increases (log MIC decreases) to a specific chain length, after which it decreases (log MIC increases) with longer chain length. One possible reason for the decreasing activity is the amphiphile's limited solubility. Another

possible reason is micelle formation, which limits the concentration of the biologically active monomer.

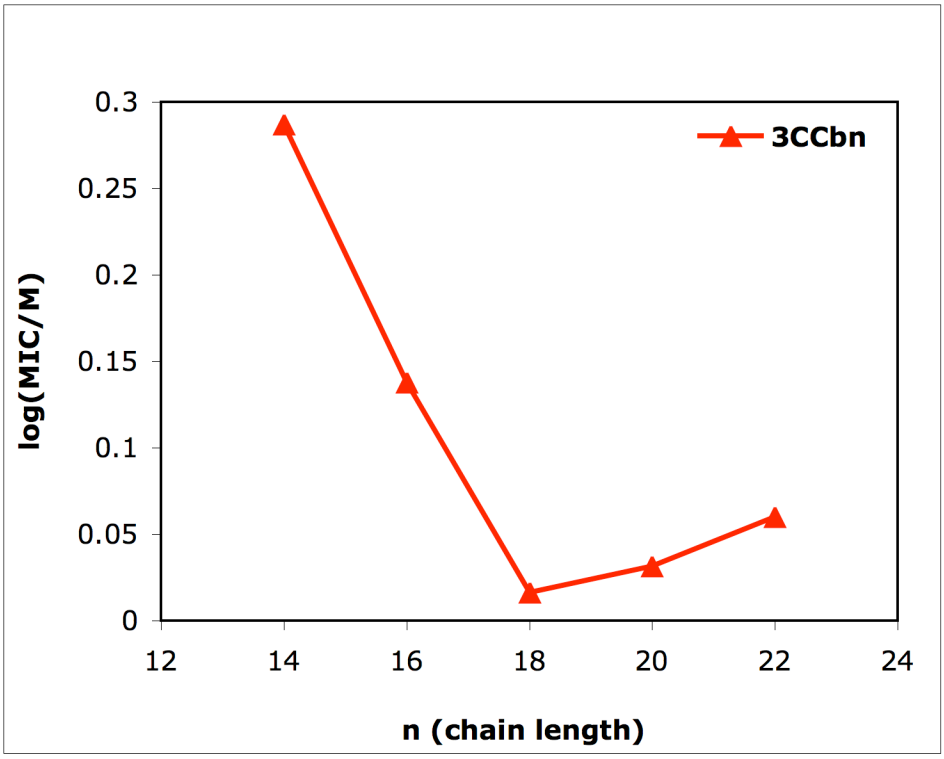

Figure 1.2 Cutoff effect for the **3CCbn** series against *M. smegmatis*

Previous work[11] in the Gandour group has demonstrated that three-headed anionic amphiphiles (Figure 1.3) are significantly more soluble than single-headed amphiphiles in aqueous media. This observation removes the solubility problem as a possible cause of the "cutoff effect". So we must determine the CMC to probe whether micelle formation is a reason for the cutoff effect. If both solubility and micelle formation are excluded as reasons, then it can be concluded that molecular structure and the biological target produce the cutoff effect.

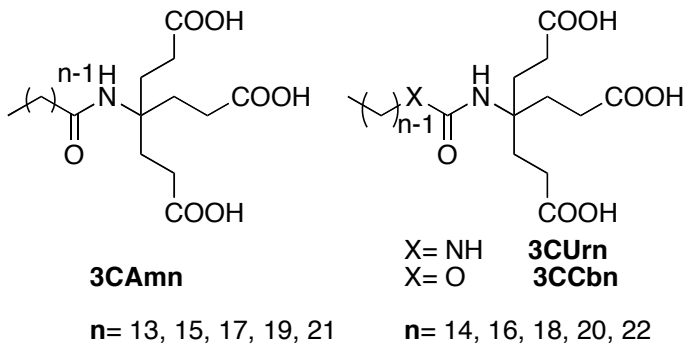

Figure 1.3 Structure of three-headed amphiphiles.

Where **3C** = three carboxyl groups, **Am** = amido linker,

Ur = ureido linker, **Cb** = carbamato linker, **n** = number of

carbons in the tail.

The ultimate goal of this project is to synthesize topical microbicides, especially those active against *S. aureus* and MRSA. The individual goals of this research include (1) synthesis and characterization of two-headed amphiphiles, (2) measurements of CMCs, and (3) measurements of antimicrobial activity.

1.3 Homologation and the Effect of Increasing Chain Length

Silverman[12] describes " A *homologous series* as a group of compounds that differ by a constant unit, generally a CH_2 group." He further states, " For many series of compounds, lengthening a saturated carbon side chain from one (methyl) to five to nine atoms (pentyl to nonyl) produces an increase in pharmacological effects; further lengthening results in a sudden decrease in potency." He suggests[12] "that this phenomenon corresponds to increased [hydrophobicity] of the molecule to permit penetration into cell membranes until its lowered water solubility becomes problematic in its transport through aqueous media." He further points out, "…another problem is

micelle formation, which begins at about C_{12}. This effectively removes the compound from potential interaction with the appropriate receptors" (sites of action).

1.4 Introduction to Amphiphiles

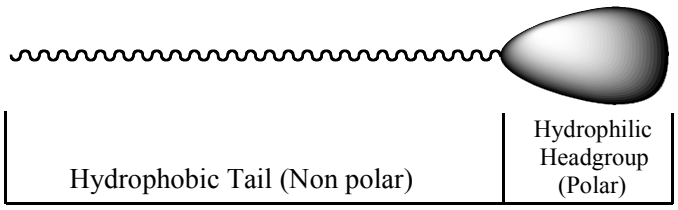

Figure 1.4 General structure of an amphiphile

Amphiphiles (Figure 1.4) are molecules with two parts: they have a water-loving part (hydrophilic) and a water-hating part (hydrophobic). In general, the hydrophobic part consists of a long-chain alkyl group. The hydrophilic part can be either ionic, nonionic and zwitterionic (Table 1.1).[13, 14] The polar head can consist of one or several phosphates, amines, hydroxyl groups or acid groups. Ionic amphiphiles can be either anionic, cationic or zwitterionic (contain both an anionic and a cationic group).

According to an article in *Chemistry in Britain*,[15] anionic surfactants consist of negatively charged polar headgroups and positively charged counterions such as sodium, potassium or ammonium ions. Anionic surfactants are excellent detergents and are widely used as soap for cleaning processes.

Cationic surfactants[15] consist of positively charged headgroups such as a quaternary ammonium and a halide ion as a counterion. Cations are generally attracted to surfaces carrying a negative charge. Surface characteristics can be measured for cationic surfactants with proteins and synthetic polymers. Hair conditioners and fabric softeners are cationic surfactants.

Amphoteric surfactants[15] consist of headgroups that have both a positive and

negative charge; therefore these surfactants are zwitterions. If zwitterions contain a carboxylate and a protonated ammonium ion, they can behave as a cation at low pH or an anion at high pH. They are often used as shampoos due to low irritancy.

Nonionic surfactants[15] are used in cleaning applications with anionic surfactants. Nonionic surfactants consist of a chain of oxyethylene groups, also called ethoxylates.

Table 1.1 Examples of anionic, cationic, zwitterionic, and nonionic amphiphiles

Amphiphiles	**General Structure**	**Examples**
Anionic (based on sulfate, sulfonate, carboxylate and phosphate anions)		
Sulfonate	$R–SO_3^-M^+$	Perfluorooctate sulfonate
		Alkyl benzene sulfonate
Sulfate	$R–OSO_3^-M^+$	Sodium dodecyl sulfate
		Ammonium lauryl sulfate
		Sodium laureth sulfate
Carboxylate	$R–COO^-M^+$	
Phosphate	$R–OPO_3^-M^+$	
Cationic (based on quaternary ammonium cations)		
Quaternary ammonium salts	$R_4N^+X^-$	Cetyl trimethylammonium bromide
		Cetylpyridinium chloride
		Benzalkonium chloride
		Benzethonium chloride
Ammonium salts	$R_xH_yN^+X^-$	
Zwitterionic (Amphoteric)		
Betains	$R–N^+(CH_3)_2CH_2CH_2COO^-$	Dodecyl betaine
Sulfobetaines	$R–N^+(CH_3)_2CH_2CH_2SO_3^-$	
Nonionic		
Polyoxyethylene	$R–CH_2CH_2(OCH_2CH_2)_nOH$	

Amphiphiles tend to migrate to the water–air interface and, thus, lower the surface tension, which makes them useful as detergents. Amphiphiles in solution can form spontaneous aggregates (micelles) above a certain concentration. Depending on the temperature and concentration, these aggregates can adopt several shapes. Different variables, such as temperature, structure, solution conditions, and counterions affect the

solubility, activity, and CMC of amphiphiles.

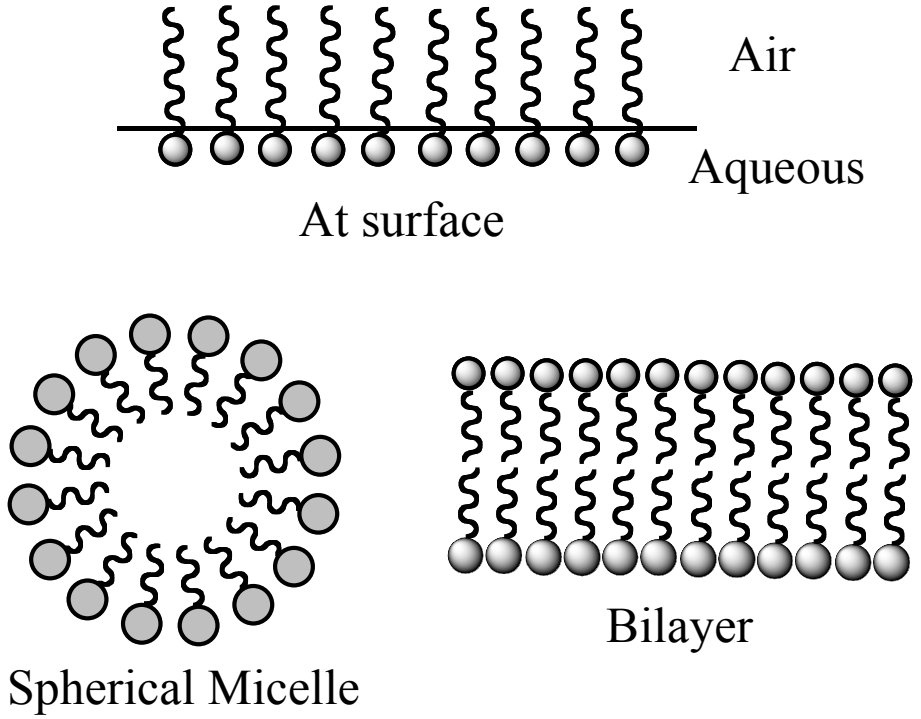

Figure 1.5 Amphiphile aggregates

Amphiphiles differ in their affinity for solutes. The hydrophilic part has an affinity for polar solutes, such as water, and the hydrophobic part has an affinity for non-polar solutes, such as hexane. Amphiphiles display distinct behavior when interacting with water. They can arrange themselves at the interface between water and air or a nonpolar solvent. The polar headgroup interacts with the water and the nonpolar alkyl chain is held above the interface (either in the air or in a nonpolar liquid) (Figure 1.5). Molecules on the interface disrupt the cohesive energy at the interface and, thus, lower the surface tension.

Another arrangement of amphiphiles allows each part to interact with its preferred environment. Amphiphiles aggregate in which the hydrophobic parts are oriented within

the cluster, and the hydrophilic parts are exposed to the water (Figure 1.5). The longer the alkyl chain of an amphiphile, the stronger the van der Waals interaction among molecules in a micelle. Such aggregates can show various shapes that depend largely on the structures of the amphiphiles.

The proportion of molecules at the interface or in aggregates in the bulk liquid depends on the concentration of the amphiphile. At low concentrations, amphiphiles will prefer the interface (Figure 1.5). At a certain concentration, the surface becomes completely loaded with amphiphiles, and further increasing the concentration leads to formation of aggregates. This concentration is called the CMC.

1.5 Aqueous Solubility of Multi-headed, Anionic Amphiphiles

In 1908,[16, 17] pure saturated fatty acids were discovered to have antimicrobial activity, and their activity was investigated as a function of chain length. In 1924, Walker found that the most active fatty acids have chain length of C_{10}–C_{14}. Longer-chain length fatty acids like C_{16}–C_{20} were not active towards a wide range of microorganisms. The inactivity was due to the poor aqueous solubility of the long alkyl chain.

With longer chains, fatty acids will have low CMCs, solubilities, and antimicrobial activities. To overcome these challenges of low aqueous solubilities and to study the better relationship between activity and chain length, the Gandour group has successfully designed and synthesized three homologous series of long-chain water-soluble amphiphiles (Figure 1.3).[11, 18]

The work done by André Williams[11] has proved that the tricarboxylato amphiphiles **3CAmn** series are more soluble in neutral phosphate buffer (pH 7.4) than the saturated fatty acids. The solubilities for **3CAm13**, **3CAm15** and **3CAm17** were

6900, 3400, and 1700 μM, respectively, while the solubilities of fatty acids like myristic, palmitic, and stearic acid were 20–30, ~1, and <<1 μM, respectively. But the question is, are the tricarboxylato amphiphiles too hydrophilic? The more hydrophilic they are, the more difficult it is to penetrate into the lipid bilayer. In order to address this issue, a series of dicarboxylato amphiphiles (Figure 1.1) have been synthesized to compare with the tricarboxylato amphiphiles (Figure 1.3). They will be compared by using their CMCs, MICs, calculated logarithm of the partition coefficient (clog *P*), and logarithm of the octanol-1-ol–water distribution coefficient (log *D*).[19]

1.6 CMCs of Multi-headed, Anionic Amphiphiles

Our goal is to measure the CMCs of the **2CCbn** series. They should have high CMCs. These CMCs are really important because if the MIC is lower than the CMC then the amphiphiles have non-detergent antimicrobial activity.[20] This would mean that activity is due to monomers and not micelles.

Shinoda[21, 22] has explored the correlation between the number of headgroups and chain length to the CMC value (Figure 1.6).[21, 23] The CMC values for multi-headed amphiphiles were larger than those of the corresponding fatty acids (Figure 1.7).[22] Shinoda attributed these larger CMCs to the increased repulsion of the headgroups in multi-headed amphiphiles.[22]

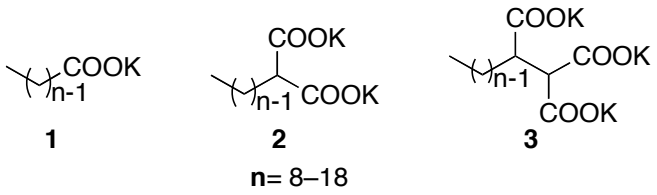

Figure 1.6 Structures of multi-headed amphiphiles studied by Shinoda[22]

CMC values were collected for a homologous series of dipotassium alkylmalonates, **2**.[23] The results showed that as the length of the alkyl chain increases, the CMC decreases. The work[21] performed also revealed that the logarithm of the CMC has a linear relationship to the alkyl chain length (Equation 1.1) (Figure 1.7), where **n** is the number of carbons in the alkyl chain and k_n is the slope of the line. From Figure 1.7, we can also see that the CMC values for **2** and **3** are not very different.

$$\log \mathrm{CMC} = -k_n \mathbf{n} + \mathrm{const.} \qquad \text{Equation 1.1}$$

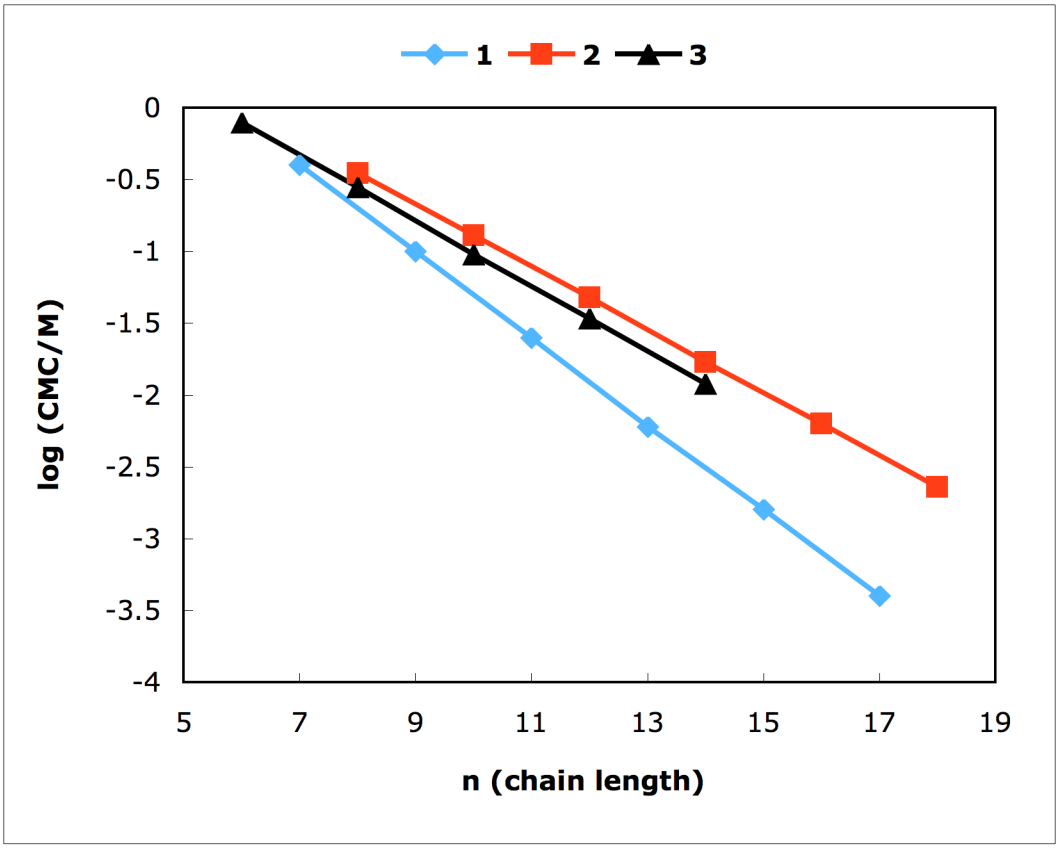

Figure 1.7 The effect of the number of headgroups on CMC

Paleos et al.[24] explored the physicochemical properties of a series of iminodiacetic acid amphiphiles **4** (Figure 1.8).

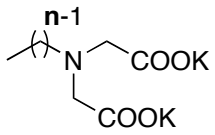

4

n= 12, 16, 18

Figure 1.8 Structure of iminodiacetic acid derivatives

The two-headed anionic amphiphiles[24] have a higher CMC than the corresponding fatty acid salts (Figure 1.9). For example, the CMC of the C_{12} dipotassium salt is 0.022 M; the CMC of the corresponding potassium salt of the C_{12} fatty acid is 0.014 M. The author[24] noted that the doubly charged ionic headgroup of the **4** makes the amphiphiles more water-soluble than the corresponding fatty acids. Comparing the works of Shinoda[21] and Paleos et al.,[24] there are no dramatic CMC differences between **1** (Figure 1.7) and **4** (Figure 1.9).

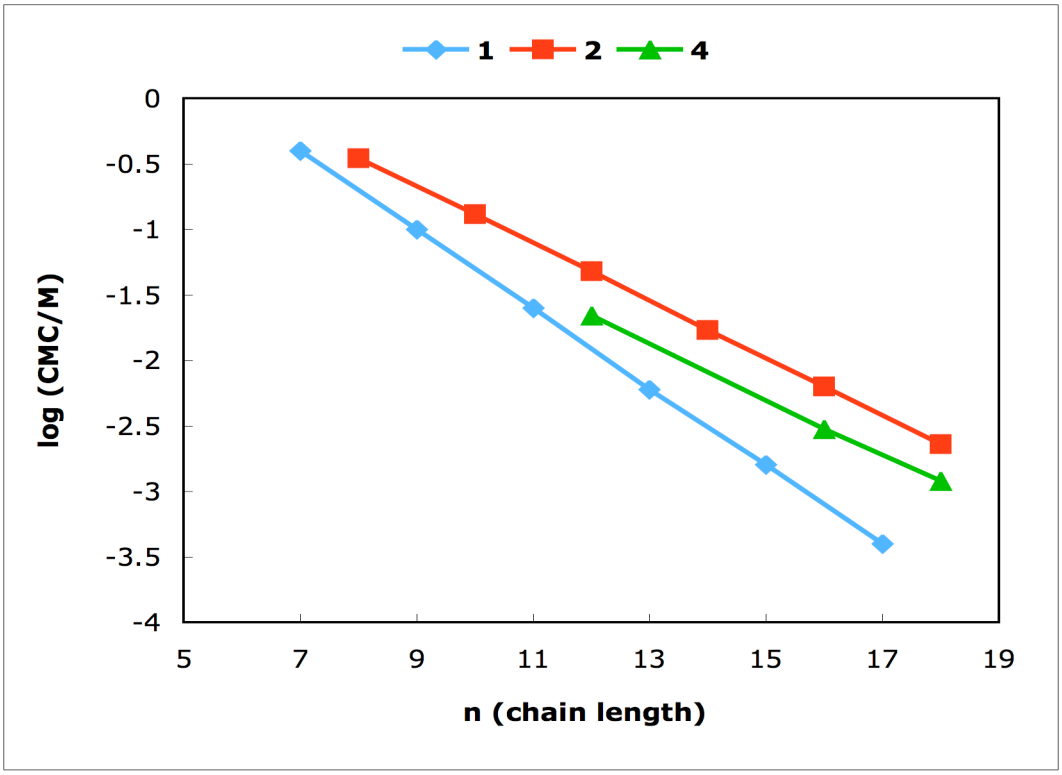

Figure 1.9 The effect of two headgroups on CMC

The Gandour[18] group has shown that three-headed anionic amphiphiles (Figure 1.3) are water-soluble and have higher CMC values than the corresponding fatty acids. Several amphiphiles[18] had CMC values ~100 times greater than the minimal inhibitory concentration (MIC). The CMC for these amphiphiles decreased with increasing chain length (Figure 1.10), which agreed with Shinoda's work.[23] Based on Figures 1.7 and 1.9, we concluded that two-headed anionic amphiphiles (**2CCbn**) should have a higher CMC than the corresponding fatty acids but slightly lower than the three-headed anionic amphiphiles (Figure 1.10).

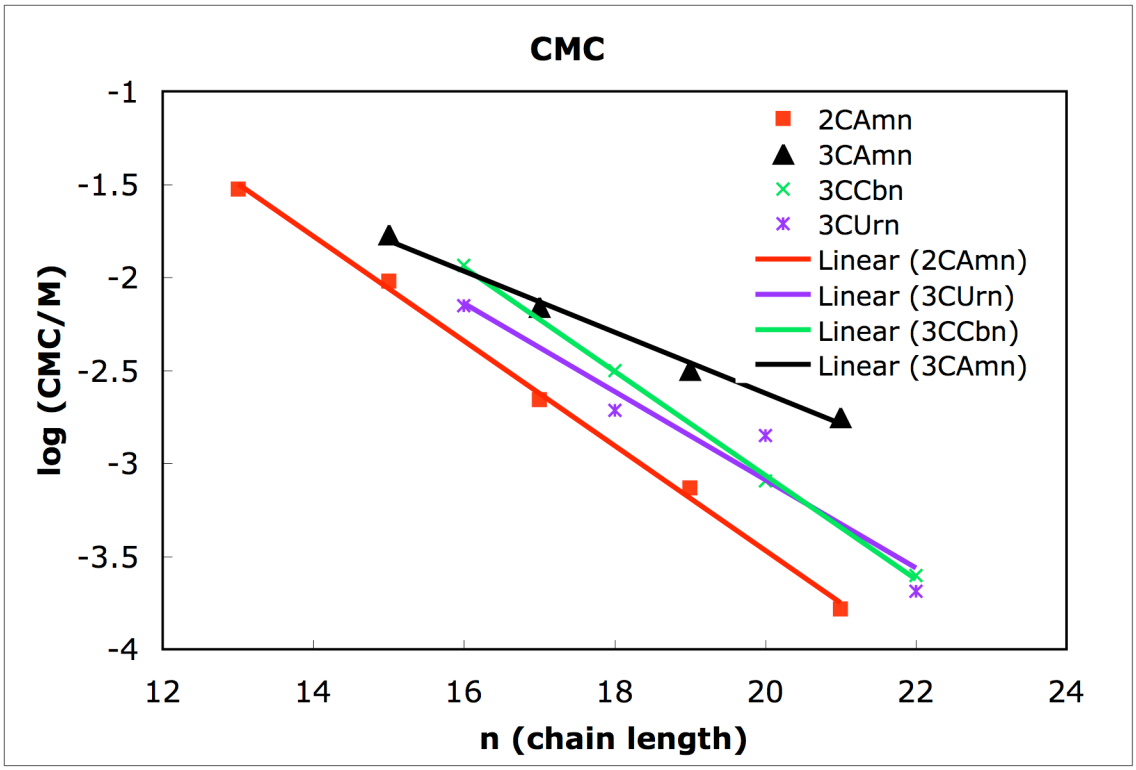

Figure 1.10 CMCs for two- and three-headed amphiphiles.

1.7 Hydrophobicity Effects

1.7.1 Importance of Hydrophobicity

Hansch and co-workers[25, 26] suggest that diffusion into a membrane is the first step in the overall drug process, in which the drug travels from a dilute solution outside of the cell to a particular site in the cell. The rate is highly dependent on the drug's molecular structure. The drug interacts with two different environments, lipophilic (e. g., membranes) and aqueous (e. g., cytoplasm) before it reaches to the site of action. The cytoplasm of a cell is made of an aqueous solution of salts and biomolecules. The functions of membranes are to protect the cell, to form a surface on which proteins can attach to produce structural organization, and to separate solutions of different electrochemical potentials. The structure of a membrane (Figure 1.11)[27] is determined by the structure of lipids, which are made of cholesterol, ionic phospholipids and glycolipids. All of these lipids are amphiphiles.

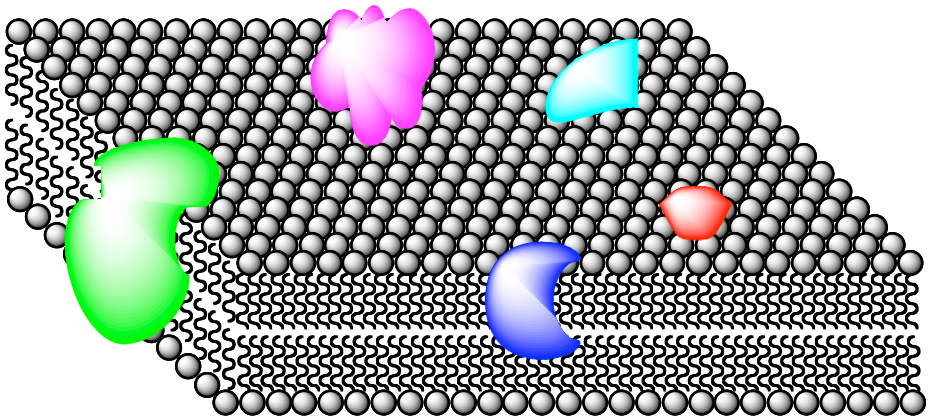

Figure 1.11 Fluid mosaic model of a membrane, inspired by Figure 2.14 in Ref [27]. The balls represent polar headgroups, and the wavy lines are the alkyl chains of the lipids. The masses embedded in the lipid bilayer are proteins.

1.7.2 Measurement of Hydrophobicity (log *P* and log *D*)

As described by Silverman,[28] Hansch and co-workers[25, 26] proposed that the *partition coefficient*, *P*, is a measure of the solubility in octan-1-ol versus water (Equation

1.1). Thus, *partition coefficient* is a measure of hydrophobicity. The logarithm of the ratio of concentrations of an un-ionized compound between two immiscible solutions (1-octanol/water) is called log *P*.

$$\log P = \log\left(\frac{[compound]_{oct}}{[compound]_{aq}(1-\alpha)}\right) \qquad \text{Equation 1.1}$$

The degree of dissociation (α) of the compound in water is calculated from ionization constants. The *P* can be measured by placing a compound in a shaking device (like a separatory funnel) with varying volumes of octan-1-ol and water, determining the concentration of the compound (by GC or HPLC) in each layer after mixing, and employing Equation 1.1.[29] The value of *P* depends on temperature and concentration of the solute. If a compound is more soluble in water than in octan-1-ol, $P < 1$ ($\log P < 0$), it is hydrophilic. If a molecule is more soluble in octan-1-ol, $P > 1$ ($\log P > 0$), it is hydrophobic. A drug with a large *P* value has more interaction with the lipid phase (i.e., membranes). Silverman states,[28] " As *P* approaches infinity, the micelle will form and/or the drug interaction will become so great that the drug will not be able to cross the aqueous phase, and will localize in the first lipophilic phase with which it comes into contact. As *P* approaches zero, the drug will be so water soluble that it will not be able to cross the lipid phase and will localize in the aqueous phase." Somewhere between $P = 0$ and $P = \infty$, the compound will have a value of *P* that will give optimal pharmacological activity.

Similarly, Silverman[28] describes log *D*, the hydrophobicity of an ionizable compound, where the distribution coefficient *D* is the ratio of the sum of the concentrations of all forms of the compound (ionized plus un-ionized) in each of the two phases (Equation 1.2). To measure *D*, the pH of the aqueous phase is buffered to a

specific value such that the pH is not significantly perturbed by the introduction of the compound.

$$\log D = \log\left(\frac{[compound]_{oct}}{\{[compound]_{ionized} + [compound]_{un\ -\ ionized}\}_{aq}}\right) \qquad \text{Equation 1.2}$$

In addition, log *D* is pH dependent; one must specify the pH at which the log *D* was measured. Of particular interest is the log *D* at pH = 7.4 (the physiological pH of blood serum). For un-ionizable compounds, log *P* = log *D* at any pH.

1.8 Cutoff Effect

In his dissertation,[30] André Williams described that one goal of the project in the Gandour group was to remove the insolubility of an amphiphile as the primary cause of the cutoff effect. The amphiphiles should be soluble in the same aqueous media used for growing a microorganism. So my goal was to synthesize the **2CCbn** series and check their aqueous solublility for measuring CMCs and MICs.

Antimicrobial properties of amphiphiles tend to increase with increasing alkyl chain length.[8, 9] However, increasing the length decreases the solubility of amphiphiles in aqueous media.[10] As shown previously in our group, cationic amphiphiles have spermicidal and anti-HIV activities that directly correlate with alkyl chain length.[31,32] However, both activities drop off after a certain chain length, e.g. >C_{16}. In those examples, longer chain homologues are insoluble in water. This phenomenon is known as the cutoff effect due to insolubility.[8]

According to Balgavý and Devinský[8] the cutoff effect can occur because of (1) limited aqueous solubility of amphiphiles, (2) size discrimination and partition coefficient, (3) kinetic effects, and (4) free volume. The reasons for (1) have been discussed above. The next few paragraphs explain (2), (3), and (4).

In explaining the cutoff effect due to the partition coefficient, one can imagine a complication in the intercalation of very long-chain amphiphiles into a lipid bilayer. The harder the entry into a lipid bilayer, the lower the biological activity, which often depends on the drug-receptor interaction. In explaining the cutoff effect due to the length size discrimination, the increasing alkyl chain length will decrease the affinity of an amphiphile for the receptor. As Williams explains,[30] "A microorganism has a receptor with a fixed volume. As alkyl chain length increases, the drug fills the volume of the receptor and becomes more active. Activity increases until the receptor's volume is completely filled with a specific chain length. This chain length is the optimal chain length. As the chain length increases further, the drug becomes too big for the receptor's volume and cannot fit into the receptor as tightly as before; consequently, activity decreases."

To explain the cutoff effect due to kinetic effects, Balgavý and Devinský suggest that time-dependent drug concentration and modification of the receptor control the antimicrobial activity.[8] Biological activity depends on the drug concentration at the receptor. The drug is separated from the receptor by several compartments (e.g. series of lipid bilayers separated by aqueous layers) (Figure 1.12). The drug concentration at the receptor depends on both the hydrophobicities of the drug and of each compartment. Biological activity depends ultimately on time required to reach the receptor.

The drug can pass through the peptidoglycan layer, lipid layer before reaching the receptor (Figure 1.12). The symbol Ra, Rb, and Rc are the rates to penetrate the peptidoglycan layer, lipid bilayer and binding with the receptor, respectively. Short-chain drugs would be unable to cross the hydrophobic compartments (lipid bilayer) whereas

long-chain drugs would be unable to penetrate the hydrophilic compartments (aqueous region). The amphiphile must be hydrophobic enough to pass through the lipid bilayer but not too hydrophobic to prevent travel across the aqueous compartments and vice versa. So only drugs with optimal properties for traveling across compartments in specified time can produce good antimicrobial activity. For any given homologous series of an amphiphile, the alkyl chain length controls the properties.

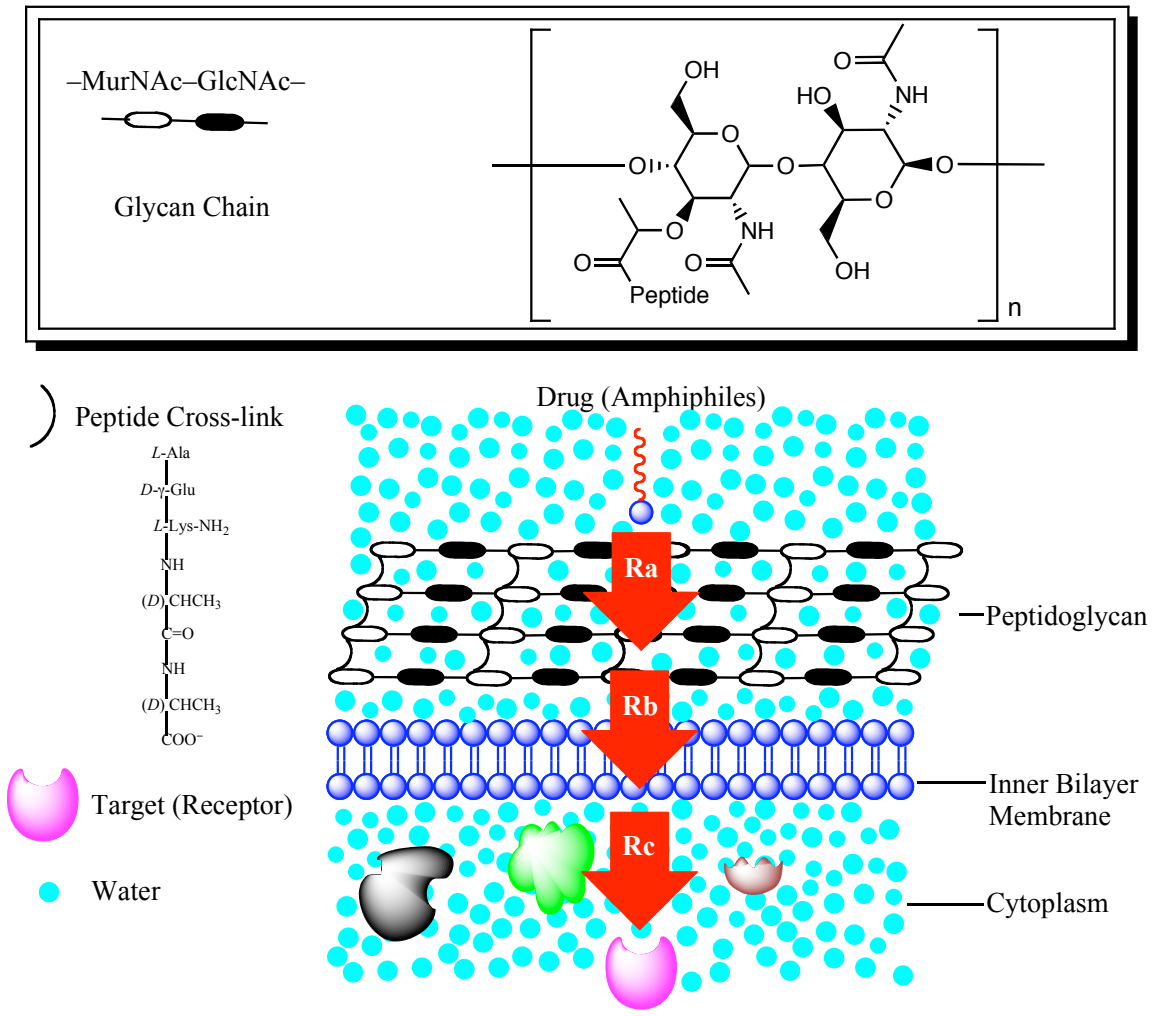

Figure 1.12 Schematic to explain cutoff effects due to kinetics in Gram-positive bacteria. Three vertical arrows indicate the rate to penetrate the peptidoglycan layer (Ra), to pass through the lipid bilayer (Rb), and to bind the receptor (Rc).

To explain the cutoff effect due to formation of free volume in a lipid bilayer, Balgavý and Devinský propose that chain length can affect the amount of free volume that is created when an amphiphile intercalates into the lipid bilayer.[8] This proposal also depends on *P* of the amphiphile. In this model, when an alkyl chain intercalates into the lipid bilayer, volume (space) is created because the alkyl chain lengths of the amphiphile and the membrane phospholipids are different. The phospholipids rearrange their alkyl chains to fill the volume. This rearrangement changes the lipid bilayer thickness, which can affect the activities of membrane-associated proteins or leakage and membrane disruption. The free-volume model proposes that short-chain amphiphiles would not exhibit antimicrobial activity. Phospholipids having much longer alkyl chain lengths than the amphiphiles create a large free volume (Figure 1.13A). Amphiphiles with short chains have low *P* values and will be present in low concentrations in the lipid bilayer. Therefore, this low concentration would only create a small free volume. As the alkyl chain length of the amphiphile increases, the amount of free volume increases because the amphiphile concentration increases due to higher values of *P* (Figure 1.13B). As an amphiphile alkyl chain length approaches the phospholipid chain length, the value of *P* increases, but the free volume decreases to zero because of the similarities in chain lengths (Figure 1.13C). High amphiphile concentration in the lipid bilayer, coupled with adequate free volume, results in decreased lipid bilayer thickness. These conditions result in cell death due to changes in the activity of membrane-associated proteins, membrane disruption, or membrane leakage.

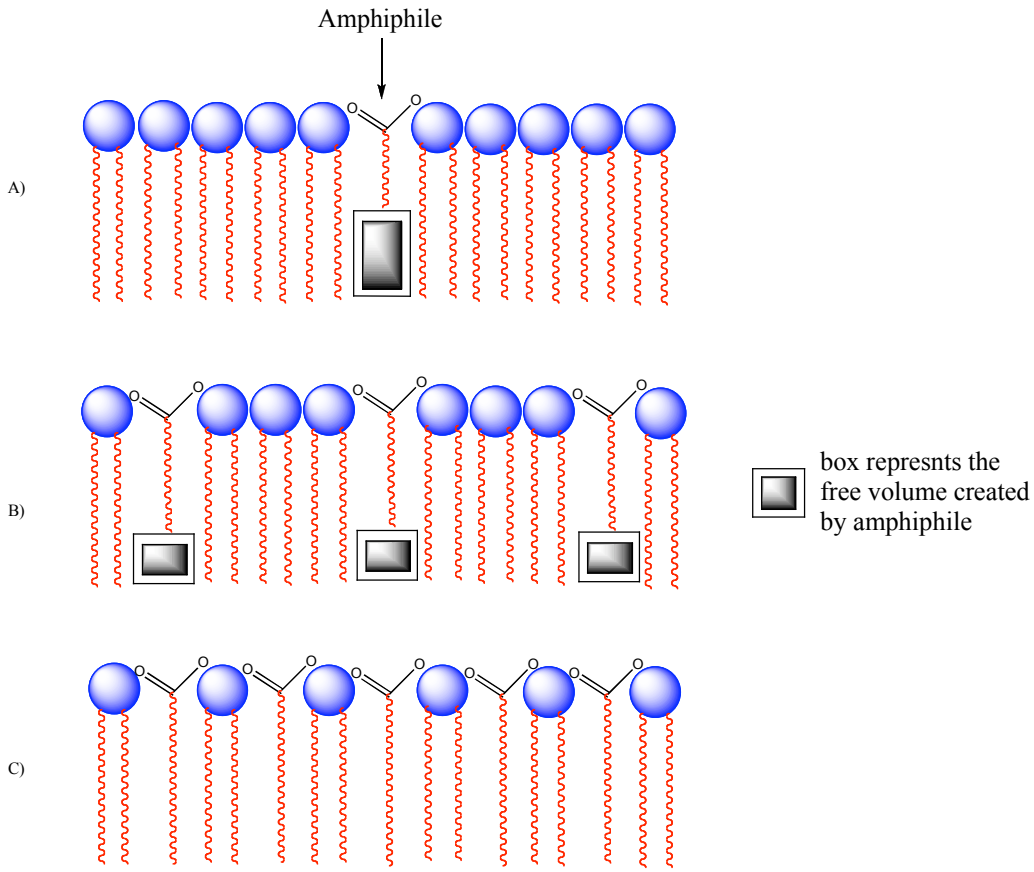

Figure 1.13 Cutoff effects: Free Volume. A) Shows a short-chain Amphiphile with a large free volume; B) shows the optimal Amphiphile; C) shows a long-chain Amphiphile with a small free volume.

1.9 The Rigid Cell Walls of Microorganisms

The cell walls of microorganisms function to prevent osmotic lysis, allow the selective passage of nutrients, exclude harmful antimicrobial agents, act as a scaffold for proteins, and maintain cell shape.[33] Cell walls protect the inner cytoplasmic membrane and can differ from one microorganism to another. The cell wall is necessary because most bacteria live in liquids whose concentration of salts and other small molecules is much lower than the concentration of these same small molecules inside the bacterial cell. In the absence of a cell wall, water flowing across the bacterial membrane

would rush into the cell, causing the cell to swell and burst. Having a cell wall will protect the cell from swelling and bursting. Many antibiotics impair the strength of the cell wall, causing swelling and bursting.[33]

The bacterial cell wall is comprised of a mesh-like polymer called peptidoglycan (Figure 1.12), which gives it strength. A staining procedure differentiates bacteria into two categories, Gram positive and Gram negative (Figure 1.14). Hans Christian Gram[33] was the inventor of this staining procedure. In the Gram stain procedure, bacteria are initially attached to a heated glass slide. Then in the first step, a combination of blue stain crystal and then in the second step, iodine as a mordant is applied to give a dark blue color to the bacteria. In the third step, washing with acetone or ethyl alcohol mixture removes the blue dye color from some bacteria, rendering them colorless under the microscope, whereas other bacteria retain their blue stain. In the fourth step, giving a second stain, safranin dye gives invisible bacteria a light red color; and the bacteria that retain the blue dye also become a deeper blue and purplish. So bacteria that stain blue are called Gram positive and bacteria that stain red are called Gram negative. These differences are due to the presence of outer bilayer membrane.

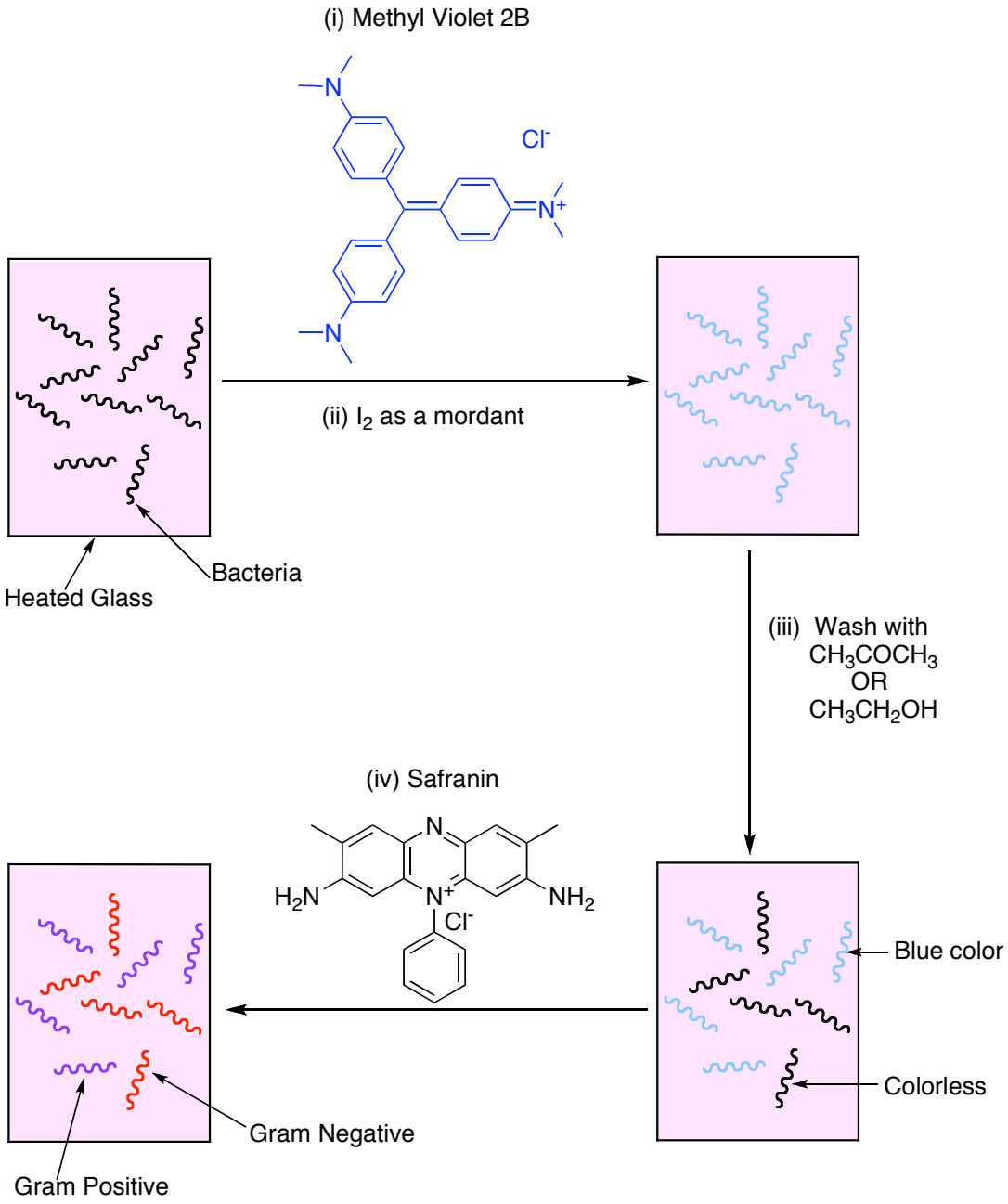

Figure 1.14 Gram stain procedure.

1.9.1 Comparison Between Gram-negative and Gram-positive Bacteria Cell Wall

The cell wall of Gram-negative bacteria is more complex than that of Gram-positive bacteria (Figure 1.15).[30] The surface of the cell wall of Gram-negative bacteria is considered hydrophilic because of the lipopolysaccharide (LPS). Gram-positive bacteria

do not contain LPS. Additionally, Gram-negative bacteria also possess an outer lipid bilayer membrane, while Gram-positive bacteria do not. However, Gram-positive and Gram-negative bacteria do share the inclusion of peptidoglycan in their cell walls. Peptidoglycan is a polymer composed of *N*-acetyl glucosamine, *N*-acetyl muramic acid, and amino acids. In Gram-positive bacteria, peptidoglycan accounts for nearly half of the entire cell and most of the cell wall (Figure 1.12). In Gram-negative bacteria, peptidoglycan only accounts for a small portion of the cell wall. The cell wall of Gram-positive bacteria is twofold to eightfold larger than the cell wall of Gram-negative bacteria. The LPS and outer bilayer membrane protect Gram-negative bacteria against membrane perturbers that destabilize the inner cytoplasmic membrane. Peptidoglycan (Figure 1.12) is such a large structure that it can not be constructed in the bacterial cytoplasm and then exported intact to the bacterial surface through the bacterial cytoplasmic membrane. Instead, bacteria construct the sugar-peptide subunits of peptidoglycan in their cytoplasm. These sugar-peptide units are then exported through the cytoplasmic membrane and assembled on the surface of the membrane into peptidoglycan.

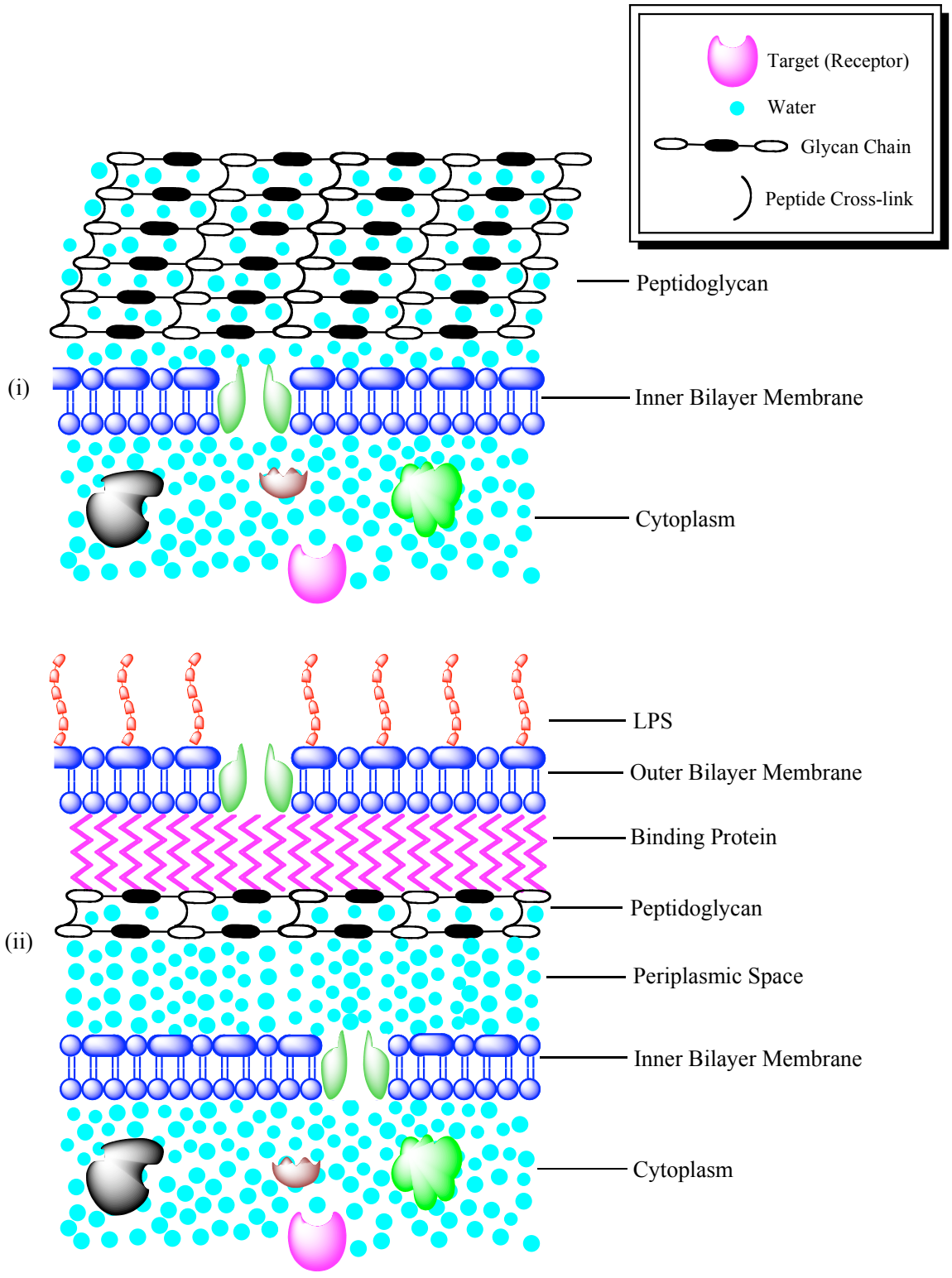

Figure 1.15 Cell wall of (i) Gram-positive, and (ii) Gram-negative bacteria.

1.9.2 Effect of Antibiotics

The peptide cross-linking gives strength to the bacterial cell wall.[33] Without cross-linking, the cell wall cannot contain the internal pressure of the bacteria, and the bacteria burst. ß-lactam antibiotics bind covalently to these cross-linking enzymes (penicillin-binding proteins, PBPs) and inactivate them. ß-lactam antibiotics are structurally similar to the D-alanyl-D-alanine residues in the peptide (Figure 1.16). Proteins for cross-linking will bind the ß-lactam antibiotics and become inhibited. The cross-linking stops and the cell dies. Whereas penicillin binds to and inactivates the enzymes that make the cross-linking, vancomycin binds to the peptides that are slated to become part of the cross-linked peptidoglycan structure. Thus, the peptides are not recognized by the cross-linking enzymes, cross-linking stops, and the cell dies.

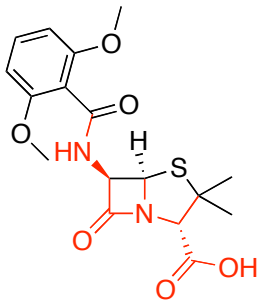

Methicillin

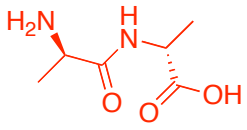

D-alanyl-D-alanine

Figure 1.16 Similarity between methicillin and D-alanyl-D-alanine

1.9.3 The Bacteria Become Resistant to Antibiotics

The first account of resistance to penicillin[33] was published at about the same time penicillin was introduced, but it took three decades to understand how bacteria protect themselves against the antibiotic. Both Gram-positive and Gram-negative bacteria cell walls use their ß-lactamase for resistance. ß-Lactamase cleaves the ß-lactam ring, thus inactivating penicillin. Bacteria developed the ß-lactamases from the PBPs. The PBPs

can start but not complete the hydrolysis of the ß-lactam ring. So a partially hydrolyzed antibiotic is trapped in the active site of the enzyme and the enzyme no longer functions. A ß-lactamase is able to complete the reaction, releasing a penicillin molecule with a broken ß-lactam ring. Gram-negative bacteria mutate proteins that make up outer membrane pores so that the opening becomes narrower. This decreases the ability of antibiotics to diffuse into the periplasmic space (Figure 1.15), thus making it easier for the periplasmic ß-lactamase to inactive all penicillin molecules. In the mechanism of resistance to vancomycin, which decreases its binding to a peptidoglycan substrate 1000-fold, bacterial enzymes replace the D-alanyl-D-alanine with D-alanyl-D-lactate.

1.10 Introduction to *Staphylococcus aureus* and Methicillin-Resistant *Staphylococcus aureus*

Deurenberg and Stobberingh recently described the history of infections caused by *Staphylococcus aureus,*[34] which was discovered in the 1880s by the surgeon Sir Alexander Ogston[35] in Aberdeen, Scotland in pus from surgical abscesses. Since then it has been considered as a pathogenic Gram-positive bacterium and the cause of a range of illnesses[36] from minor skin infections, such as pimples, to life-threatening diseases, such as pneumonia, meningitis, osteomyelitis, endocarditis, etc. It was identified[36] to occur in skin, soft tissue, respiratory tissue, bone, joint, endovascular, and wound infections. It was also identified as one common cause of nosocomial infections.

Deurenberg and Stobberingh[34] further described the origin of methicillin-resistant *S. aureus* (MRSA). In 1942, the first penicillin-resistant *S. aureus* isolate was observed in a hospital and in the community. Since 1960, more than 80% of *S. aureus* strains have been resistant to penicillin. In 1959, methicillin was introduced and two years later a *S.*

aureus developed methicillin-resistant strain. During the last 45 years, various hospital-associated MRSA (HA-MRSA) isolates have spread around the world.

There are few drugs for the treatments of MRSA infections. Vancomycin, daptomycin, and mupirocin (Figure 1.17) are the most popular drugs. With the increasing use of these drugs, rare strains of MRSA have been found to be susceptible only to a short list of antibiotics.

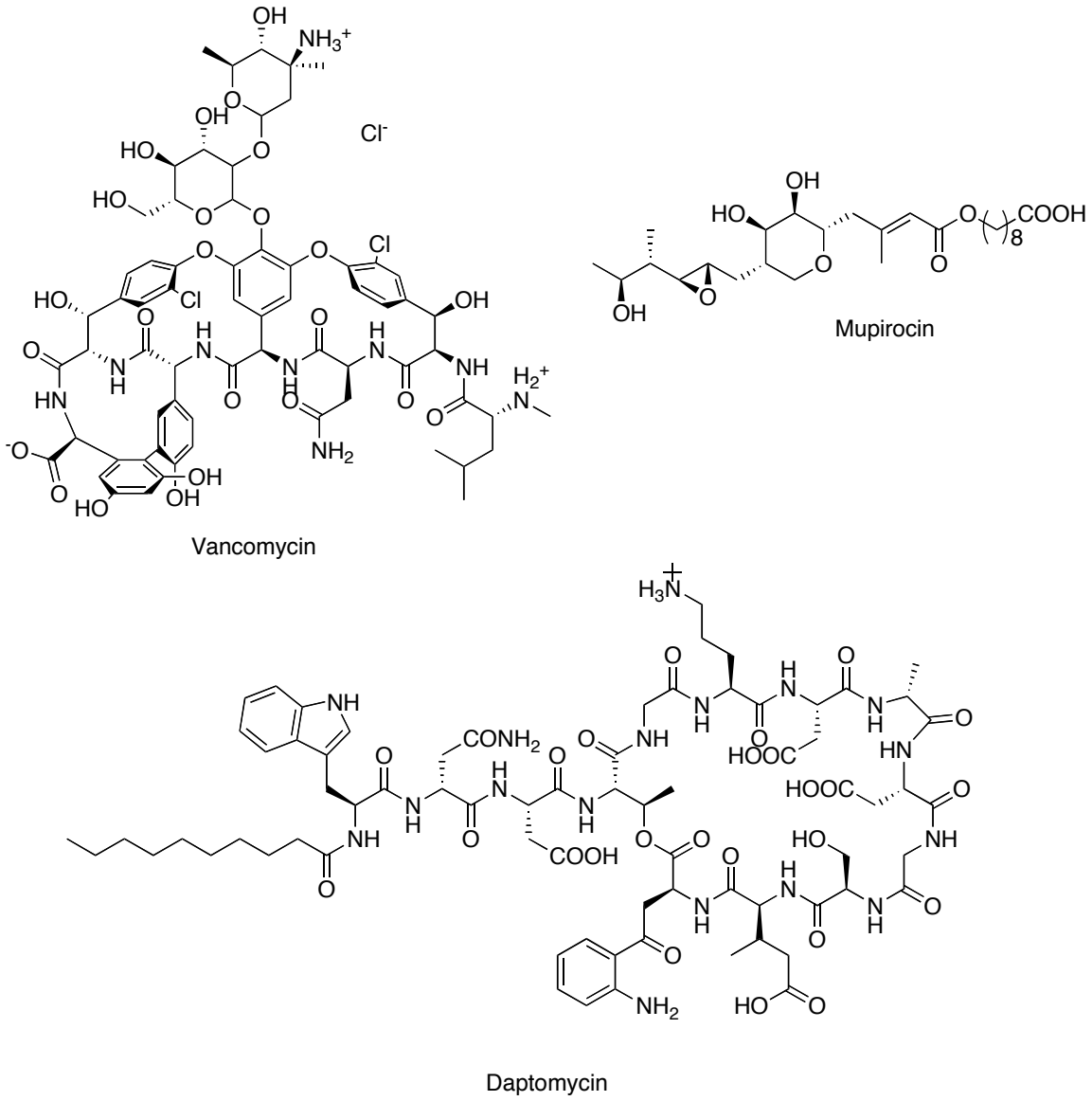

Figure 1.17 Examples of drugs used to treat MRSA

1.11 Antimicrobial Activity of Fatty Acids

1.11.1 Introduction of Antibacterial and Antifungal Activities of Fatty Acids

Fatty acids (FAs) have been known for their antimicrobial activity for over a hundred years as noted in several reviews.[37, 38] New antimicrobial agents are needed with the increasing resistance power of microorganisms. As described above, *Staphylococcus aureus* has become resistant to penicillin-type drugs, e.g. methicillin (Figure 1.16), which is commonly used to treat microbial infections.[39]

FAs inhibit the growth of a wide variety of microorganisms, like Gram-negative bacteria, Gram-positive bacteria, mycobacteria, and fungi.[20, 40-48] FAs tend to have better antimicrobial activity against Gram-positive bacteria than against Gram-negative bacteria.[43, 49] The **2CCbn** series will be tested against *S. aureus* and MRSA. We will attempt to determine (1) which chain length gives good antimicrobial activity, and (2) where the cutoff occurs for optimal activity versus chain length.

1.11.2 Antimicrobial Activity of Fatty Acids against *S. aureus*

Many studies have been done to observe the relationship between FAs and their activity against *S. aureus*. The saturated C_{12} and C_{14} FAs are the most active.[17, 38, 39, 44, 46, 50, 51] The cutoff effect was observed with longer-chain ($>C_{14}$) fatty acids showing decreased activity. Ohta et al.[52] showed that unsaturated fatty acids were considerably more active than saturated fatty acids against *S. aureus*.

1.11.3 Antimicrobial Activity of Fatty Acids against MRSA

MRSA is susceptible to both saturated and unsaturated FAs.[52] The susceptibility to the FAs increases with the number of double bonds. Three double bond FAs were

found to be more active than single double bond FAs. Oleic acid ($C_{18:1}$) was inactive, while linolenic acid ($C_{18:3}$) was active at 72 μM.

The susceptibilities of five strains of MRSA to saturated FAs was studied by Kitahara et al.[39] In all cases, susceptibility increased with chain length., from C_8 (>11 mmol) to a maximum at C_{12} (2.0 mmol). In four of the five strains, the longer-chain fatty acids (C_{14}-C_{18}) were mostly inactive (≥11 mmol).

1.12 Antimicrobial Activity of Dendritic Amphiphiles against *S. aureus*

The **3CAmn**, **3CCbn**, and **3CUrn** (Figure 1.3), C_{13}–C_{22} water-soluble homologous amphiphiles, are active against *S. aureus*.[11] The activity increases (log MIC is lower) with increasing chain length (Figure 1.18). The **3CCb22** was the most active amphiphile against *S. aureus* (MIC, 333 μM) at a high inoculum density [10^8 colony-forming units (CFU/mL)]. The **3CAmn** and **3CCbn** series showed increasing activity (log MIC still decreasing) with longer chain length. The **3CUr16** (MIC, 758 μM) was the most effective amphiphile, but the cutoff effect was observed in **3CUrn** series.

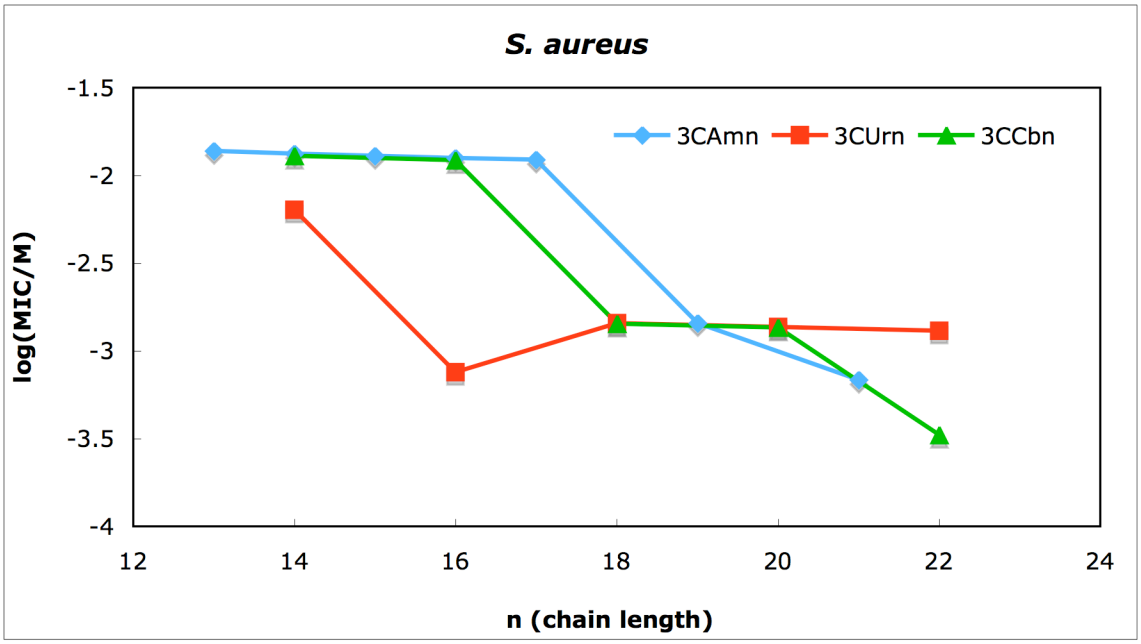

Figure 1.18 *S. aureus* MICs for three-headed amphiphiles at high inoculum density

This work[11] against *S. aureus* demonstrated that long chain ($\geq C_{20}$) water-soluble amphiphiles are more active than FAs. After this work was published, we discovered that antibiotics are typically assayed at lower inoculum density, typically 10^5 CFU. Marcelo Actis[53] described that *S. aureus* was susceptible at this inoculum density to **2CAmn** series. Further, this series was more active than **3CAmn** or even **3CCbn**, and **3CUrn** series (Figure 1.19). The compound **2CAm21** was the most active (MIC, 2.0 ± 1.0 μM). Actis compared the CMC to the MIC to determine the safety potential (>100 is considered safe) of all amphiphiles. The CMC and MIC concentration ratio of the active **2CAmn** amphiphiles against *S. aureus* are better than those of active three-headed amphiphiles (Table 1.2).

These results suggest that the **2CCbn** series might be as active as **2CAmn** and more active than **3CCbn**, **3CAmn**, and **3CUrn** series. Perhaps even the CMC/MIC ratio

for **2CCbn** series will be as good as that of the **2CAmn** series and may be better than that of three-headed amphiphiles.

Table 1.2 Concentration ratio between CMC and MIC against *S. aureus*

Amphiphiles	CMC/MIC
3CCb20	54
3CCb22	22
3CUr20	81
3CUr22	57
3CAm19	45
3CAm21	94
2CAm19	205
2CAm21	84

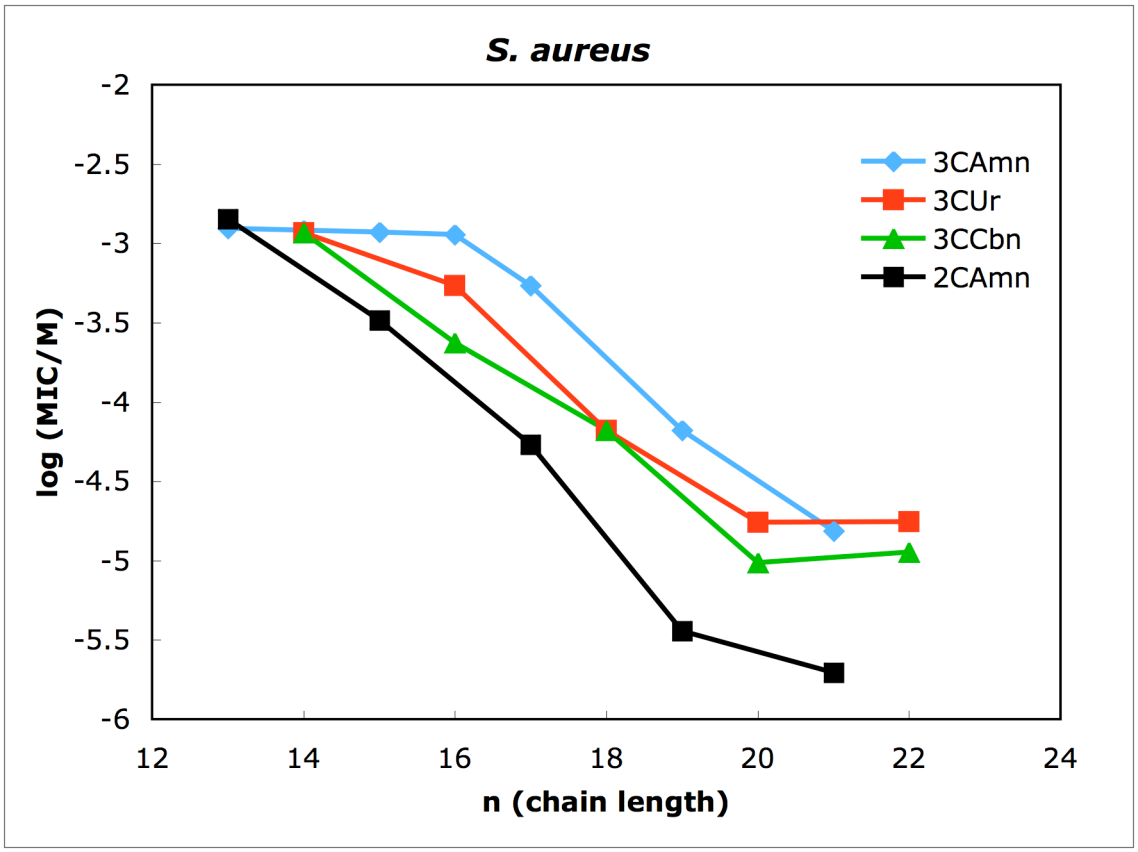

Figure 1.19 MIC comparison for *S. aureus*.[11]

1.13 Antimicrobial Activity of Dendritic Amphiphiles against MRSA

The same sets of compounds[11] were also active against MRSA. The **3CAm19** was active against MRSA (MIC of 64 μM) at a high inoculum density [10^8 colony-forming units (CFU/mL)] (Figure 1.20). The cutoff effect was observed with **3CAmn** and **3CUrn** while **3CCbn** still increased in activity with increasing alkyl chain length.

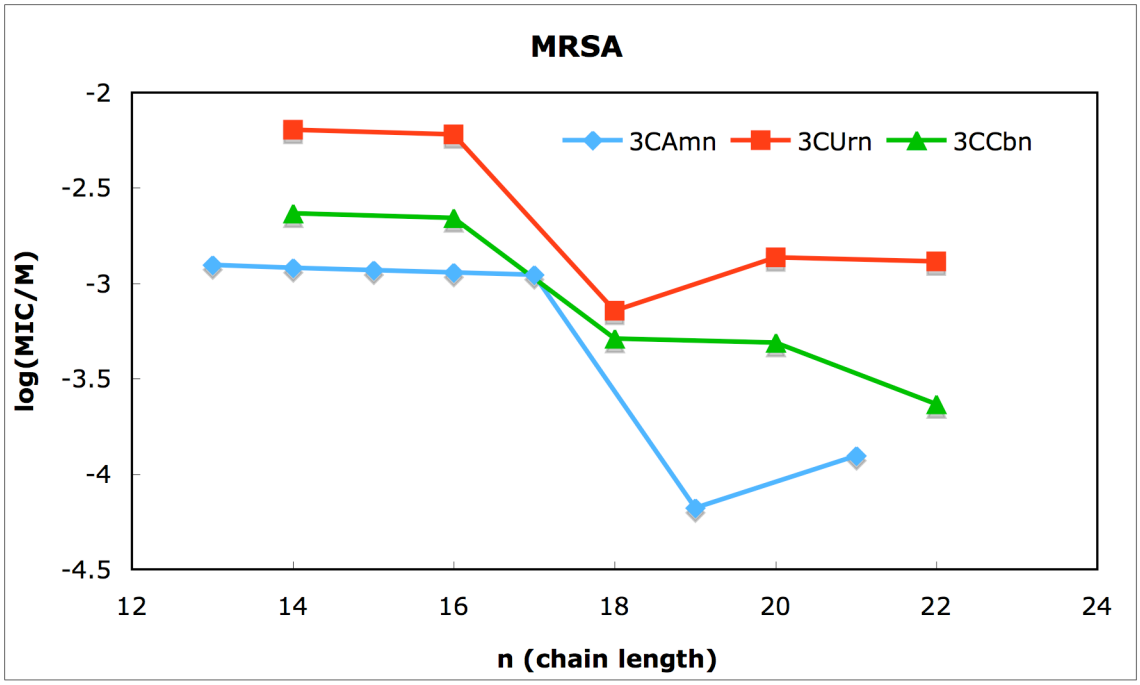

Figure 1.20 MRSA MICs for three-headed amphiphiles at high inoculum density

Marcelo Actis[53] has described that the **2CAmn** series at the lower inoculum density (10^5 CFU) are as active as **3CCbn** and **3CUrn**, but more active than the **3CAmn** series against MRSA (Figure 1.21). The difference between **2CAmn** and **3CAmn** suggests that if the difference in activity between the two- and three-headed amphiphiles holds for the **3CCbn** series, then the **2CCbn** series may be even more active than the **2CAmn** series.

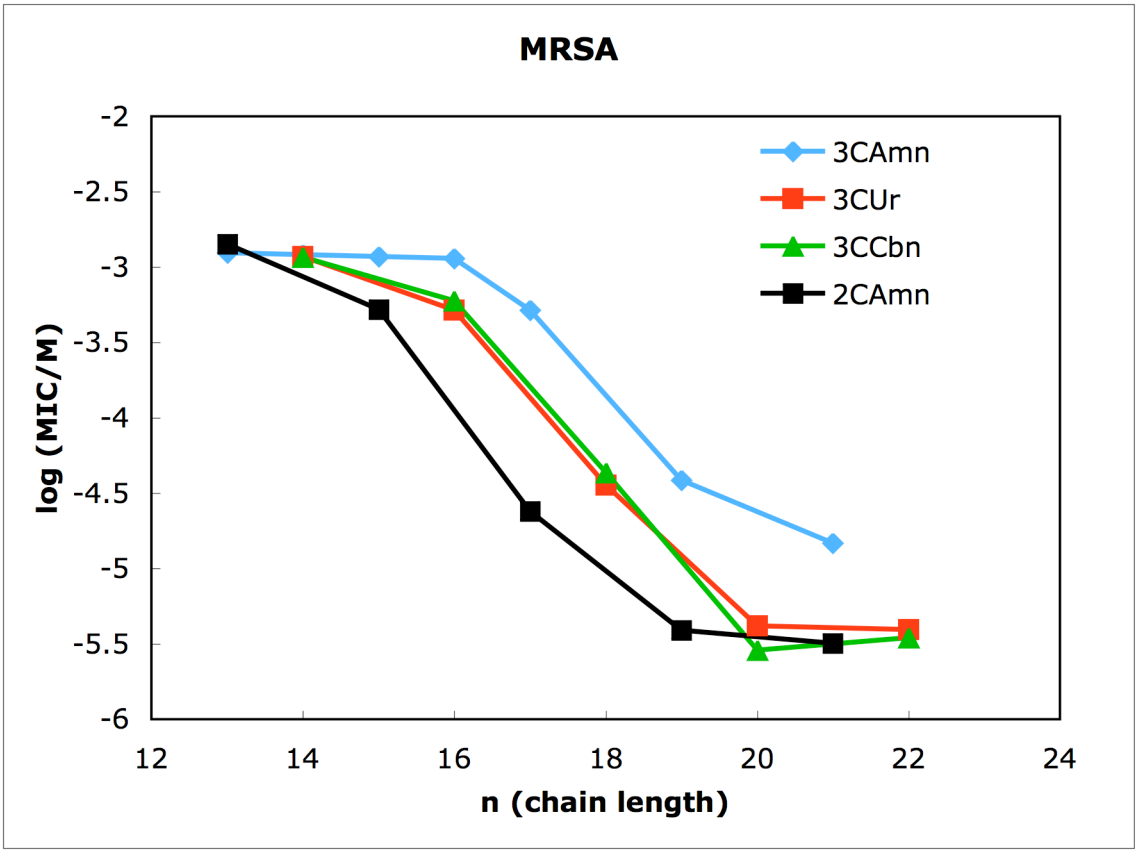

Figure 1.21 MIC comparison for MRSA.[11]

The CMC and MIC concentration ratio of the **2CAmn** series against MRSA are almost the same as three-headed amphiphiles (Table 1.3).[53] These results suggest that the CMC/MIC ratio for **2CCbn** series may be as good as that of two- and three-headed amphiphiles.

Table 1.3 Concentration ratio between CMC and MIC against MRSA

Amphiphiles	CMC/MIC
3CCb20	183
3CCb22	72
3CUr20	339
3CUr22	256
3CAm19	76
3CAm21	120
2CAm19	190

2CAm21	52

1.14 Conclusion

The three-headed amphiphiles (Figure 1.3) have been shown to be water-soluble, and to have high CMCs relative to the MIC.[11, 18] So we anticipate that the **2CCbn** series will be water-soluble, and have higher CMCs than the corresponding fatty acids and lower CMCs than the corresponding homologues in the **3CCbn** series. We also anticipate that the **2CCbn** series will demonstrate good antimicrobial activity against *S. aureus* and MRSA. The **2CCbn** series might be as active as the **2CAmn** series but more active than the **3CCbn**, **3CAmn**, and **3CUrn** series. The difference between **2CAmn** and **3CAmn** against MRSA suggests that if the difference in activity between the two- and three-headed amphiphiles holds for the **3CCbn** series, then the **2CCbn** series may be even more active than the **2CAmn** series. Perhaps the CMC/MIC ratio for the **2CCbn** series will be as good as that of the **2CAmn** series and may be even better than that of three-headed amphiphiles against *S. aureus* and MRSA.

1.14 References for Chapter 1

1. Actis, M. L. Synthesis, Characterization, Critical Micelle Concentration and Biological Acitivity of two-Headed Amphiphiles: Master of Science Thesis. Virginia Tech, Blacksburg, VA, November 6, 2008.
2. Cross, J.; Singer, E. J., *Cationic Surfactants: Analytical and Biological Evaluation. Surfactant science series. Vol. 53*. Marcel Dekker: New York, 1994.
3. Urizzi, P.; Souchard, J.-P.; Nepveu, F., EDTA and DTPA analogues of dipalmitoylphosphatidylethanolamine as lipopphilic chelating agents for metal labeling of LDL. *Tetrahedron Lett.* **1996,** *37* (27), 4685–4688.
4. Lawrence, C. A., Surfactant Science, ed. E. E. Jungermann. *New York: Marcel Dekker.* **1970,** *Vol. 4*, 491–495.
5. Myers, D., *Surfactant Science and Technology*. VCH: New York, 1988; p 65.
6. Lichtenberg, D., Characterization of the solubilization of lipid bilayers by surfactants. *Biochim. Biophys. Acta* **1985,** *821* (3), 470–478.
7. Dennis, E. A., Micellization and solubilization of phospholipids by surfactants. *Adv.Colloid Interface Sci.* **1986,** *26*, 155–175.

8. Balgav″, P.; DevÌnsky, F., Cut-off effects in biological activities of surfactants. *Adv. Colloid Interface Sci.* **1996,** *66*, 23–63.
9. Devinský, F. A.; Sersen, F.; Balgavý, P., interaction of surfactant with model and biological membranes. Part VIII. Cut-off effect in antimicrobial activity and in membrane perturbation efficiency of the homologous series of *N*, *N*-dimethylalkylamine oxides. *J. Pharm. Pharmacol.* **1990,** *42* (11), 790–794.
10. Klevens, H. B., Solubilization. *Chem. Rev.* **1950,** *47* (1), 1–74.
11. Willilam, A. A.; Sugandhi, E. K.; Macri, R. V.; Falkinham, J. O., III; Gandour, R. D., Antimicrobial activity of long-chain, water-soluble, dendritic tricarboxylato amphiphiles. *J. Antimicrob. Chemother.* **2007,** *59*, 451–458.
12. Silverman, R. B., Lead Modification: Drug Design and Development: Structure Modifications to Intcrease Potency and the Therapeutic Index. *The Organic Chemistry of Drug Design and Drug Action* **2003,** *2*, 27-86.
13. Clint, J. H., Surfactant Aggregation. *New York: Chapman and Hall* **1991**, 5.
14. Myers, D., Surfactant Science and Technology. *New York, N. Y.: VCH* **1988**, 33.
15. Surfactants: the ubiquitous amphiphiles. http://www.rsc.org/chemistryworld/Issues/2003/July/amphiphiles.asp (accessed March 30, 2009).
16. Reichenbach, H., The effect of soaps on *E. coli*. *Z. Hyg. Infectionskrankh.* **1908,** *59*, 296.
17. Bayliss, M., Effect of the Chemical Constitution of Soaps upon their Germicidal Properties. *J. Bacteriol.* **1936,** *31* (5), 489–504.
18. Sugandhi, E. W.; Macri, R. V.; Williams, A. A.; Kite, B. L.; Slebodnick, C.; Falkinham, J. O., III; Esker, A. R.; Gandour, R. D., Synthesis, Critical Micelle Concentrations, and Antimycobacterial Properties of Homologous, Dendritic Amphiphiles. Probing Intrinsic Activity and the "Cutoff Effect". *J. Med. Chem.* **2007,** *50* (7), 1645–1650.
19. Scherrer, R. A.; Howard, S. M., Use of distribution coefficients in quantitative structure–activity relations. *J. Med. Chem.* **1977,** *20* (1), 53–58.
20. Miller, R. D.; Brown, K. E.; Morse, S. A., Inhibitory action of fatty acids on growth of *Neisseria gonorrhoeae*. *Infect. Immun.* **1977,** *17* (2), 303–312.
21. Shinoda, K., The Critical Micelle Concentrations in Aqueous Solutions of Potassium Alkyl Malonates. *J. Phys. Chem.* **1955,** *59* (5), 432–435.
22. Shinoda, K., The Critical Micelle Concentrations in Aqueous Solutions of Potassium Alkane Tricarboxylates. *J. Phys. Chem.* **1956,** *60* (10), 1439–1441.
23. Shinoda, K., The Effect of Alcohols on the Critical Micelle Concentrations of Fatty Acid Soaps and the Critical Micelle Concentration of Soap Mixtures. *J. Phys. Chem.* **1954,** *58* (12), 1136–1141.
24. Paleos, C. M.; Michas, J.; Malliaris, A., Alkyl derivatives of iminodiacetic acid: A novel class of compounds forming thermotropic liquid crystals and aqueous micelles. *Mol. Cryst. Liq. Cryst.* **1990,** *186*, 251–260.
25. Hansch, C.; Maloney, P. P.; Fujita, T.; Muir, R. M., Correlation of biological activity of phenoxyacetic acids with Hammett substituent constants and partition coefficients. *Nature (London)* **1962,** *194*, 178.
26. Fujita, T.; Iwasa, J.; Hansch, C., A new substituent constant, π, derived from partition coefficients. *J. Am. Chem. Soc.* **1964,** *86*, 5175–5180.

27. Singer, S. J.; Nicolson, G. L., The Fluid Mosaic Model of the Structure of Cell Membranes. *Science* **1972,** *175* (4023), 720–731.
28. Silverman, R. B., *The Organic Chemistry of Drug Design and Drug Action*. 2nd ed.; Elsevier Academic Press: Amsterdam, 2004; p. 55–57.
29. Sangster, J., *Octanol–Water Partition Coefficients: Fundamentals and Physical Chemistry*. Wiley series in solution chemistry, v. 2. Wiley: Chichester, 1997.
30. Williams, A. A. Syntheses, Characterization, Physical and Biological Properties of Long-chain, Water-soluble, Dendritic Amphiphiles: Doctor of Philosophy Thesis. Virgnia Tech, Blacksburg, VA, 2008.
31. Wong, Y. L.; Hubieki, M. P.; Curfman, C. L.; Doncel, G. F.; Dudding, T. C.; Savle, P. S.; Gandour, R. D., A structure–activity study of spermicidal and anti-HIV properties of hydroxylated cationic surfactants. *Bioorg. Med. Chem.* **2002,** *10*, 3599–3608.
32. Wong, Y. L.; Curfman, C. L.; Doncel, G. F.; Hubieki, M. P.; Dudding, T. C.; Savle, P. S.; Gandour, R. D., Spermicidal, anti-HIV, and micellar properties of di- and trihydroxylated cationic surfactants. *Tetrahedron* **2002,** *58* (1), 45–54.
33. Salyers, A. A.; Whitt, D. D., *Revenge of the Microbes: How Bacterial Resistance is Undermining the Antibiotic Miracle*. ASM Press: Washington, D. C., 2005.
34. Deurenberg, R. H.; Stobberingh, E. E., The evolution of *Staphylococcus aureus*. *Infect. Genet. Evol.* **2008,** *8* (6), 747–763.
35. Ogston, A., Classics in Infectious Diseases. *Rev. Infect. Dis.* **1984,** *6* (1), 122–128.
36. Kluytmans J, v. B. A., Verbrugh H, Nasal carriage of *Staphylococcus aureus*: epidemiology, underlying mechanisms, and associated risks. *Clin. Microbiol. Rev.* **1997,** *10* (3), 505–520.
37. Nieman, C., Influence of trace amounts of fatty acids on the growth of microorganisms. *Bacteriol Rev.* **1954,** *18*, 147–163.
38. Walker, J. E., The germicidal properties of chemically pure soaps. *J. Infect. Dis.* **1924,** *35*, 557–566.
39. Kitahara, T.; Koyama, N.; Matsuda, J.; Aoyama, Y.; Hirakata, Y.; Kamihira, S.; Kohno, S.; Nakashima, M.; Sasaki, H., Antimicrobial activity of saturated fatty acids and fatty amines against methecillin-resistant *Staphylococcus aureus*. *Biol. Pharm. Bull.* **2004,** *27(9)*, 1321–1326.
40. Saito, H.; Tomioka, H.; Yoneyama, T., Growth of Group-IV mycobacteria on medium containing various saturated and unsaturated fatty acids. *Antimicrob. Agents Chemother.* **1984,** *26* (2), 164–169.
41. McGaw, L. J.; Jager, A. K.; Van Staden, J., Antibacterial effects of fatty acids and related compounds from plants. *S. Afr. J. Bot.* **2002,** *68*, 417–423.
42. Kondo, E.; Kanai, K., Lethal effect of long-chain fatty acids on mycobacteria. *Jpn. J. Med. Sci. Biol.* **1972,** *25* (1), 1–13.
43. Kanai, K.; Kondo, E., Antibacterial and cytotoxic aspects of long-chain fatty acids as cell-surface events-selected topics. *Jpn. J. Med. Sci. Biol.* **1979,** *32* (3), 135-174.
44. Kabara, J. J., Lipids as host-resistance factors of human milk. *Nutr. Res. (N. Y.)* **1980,** *38* (2), 65–73.
45. Kabara, J. J.; Swieczkowski, D. M.; Conley, A. J.; Truant, J. P., Fatty acids and derivatives as antimicrobial agents. *Antimicrob. Agents Chemother.* **1972,** *2* (1), 23–28.

46. Kabara, J.; Vrable, R.; Lie Ken Jie, M., Antimicrobial lipids: Natural and synthetic fatty acids and monoglycerides. *Lipids* **1977,** *12* (9), 753–759.
47. Kabara, J., Structure–Function Relationships of Surfactants as Antimicrobial Agents. *J. Soc. Cosmet. Chem.* **1978,** *29* (11), 733–741.
48. Bergsson, G.; Arnfinnsson, J.; Steingrímsson, O.; Thormar, H., In vitro killing of *Candida albicans* by fatty acids and monoglycerides. *Antimicrob. Agents Chemother.* **2001,** *45* (11), 3209–3212.
49. Thomar, H.; Bergsson, G., Antimicrobial effects of lipids. *Recent Dev. Antiviral Res.* **2001,** *1*, 157–173.
50. Kabara, J., Toxicological, bacteriocidal and fungicidal properties of fatty acids and some derivatives. *J. Am. Oil Chem. Soc.* **1979,** *56* (11), 760A–767A.
51. Kabara, J. J., Structure-function relationship of anti-microbial lipids - review. *J. Am. Oil Chem. Soc.* **1978,** *55* (3), A235–235.
52. Ohta, S.; Shiomi, Y.; Kawashima, A.; Aozasa, O.; Nakao, T.; Nagate, T.; Kitamura, K.; Miyata, H., Antibiotic effect of linolenic acid from *Chlorococcum* strains Hs-101 and *Dunaliella primolecta* on methicillin-resistant *Staphylococcus aureus*. *J. Appl. Phycol.* **1995,** *7* (2), 121–127.
53. Actis, M. L., Synthesis, Characterization, Critical Micelle Concentration and Biological Acitivity of two-Headed Amphiphiles: Master of Science Thesis. *VT* **2008**.

Chapter 2: Synthesis of the 2CCbn Series

2.1 Introduction to Synthesis of the 2CCbn Series

The synthesis of the **2CCbn** series can be carried out in five steps (Scheme 2.1). The first step involves a reaction of nitroethane and two equivalents of *tert*-butyl acrylate (TBA) to form nitrodiester headgroups **1** by successive Michael additions. The second step is reduction of **1** to form aminodiester **2**. The third step involves a reaction of **2** with di-*tert*-butyl dicarbonate [$(Boc)_2O$] to form isocyanatediester **3**. The fourth step is addition of **3** with aliphatic alcohol to give alkyl carbamate diester **(2ECbn) 5**. The resulting compounds are abbreviated as **2ECbn**, where **"2E"** represents two *tert*-butyl ester headgroups, **"Cb"** represents the carbamate linker, and **"n"** represents the number of carbons in the hydrophobic tail. The final step is the removal of the *tert*-butyl protecting groups to give **2CCbn** series **6**. Here **"2C"** represents two carboxylic acid containing headgroups or carboxylate headgroups, again **"Cb"** represents the carbamate linker and **"n"** represents the number of carbons in the hydrophobic tail.

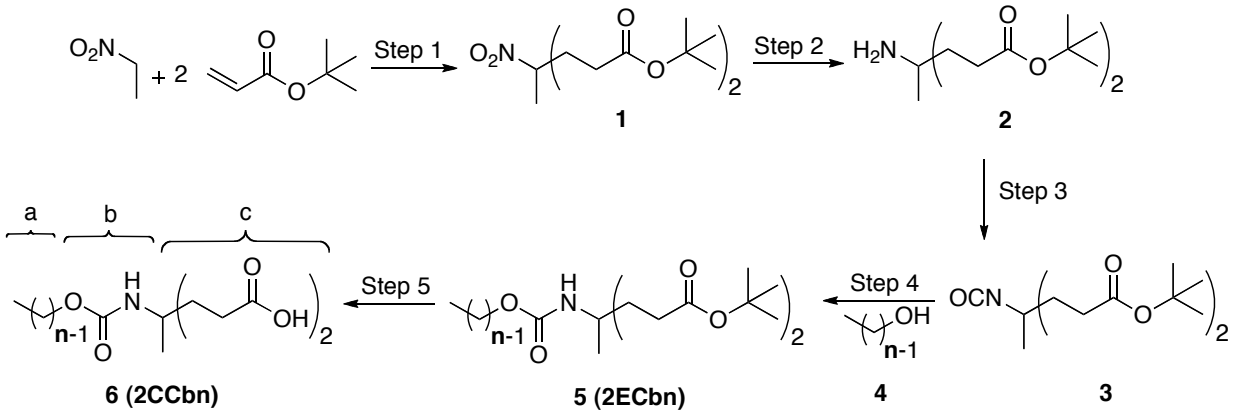

a. hydrophobic tail; b. carbamate linker; c. hydrophilic headgroup

Scheme 2.1 Synthesis of the **2CCbn** series

2.2 Synthesis of Di-*tert*-butyl 4-Methyl-4-nitroheptanedioate, Nitrodiester (1)

Newkome et al. published several methods for preparing dendritic headgroups with two *tert*-butyl ester groups (Scheme 2.2),[1-3] including synthesis of **1**. In an effort to avoid using liquid NH_3, Marcelo Actis[4] accomplished the synthesis of **1** by a reaction of nitroethane and two equivalents of *tert*-butyl acrylate with Triton B (benzyltrimethylammonium hydroxide, 40 wt % solution in methanol) as a catalyst (Scheme 2.3). The reaction was run in a 2.0-mol excess of *tert*-butyl acrylate. The purified yield was modest because of the difficulty in removing excess acrylate.

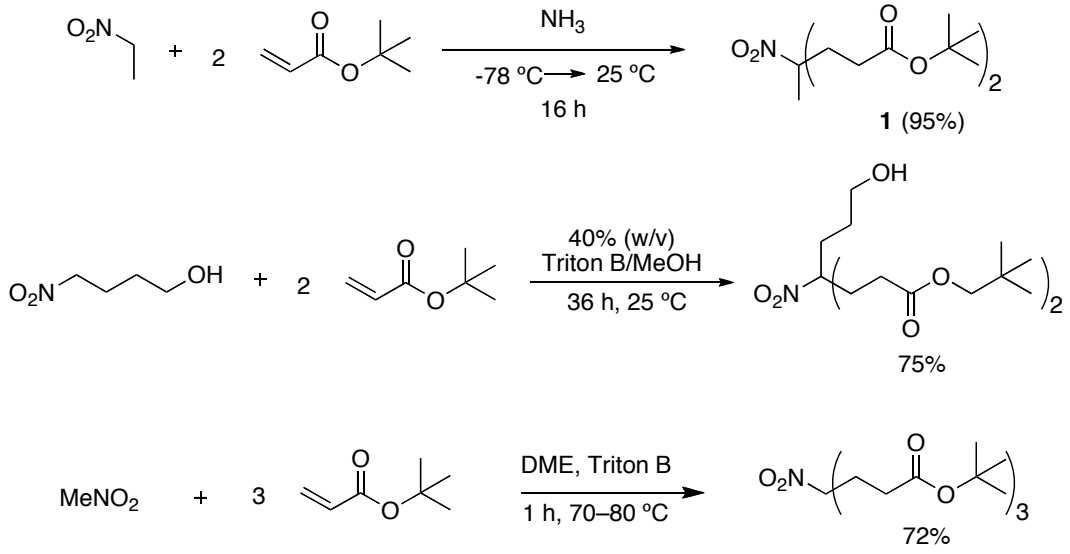

Scheme 2.2 Published methods for addition of *tert*-butyl acrylate to nitroalkanes. DME = 1,2-dimethoxyethane, Triton B = benzyltrimethylammonium hydroxide.

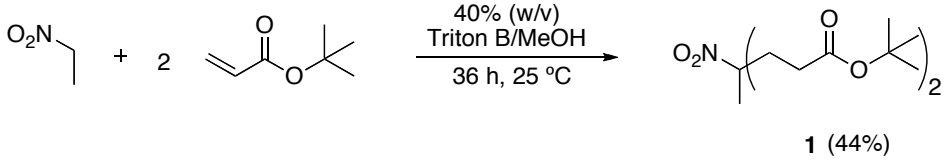

Scheme 2.3 Synthesis of nitrodiester catalyzed by Triton B

In an effort to increase the yield, another method was tried. Tishkov et al. (Scheme 2.4.a)[5] synthesized γ-functionalized ß-aryl-substituted primary nitro compounds

by using 100 mol% DBU (1,8-diazabicyclo[5.4.0]undec-7-ene). Initially, Actis and I used 15% DBU as a catalyst for the Michael addition reaction (Scheme 2.4.b). Later, I compared using 15, 10, and 5 mol % DBU in the reaction. The best result was achieved with 5 mol % DBU. However, the % crude yield (100%) and % recovery (81%) of nitrodiester was almost the same for all three. But by using less base, it was easier to purify the crude product with one-inch diameter flash column chromatography (97.5:2.5 chloroform/ethyl acetate) and less expensive. The compound had a narrow melting range (52.6–53.0 °C), which was higher than the reported value (46.0–47.0 °C),[1] and was fully characterized by ^{1}H, ^{13}C NMR, IR, HRMS, and elemental analysis.

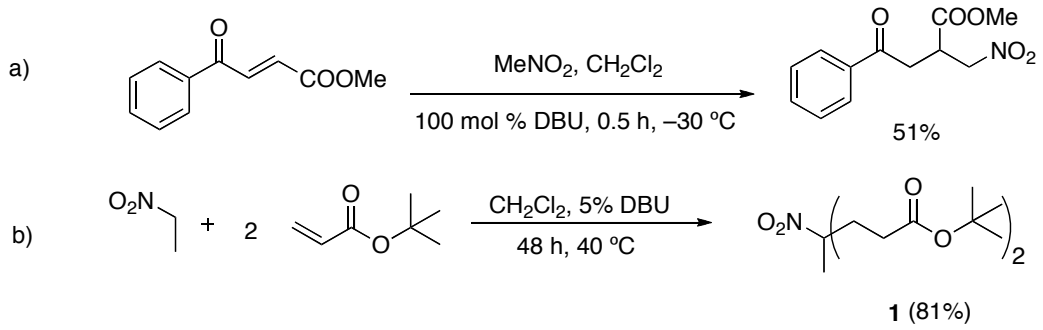

Scheme 2.4: a) Published example with DBU. b) Current work with DBU.

2.3 Synthesis of Di-*tert*-butyl 4-Amino-4-methylheptanedioate, Aminodiester (2)

Synthesis of **2** is accomplished via catalytic hydrogenation of **1** (Scheme 2.5).[1] Newkome et al.[3] stated that a *tert*-butyl ester was needed, instead of a less bulky alkyl (methyl) group to prevent intramolecular cyclization, i.e. the formation of a lactam **7** (Scheme 2.6). Typically, the reaction was run in an alcoholic solvent.

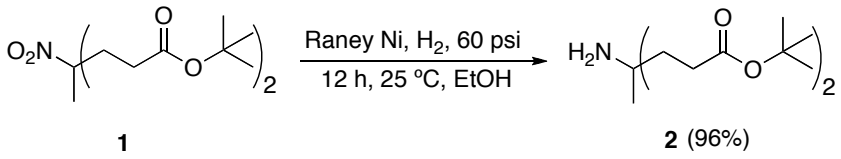

Scheme 2.5 Reported method for the synthesis of aminodiester

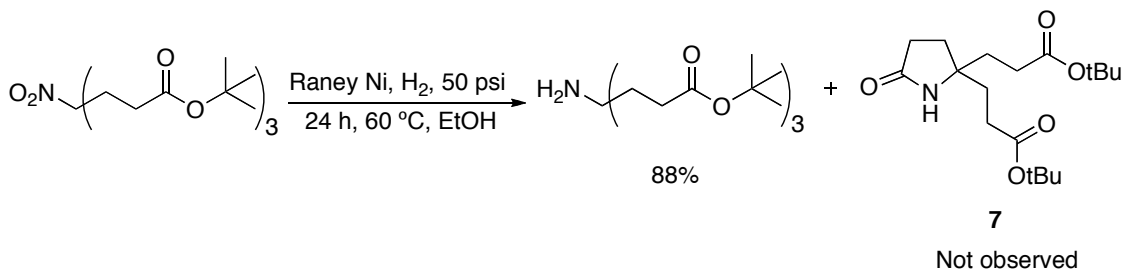

Scheme 2.6 The use of *tert*-butyl groups to prevent lactam formation

An alternative method[6] for the reduction of **8** used heptane instead of ethanol (Scheme 2.7), and resulted in a product with higher purity and yield (98%) compared to Newkome et al.[3] (88%). The hydrogenation was carried out in a mechanically stirred sealed reactor, which was unavailable to us for the desired scale of the reaction. Hardrict (unpublished) attempted the reaction with shaking in a Parr hydrogenator but **9** was not formed. Cefalo and Huang (personal communication to Gandour) at Frontier Scientific confirmed Hardrict's results.

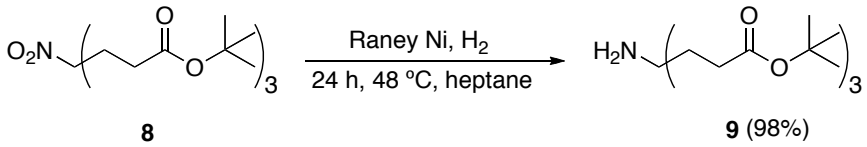

Scheme 2.7 Reduction procedure of Akpo et al.

The synthesis of **2** was accomplished by modifying the method in Scheme 2.5 by allowing the reaction to proceed for only 3 h (Scheme 2.8). The white low-melting solid gave a ^{1}H NMR spectrum that agreed with that published for **2**, reported as an oil.[1]

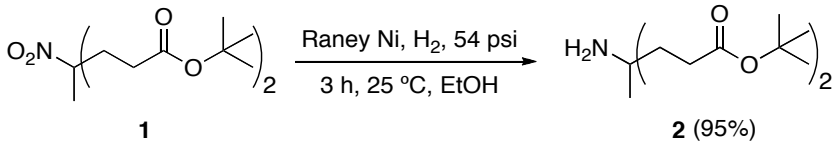

Scheme 2.8 Synthesis of aminodiester

2.4 Synthesis of Di-*tert*-butyl 4-Isocyanato-4-methylheptanedioate, Isocyanatediester (3)

Newkome et al.[7] have published the method for preparing isocyanatetriester dendritic building block. Isocyanatetriester **11** (Scheme 2.9) can be prepared with the treatment of **10** with triphosgene in the presence of an inorganic or organic base.

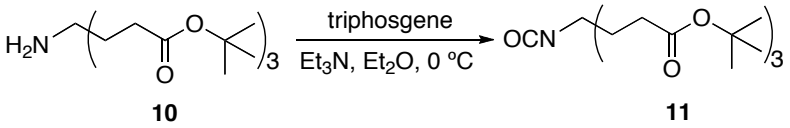

10 **11**

Scheme 2.9 Synthesis of the isocyanatetriester

Isocyanatediester was prepared by combining aminodiester **2** (Scheme 2.10) with dimethyl amino pyridine (DMAP) **12** and di-*tert*-butyl dicarbonate $(Boc)_2O$ **13** in methylene dichloride solvent at room temperature for 15 minutes to give isocyanatediester **3**.[8, 9] Compound **3** was fully characterized by ^1H, ^{13}C NMR, IR, HRMS, and elemental analysis.[7] The isocyanatediester was a colorless viscous liquid, which contrasted to the solid isocyanatetriester.

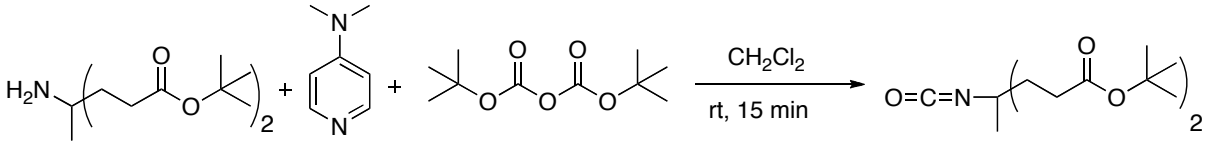

2 **12** **13** **3**

Scheme 2.10 Synthesis of isocyanatediester

2.5 Synthesis of Carbamate Linked Diesters

A carbamate bond was created in all homologues of **5** and steroid **15** (Scheme 2.11) by combining a slight excess of alkan-1-ol **4** and 5α-cholestan-3ß-ol **14**, respectively, with isocyanatediester **3** in triethylamine as the solvent[10] at 95 °C for 24 h. Crude product had unreacted alcohol and another impurity. Over sixty different solvent

systems were tried to find out the best for flash column chromatography. A mixture of 6:2.5:2.5 (v/v/v) hexane:diethyl ether:methanol gave the best separation. The purified yield was more than 98 %. All homologues of the **2ECbn** series gave narrow melting point range and were fully characterized by ^{1}H NMR, ^{13}C NMR, IR, HRMS and elemental analysis.

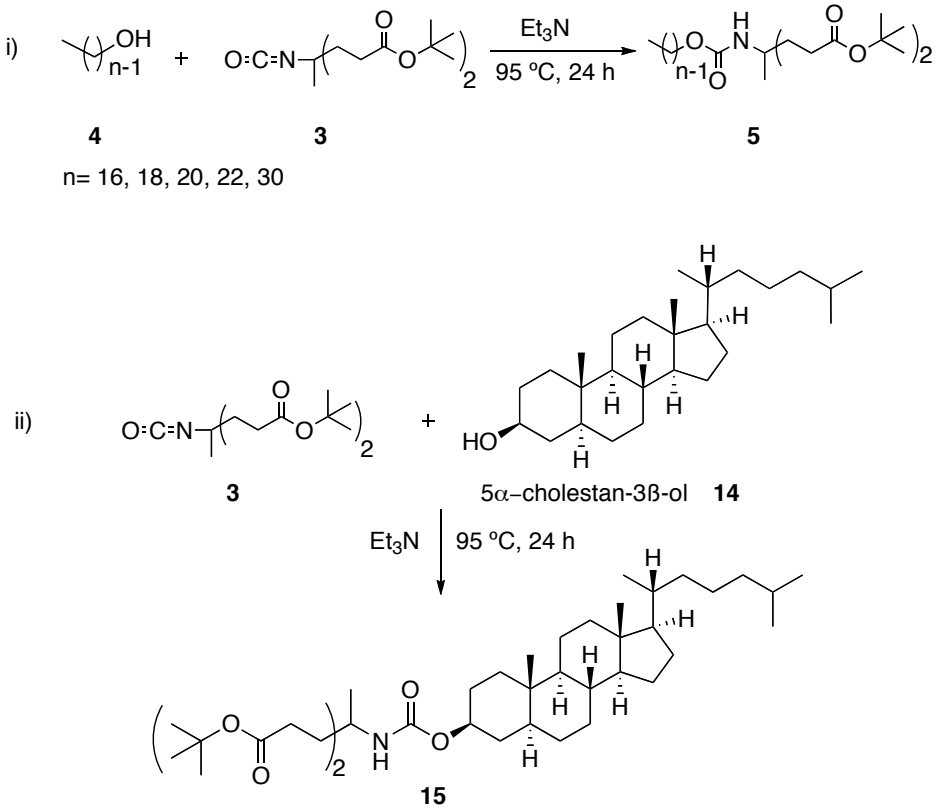

Scheme 2.11 Synthesis of the **2ECbn** series

2.6 Removal of the *tert*-Butyl Group from the 2ECbn Series

Generally, *tert*-butyl groups were removed with trifluoroacetic acid (TFA) because Marcelo Actis[4] discovered that removal of *tert*-butyl group from the **2CAmn** series took 1 hour with TFA compared to 24 hours with formic acid. The homologues of **5** and steroid **15** were combined with TFA to give diacids **6** and **16**, respectively (Scheme 2.12). Removing TFA by rotary evaporation, including three treatments with chase

solvents, and drying under high vacuum gave a product with a narrow melting range. All compounds were fully characterized by ^{1}H NMR, ^{13}C NMR, IR, HRMS, and elemental analysis.

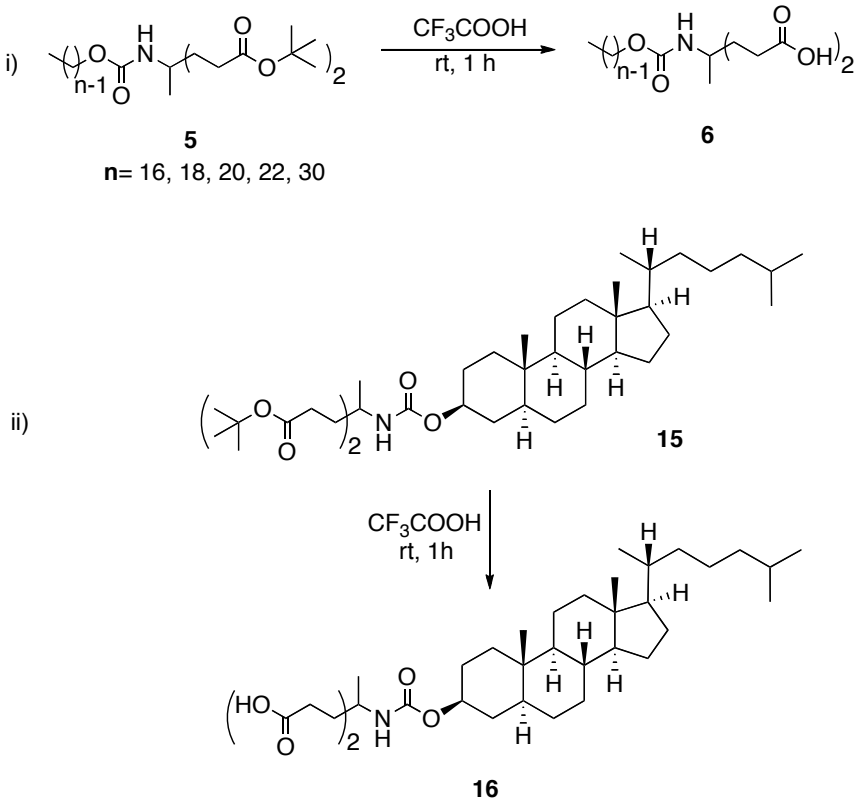

Scheme 2.12 Removal of *tert*-butyl group

2.7 Overall Synthesis of the 2CCbn Series

In summary, five different steps are needed to form the **2CCbn** series (Scheme 2.13). The first step, synthesis of nitrodiester, occurs with good yield via Michael addition reaction. The second step, reduction of nitrodiester, give aminodiester in high yield. The third step, synthesis of isocyanatediester, gives good yield. In the fourth step, synthesis of **2ECbn**, the yield varies with the alcohol. The fifth step, deprotection of **2ECbn**, occurs in very high yield. No reaction has been fully optimized. Higher yields

would be expected by optimizing reaction times, and developing purification techniques that avoid column chromatography.

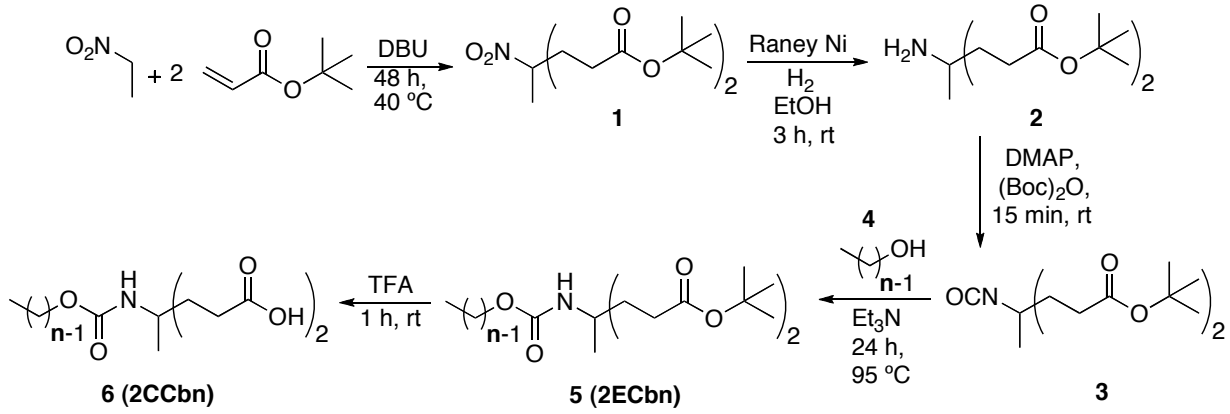

Scheme 2.13 Overall synthesis of the **2CCbn** series

2.8 Comment on NMR Characterization: Diastereotopic Protons

The ^{1}H NMR spectrum in deuterated chloroform of the nitrodiester (Figure 2.3), displays complex splitting for the eight-methylene protons. This phenomenon can be explained by looking at the environment surrounding the protons. Figure 2.1.is a three-dimensional representation of nitrodiester.

According to Ault[11] and Silverstein and Lalonde,[12] nuclei are chemical shift equivalent if they are interchangeable by a rapid process or through any symmetry operation like (1) rotation about a simple symmetry axis (C_n), (2) reflection through a plane of symmetry (σ), (3) inversion through a center of symmetry (i), (4) higher orders of rotation about an axis followed by reflection in a plane normal to this axis (S_n). Nuclei that are interchangeable through an axis of symmetry (C_n) are chemical shift equivalent in any environment (solvent or reagent) whether achiral, racemic, or chiral.

In the nitrodiester, there is no plane of symmetry (Figure 2.1 B) for each –CH_2CH_2– group. So all four protons are not interchangeable; as a result, they are not

chemical shift equivalent. Changing either Ha or Hb of the respective methylene groups gives two chiral centers; this means that Ha and Hb are diastereotopic protons. An individual proton couples with two vicinal protons and one geminal proton to give a ddd splitting pattern (Figure 2.2). So for one proton there are eight lines. One headgroup contains four protons, so a total of 32 lines are possible (Figure 2.3). At 500 MHz, 30 lines are clearly viewable. In this nitrodiester, the two headgroups are related by a plane of symmetry (Figure 2.1 A). All four protons of one headgroup are interchangeable with those of the other headgroup (Figure 2.1 A, 2.3).

In comparing the spectra of nitrodiester (Figure 2.3) and aminodiester (Figure 2.4), there is a huge difference. In the nitrodiester, two different electron-withdrawing functional groups ($–NO_2$, –COO) are present. While in amino diester there are $–NH_2$ and –COO are present. Between, nitro and amino groups, the nitro group is more electron withdrawing. The positions of functional groups affect the chemical shift. In the structure, $X_2N–C(\alpha')–CH_2$ (ß, ß′)$–CH_2(\alpha)–COO–$, one methylene is ß′ to the amino (or nitro) and ß to the carboxyl group; the other methylene is α to the carboxyl group. In the nitrodiester and the aminodiester, methylene protons on the ß carbon are predicted[13] to have different chemical shifts, 2.22 and 1.86 δ, respectively. In both nitrodiester and aminodiester, the methylene protons on the α carbon are predicted to have chemical shift 2.32 δ.

But splitting is more complex for the nitrodiester than the aminodiester. In the nitrodiester, the differences in chemical shifts ($\Delta\nu^{vic}$) between methylene groups is small such that $\Delta\nu^{vic}/J < 8$. For the simple pattern, "the arbitrarily $\Delta\nu^{vic}/J$ is greater than about 8".[14] In order to see geminal coupling (^2J, typically 12–15 Hz), the $\Delta\nu^{gem}/J$ should be

greater than 1. In the aminodiester, the $\Delta\nu^{vic}$ between methylene groups, $\Delta\nu^{vic}/J$, is very large. Thus, it gives simpler spectrum than that of the nitrodiester. With respect to $\Delta\nu^{gem}/J$ for geminal coupling in the aminodiester (Figure 2.4), the value is larger for the α methylene group than the ß methylene group, which appears as a triplet.

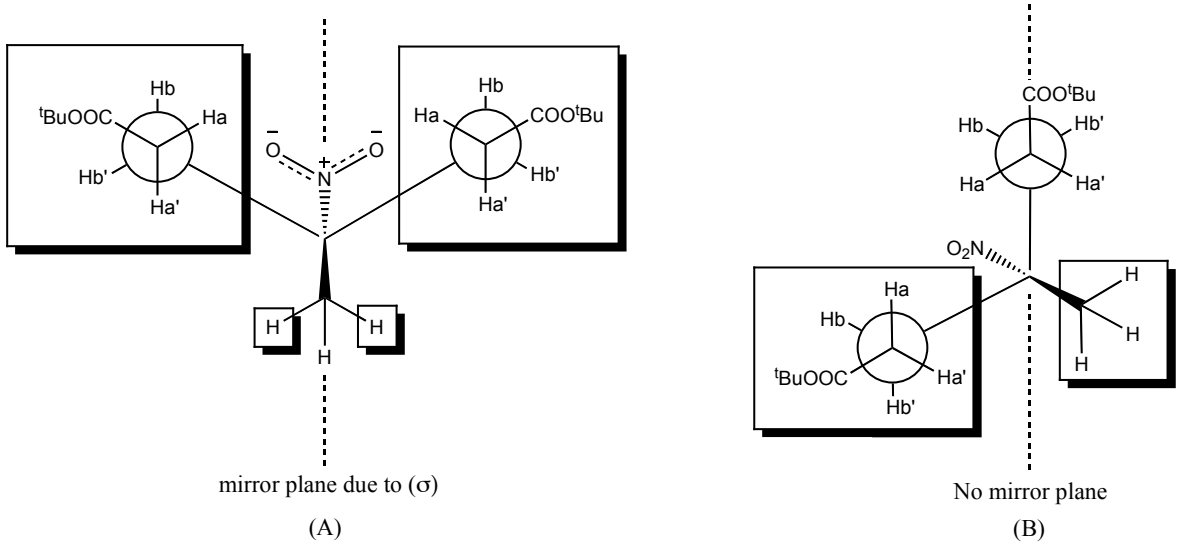

Figure 2.1 Three-dimensional representation of nitrodiester (A, B).

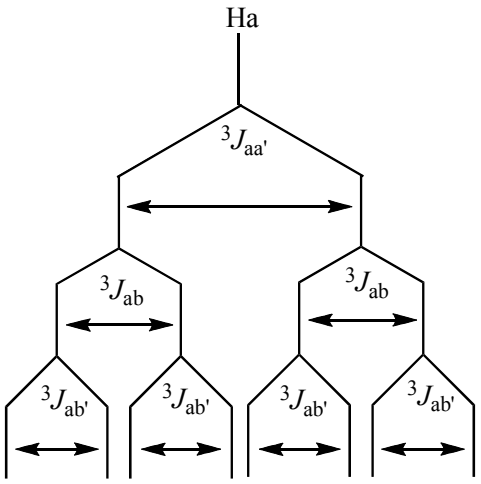

Figure 2.2 Splitting of one-methylene proton nuclei with other three in nitrodiester

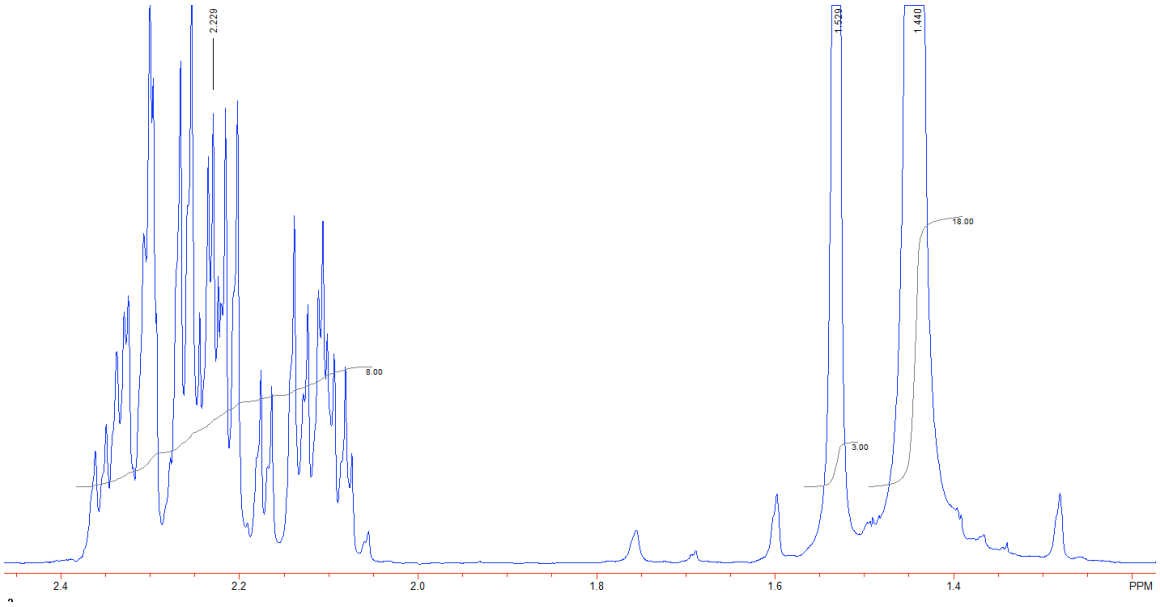

Figure 2.3 ^{1}H NMR spectrum for nitrodiester

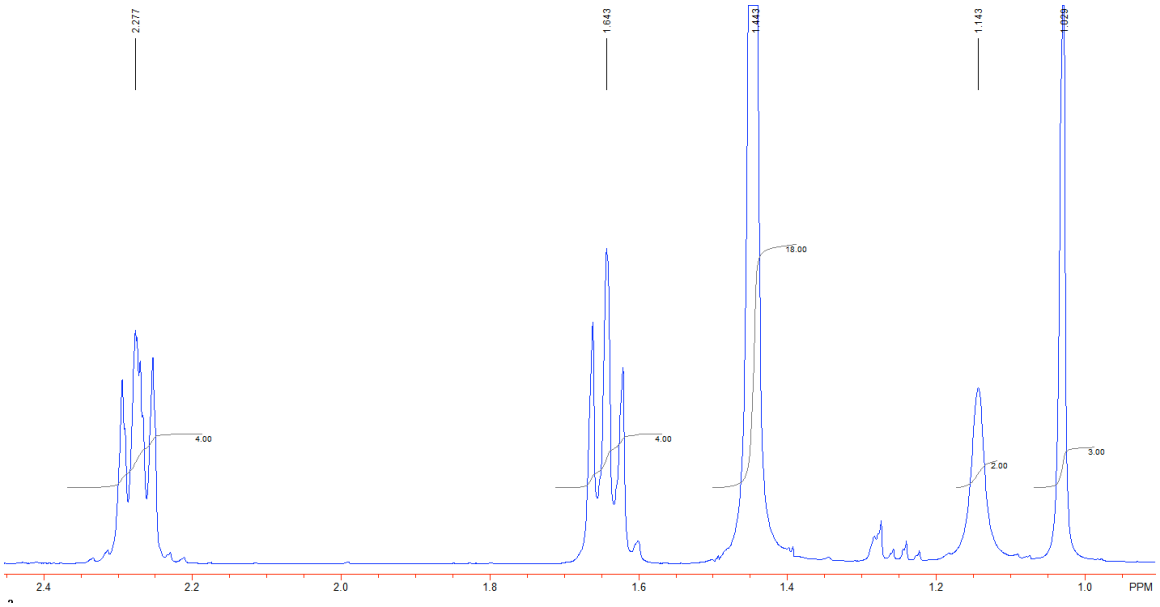

Figure 2.4 ^{1}H NMR spectrum for aminodiester

In the isocyanatediester, the $\Delta\nu^{vic}$ between methylene groups, $\Delta\nu^{vic}/J$, is very large. Thus, it gives simpler spectrum than that of the nitrodiester. With respect to $\Delta\nu^{gem}/J$ for geminal coupling in the isocyanatediester (Figure 2.5), the value is larger for

the ß methylene group, which appears as an overlapping ddd pattern, than the α methylene group, which appears as a triplet.

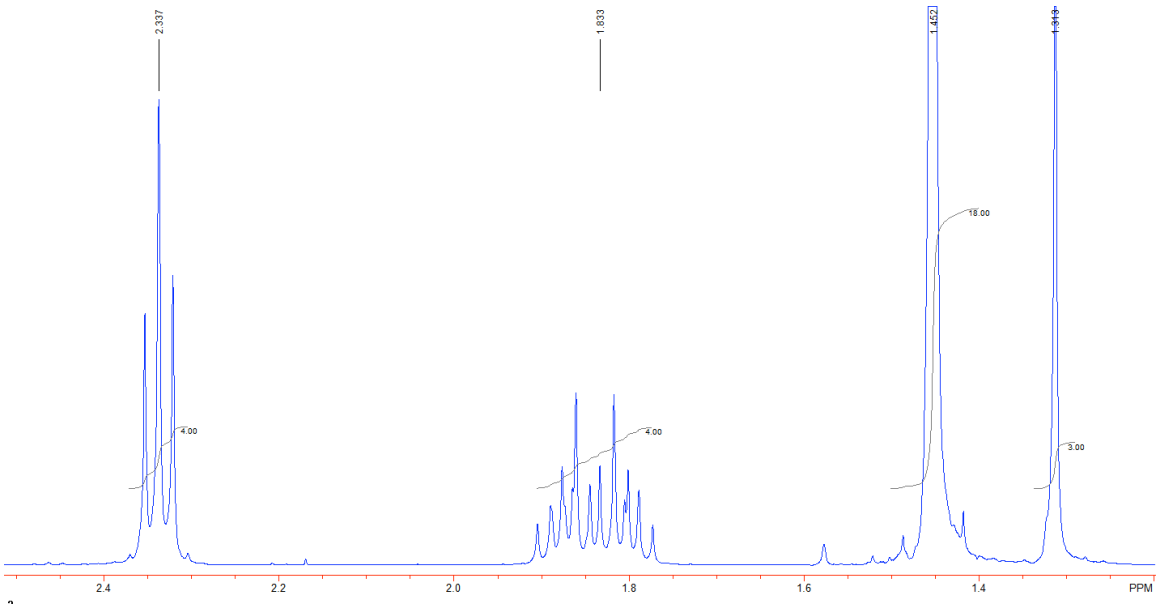

Figure 2.5 ^{1}H NMR spectrum for isocyanatediester

The ^{1}H NMR spectra of **2ECbn** (Figure 2.6) and **2CCbn** (Figure 2.7) series are simpler than the others. The $\Delta\nu^{vic}$ between methylene groups is very large. With respect to $\Delta\nu^{gem}/J$ for geminal coupling (Figure 2.6, 2.7), the value is small for the α methylene group and very large for the ß methylene group, which appear as two separate triplets of doublets.

In conclusion, these compounds were made successfully, and they were very sensitive to NMR. The methylene protons showed different splitting behavior under NMR.

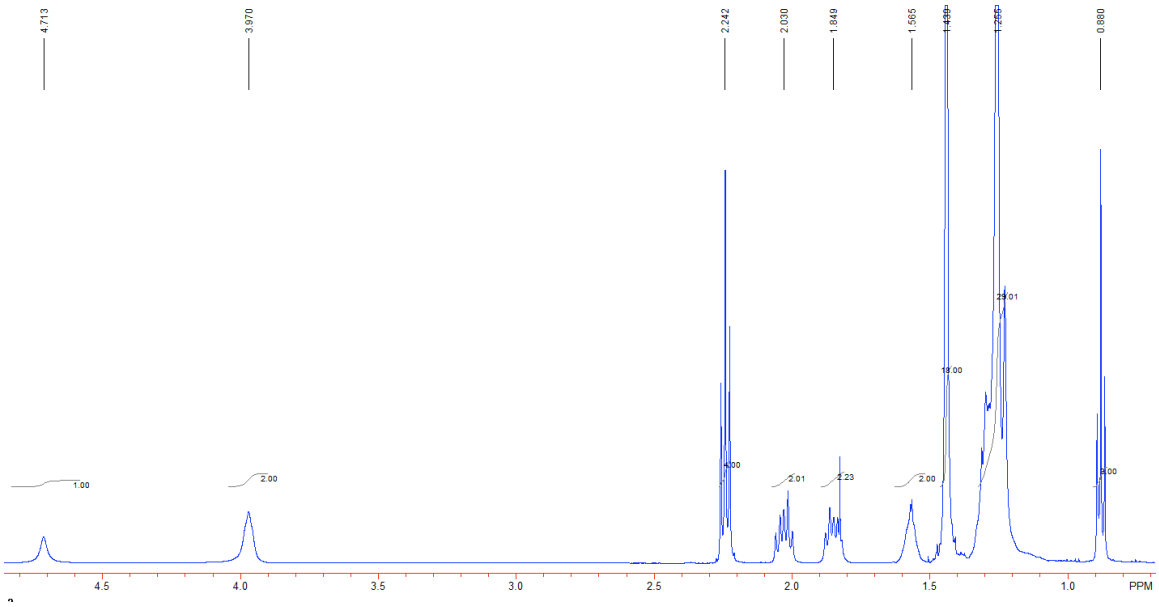

Figure 2.6 ^{1}H NMR spectrum for diester (**2ECbn**) series

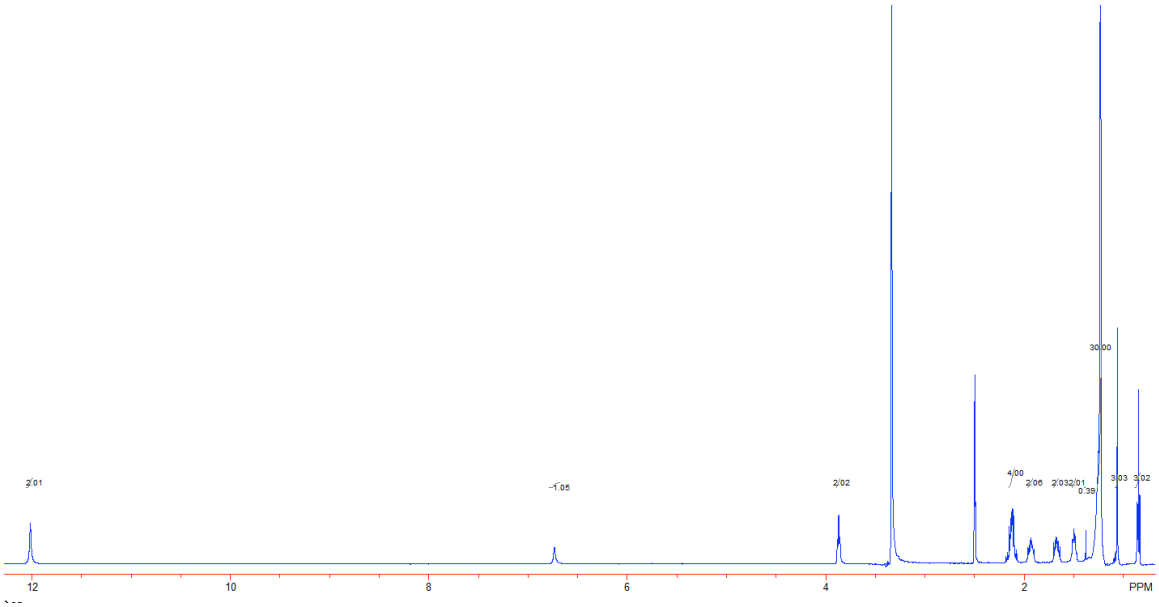

Figure 2.7 ^{1}H NMR spectrum for diacid (**2CCbn**) series

2.9 Experimental Sections

2.9.1 General Procedures for Synthetic Work

All solvents and reagents were used as received. Analytical thin layer chromatography was performed on plastic-coated silica gel 60 Å. Dipping the TLC plates

into a phosphomolybdic acid (PMA) reagent in a 5% ethanol (20 wt % solution in ethanol) followed by heating with a heat gun was used to visualize the spots. The R_f value for a given **2ECbn** and **2CCbn** ranged from 0.3–0.5; the compounds were eluted in the different solvent mixtures (see below for details). Preparative flash column chromatography was carried out on silica gel (60 Å). All solutions were concentrated by rotary evaporation. Melting points were determined in open capillary tubes at 1 °C/min and were uncorrected. NMR spectra of all compounds were recorded at 400 or 500 MHz for ^{1}H and 100.6 or 125.8 MHz for ^{13}C, respectively, and reported in ppm relative to TMS in $CDCl_3$, THF, and DMSO (2.54 δ for ^{1}H and 40.45 δ for ^{13}C) in DMSO. IR spectra were recorded on neat samples with a Fourier Transform IR (FTIR) equipped with a diamond attenuated total reflectance (ATR) system, and reported in cm^{-1}. The high-resolution mass spectrometric (HRMS) data were obtained on the Agilent 6220 series Accurate-MASS Time-of-Flight (TOF) LC/MS operating under electrospray ionization (ESI) or atmospheric pressure chemical ionization (APCI). Elemental analyses were performed by a commercial vendor.

2.9.2 Experimental Procedure for Synthesis of Di-*tert*-butyl 4-Methyl-4-nitroheptanedioate, Nitrodiester (1).

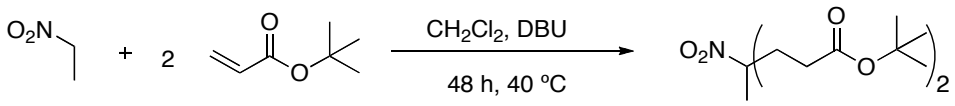

Nitroethane (1.01 g, 13.3 mmol) and *tert*-butyl acrylate (3.50 g, 27.3 mmol) were dissolved in CH_2Cl_2 (13 mL) and heated at 40 °C. To this colorless solution, DBU (0.100 mL, 0.67 mmol) was added in 0.025-mL portion every 10 min. The brown solution was stirred for 24 h; after 6 h the solution turned yellow and then green the following

morning. The solution was allowed to sit for 24 h without heating and stirring. The green solution was concentrated at 30 °C to form a green solid, which was dried under high vacuum for 24 h (4.30 g, 97%). Eluting with 97.5:2.5 (v/v) $CHCl_3$:EtOAc, the TLC showed two spots with R_f values 0.63 and 0.26. The green solid (2.13 g) was purified by flash column chromatography—6.5 cm ID column, 97.5:2.5 (v/v) $CHCl_3$/EtOAc, silica gel (40.30 g)—to produce a white solid (1.66 g, 5.0 mmol, 78% yield): mp 52.6–53.0 °C (lit.[1] 46–47 °C); ^{1}H NMR (400 MHz, $CDCl_3$, δ): 1.44 (s, 18H), 1.53 (s, 3H), 2.05–2.38 (m, 8H) (lit.[1] 250 MHz); ^{13}C NMR (125.8 MHz, $CDCl_3$, δ): 22.0, 28.3, 30.4, 34.6, 81.3, 90.2, 171.6; IR: 2981, 1722, 1533, 1160 cm^{-1}. HRMS–ESI (*m*/*z*): $[M + Na]^+$ calcd for $C_{16}H_{29}O_6NNa$, 354.1887; found, 354.1889.

2.9.3 Experimental Procedure for Synthesis of Di-*tert*-butyl 4-Amino-4-methylheptanedioate, Aminodiester (2)

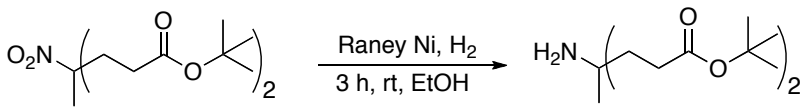

An aqueous slurry of Raney Ni (~ 11 g, Raney® 2800 nickel, slurry in H_2O) was placed in a hydrogenation flask; excess H_2O was removed by pipette to give a final weight of 10.290 g (~78 mmol of Ni, presuming 50% H_2O and 89% Ni). To the wet catalyst, nitrodiester (**1**)(8.368 g, 25.25 mmol) in 95% EtOH (160 mL) was added. The reaction mixture was shaken in a sealed container under H_2 (52.5 psi) for 3 h at 25 °C. The mixture was filtered cautiously through Celite® under continuous flow of N_2 to remove the catalyst. The clear filtrate was concentrated at rt and dried under high vacuum for 48 h to give white solid (7.25 g, 95%): mp 36.3–37.0 °C, lit.[1] as a white oil; ^{1}H NMR (400 MHz, $CDCl_3$, δ): 1.03 (s, 3H), 1.142 (s, 2H), 1.44 (s, 18H), 1.64 (m, 4H), 2.27 (m,

4H), lit.[1] 250 MHz; ^{13}C NMR (100.6 MHz, $CDCl_3$, δ): 27.1, 28.0, 30.4, 37.4, 50.7, 80.3, 173.2; IR: 2977.93, 1725, 1249, 1160 cm^{-1}; HRMS–ESI (*m*/*z*): $[M + H]^+$ calcd for $C_{16}H_{32}O_4N$, 302.2326; found, 302.2334.

2.9.4 Experimental Procedure for Synthesis of Di-*tert*-butyl 4-Isocyanato-4-methylheptanedioate, Isocyanatediester (3)

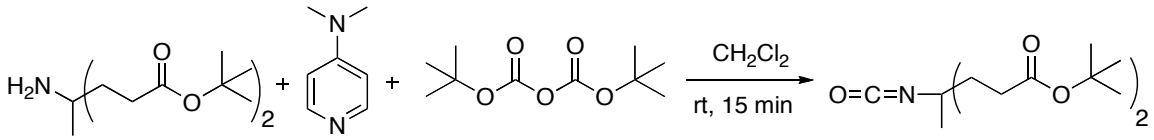

A solution of aminodiester (**2**) (0.550 g, 1.80 mmol) and DMAP (0.216 g, 1.80 mmol) in CH_2Cl_2 (20 mL) were mixed with a solution of $(Boc)_2O$ (0.390 g, 1.80 mmol) in CH_2Cl_2 (10 mL). This mixture was stirred for total 15 min. at rt. TLCs, eluting with 50:50 (v/v) hexane/EtOAc, were run to check for completion of reaction. Upon completion of reaction, TLC showed three spots with R_f values of 0.64, 0.53, and 0.03. The solution was washed with 10% HCl (5 mL) and deionized H_2O (5 mL). The organic solution was dried overnight with $MgSO_4$. The filtrate was concentrated at rt and placed under high vacuum pump for overnight to get colorless viscous liquid (0.51 g, 85%). TLC showed two spots with R_f values 0.64 and 0.53. Several reactions on larger scale were run by this method.

In order to purify the sample further, additional TLCs were run to find the better separation. Eluting with 90:10 (v/v) hexane/EtOAc showed two spots with R_f values of 0.24 and 0.00. Colorless viscous liquid (27.67 g) was purified by flash column chromatography—4.0 cm ID, silica gel (160.43 g), 90:10 (v/v) hexane/EtOAc, fraction size (50 mL), collecting and concentrating fractions 10 through 18—to produce a colorless viscous liquid (22.07 g, 79%). ^{1}H NMR (500 MHz, $CDCl_3$, δ): 1.31 (s, 3H),

1.45 (s, 18H), 1.75–1.95 (m, 4H), 2.33 (m, 4H); ^{13}C NMR (125.8 MHz, $CDCl_3$, δ): 27.6, 28.3, 30.8, 37.1, 60.1, 80.9, 122.8, 172.4; IR: 2979, 2256, 1728, 1160 cm^{-1}; HRMS–APCI (*m*/*z*): calcd for $C_{17}H_{29}O_5N$, 327.2046; found 325.1794. Anal. Calcd for $C_{17}H_{29}O_5N$: C, 62.36; H, 8.93; N, 4.28. Found: C, 62.59; H, 8.95; N, 4.35.

2.9.5 Experimental Procedure for Synthesis of Di-*tert*-butyl 4-(Hexadecyloxycarbonylamino)-4-methylheptanedioate, 2ECb16

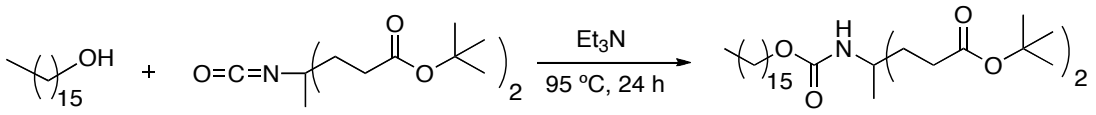

Isocyanatediester (**3**) (1.73 g, 5.28 mmol) and hexadecan-1-ol (99%) (1.28 g, 5.27 mmol) were dissolved in Et_3N (8 mL). The clear solution was refluxed in an oil bath at 95 °C for 24 h. The pale yellow solution was concentrated; diethyl ether (150 mL) was added and the solution was concentrated to get a viscous liquid (3.05 g, 100%). Eluting with 6:2.5:2.5 (v/v/v) hexane/Et_2O/MeOH, the TLC showed three spots with R_f values 0.52, 0.24, and 0.08. The liquid (3.05 g) was purified by flash column chromatography—4.2 cm ID, silica gel (125.03 g), 6:2.5:2.5 (v/v/v) hexane/Et_2O/MeOH, fraction size (20 mL), collecting and concentrating fractions 12 through 27—to give a clear viscous liquid (2.63 g, 86%), which solidified when placed in freezer (–20 °C). The melting range, mp 20–23 °C, was determined by attaching a capillary of frozen liquid to a thermometer and then placed in the reservoir of a circulating water bath. ^{1}H NMR (500 MHz, $CDCl_3$, δ): 0.88 (t, 3H), 1.26 (m, 29H), 1.44 (s, 18H), 1.57 (m, 2H), 1.85 (m, 2H), 2.03 (m, 2H), 2.24 (t, 4H), 3.97 (s, 2H), 4.71 (s, 1H); ^{13}C NMR (125.8 MHz, $CDCl_3$, δ): 14.4, 23.0, 24.1, 26.2, 28.4, 29.3, 29.63, 29.67, 29.87, 29.91, 29.97, 29.99, 30.01, 30.6, 32.2, 34.0, 54.6, 64.8, 80.7, 155.2, 173.2; IR: 3377, 2924, 2854, 1730, 1694, 1524, 1160 cm^{-1}; HRMS–ESI

(*m*/*z*): $[M + Na]^+$ calcd for $C_{33}H_{63}O_6NNa$, 592.4548; found 592.4540. Anal. Calcd for $C_{33}H_{63}O_6N$: C, 69.55; H, 11.14; N, 2.46. Found: C, 69.58; H, 11.10; N, 2.53.

2.9.6 Experimental Procedure for Synthesis of Di-*tert*-butyl 4-(Octadecyloxycarbonylamino)-4-methylheptanedioate, 2ECb18

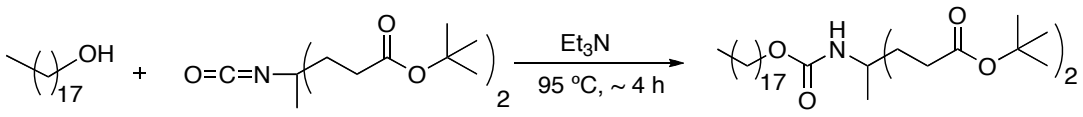

Isocyanatediester (**3**) (1.56 g, 4.96 mmol) and octadecan-1-ol (1.42 g, 5.25 mmol) were dissolved in Et_3N (4.2 mL). The clear solution was refluxed in an oil bath at 95 °C for ~ 4 h. After cooling, Et_2O (50 mL) was added. The organic solution was washed with 2 M HCl (3×10 mL), saturated $NaHCO_3$ (3×10 mL), and saturated NaCl (30 mL). The solution was dried with $MgSO_4$ for overnight. The organic solution was concentrated to give colorless viscous liquid (2.67 g, 94 %). Eluting with 10:2:1 (v/v/v) hexane/EtOAc/MeOH, the TLC showed three spots with R_f values of 0.66, 0.34, and 0.14. The viscous liquid (2.50 g) was purified by flash column chromatography—1.5 cm ID, 6″ height, silica gel (11.32 g), 10:2:1 (v/v/v) hexane/EtOAc/MeOH, fraction size (5 mL), collecting and concentrating fractions 1 through 6—to give, after concentrating and drying under high vacuum, a viscous liquid (2.47 g). This procedure did not give complete separation as the desired compound and impurities appeared in fractions 7–16. A sample (0.69 g) was purified again—2.4 cm ID, 1.5″ height, silica gel (7 g), 11:5 (v/v) hexane/CH_2Cl_2, fraction size (5 mL)—to give, after concentration and drying under high vacuum, a viscous liquid (0.61 g). Eluting with 6:2.5:2.5 (v/v/v) hexane/Et_2O/MeOH, the TLC showed two spots with R_f values of 0.39 and 0.18. A viscous liquid (0.61 g) was purified by—4.2 cm ID, 5″ height, silica gel (70.12 g), 6:2.5:2.5 (v/v)

hexane/Et_2O/MeOH, fraction size (30 mL), collecting and concentrating fractions 13 through 26—to give clear viscous liquid (0.59 g, 97%). Extended (4 d) drying under high vacuum gave a white solid: mp 33.4–34.0 °C; ^{1}H NMR (500 MHz, $CDCl_3$, δ): 0.88 (t, 3H), 1.25 (m, 33H), 1.44 (s, 18H), 1.57 (m, 2H), 1.85 (m, 2H), 2.03 (m, 2H), 2.24 (t, 4H), 3.97 (s, 2H), 4.68 (s, 1H); ^{13}C NMR (125.8 MHz, $CDCl_3$, δ): 14.5, 23.0, 24.2, 26.3, 28.4, 29.4, 29.67, 29.71, 29.90, 29.95, 30.00, 30.03, 30.05, 30.6, 32.3, 34.0, 54.6, 64.8, 80.8, 155.3, 173.3; IR: 3344, 2919, 2849, 1726, 1691, 1532, 1255, 1160 cm^{-1}; HRMS–ESI (*m*/*z*): $[M + H]^+$ (*m*/*z*): calcd for $C_{35}H_{68}O_6N$, 598.5041; found 598.5043. Anal. Calcd for $C_{35}H_{67}O_6N$: C, 70.31; H, 11.29; N, 2.34. Found: C, 70.26; H, 11.28; N, 2.32.

2.9.7 Experimental Procedure for Synthesis of Di-*tert*-butyl 4-(Icosyloxycarbonylamino)-4-methylheptanedioate, 2ECb20

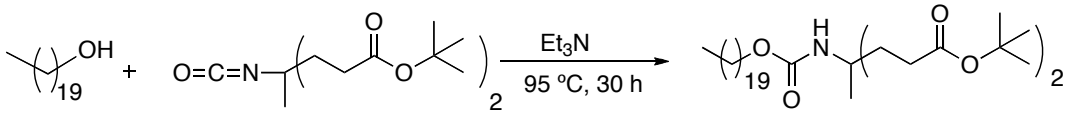

Isocyanatediester (**3**) (2.02 g, 6.14 mmol) and icosan-1-ol (96%) (1.91 g, 6.38 mmol) were dissolved in Et_3N (6.5 mL). The clear solution was refluxed in an oil bath at 95 °C for 30 h. After cooling, Et_2O (100 mL) was added. The organic solution was washed with 2.0 M HCl (2×10 mL), saturated $NaHCO_3$ (10 mL), and saturated NaCl (10 mL). The solution was dried with $MgSO_4$ for overnight. The organic solution was concentrated to give a white solid (3.65 g, 95%). Eluting with 6:5:5 (v/v/v) hexane/Et_2O/MeOH, the TLC showed two spots with R_f values of 0.19 and 0.09. The white solid (3.65 g) was purified by flash column chromatography—4.0 cm ID, 7″ height, silica gel (102.59 g), 6:5:5 (v/v/v) hexane/Et_2O/MeOH, fraction size (20 mL), collecting and concentrating fractions 6 through 24—to get (2.56 g, 70%) pure product: mp 37.6–

38.0 °C; ^{1}H NMR (500 MHz, $CDCl_3$, δ): 0.88 (t, 3H), 1.25 (m, 37H), 1.44 (s, 18H), 1.57 (m, 2H), 1.85 (m, 2H), 2.03 (m, 2H), 2.24 (t, 4H), 3.97 (s, 2H), 4.68 (s, 1H); ^{13}C NMR (125.8 MHz, $CDCl_3$, δ): 14.5, 23.0, 24.2, 26.3, 28.4, 29.4, 29.68, 29.71, 29.91, 29.95, 30.00, 30.01, 30.04, 30.05, 30.6, 32.3, 34.0, 54.6, 64.8, 80.8, 155.3, 173.2; IR: 3340, 2918, 2849, 1727, 1692, 1532, 1254, 1160 cm^{-1}; HRMS–ESI (*m*/*z*): $[M + Na]^+$ calcd for $C_{37}H_{71}O_6NNa$, 648.5174; found 648.5154. Anal. Calcd for $C_{37}H_{71}O_6N$: C, 70.99; H, 11.43; N, 2.24. Found: C, 70.99; H, 11.20; N, 2.21.

2.9.8 Experimental Procedure for Synthesis of Di-*tert*-butyl 4-(Docosyloxycarbonylamino)-4-methylheptanedioate, 2ECb22

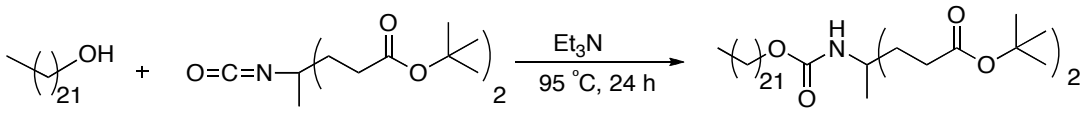

Isocyanatediester (**3**) (2.33 g, 7.10 mmol) and docosan-1-ol (2.37 g, 7.20 mmol) were dissolved in Et_3N (12 mL). The clear solution was refluxed in an oil bath at 95 °C for 24 h. After cooling, Et_2O (200 mL) was added. The organic solution was concentrated to give a white solid (4.89 g, 100%). Eluting with 6:2.5:2.5 (v/v/v) hexane/Et_2O/MeOH, the TLC showed two spots with R_f values 0.22 and 0.12. The white solid (4.89 g) was purified by flash column chromatography—4.2 cm ID, 8.5″ height, silica gel (127.58 g), 6:2.5:2.5 (v/v/v) hexane/Et_2O/MeOH, fraction size (10 mL), collecting and concentrating fractions 12 through 24—to give clear white solid (4.29 g, 88%): mp 48.7–49.0 °C; ^{1}H NMR (500 MHz, $CDCl_3$, δ): 0.88 (t, 3H), 1.25 (m, 41H), 1.44 (s, 18H), 1.58 (m, 2H), 1.85 (m, 2H), 2.03 (m, 2H), 2.24 (t, 4H), 3.97 (s, 2H), 4.68 (s, 1H); ^{13}C NMR (100.6 MHz, $CDCl_3$, δ): 14.5, 23.0, 24.2, 26.3, 28.4, 29.4, 29.68, 29.71, 29.91, 29.95, 30.01, 30.05, 30.6, 32.3, 34.0, 54.6, 64.8, 80.8, 155.4, 173.2; IR: 3346, 2910, 2849, 1723, 1690,

1531, 1160 cm^{-1}; HRMS–ESI (*m*/*z*): $[M + Na]^+$ calcd for $C_{39}H_{75}O_6NNa$, 676.5487; found 676.5466. Anal. Calcd for $C_{39}H_{75}O_6N$: C, 71.62; H, 11.56; N, 2.14. Found: C, 71.56; H, 11.75; N, 2.16.

2.9.9 Experimental Procedure for Synthesis of Di-*tert*-butyl 4-(Triacontyloxycarbonylamino)-4-methylheptanedioate, 2ECb30

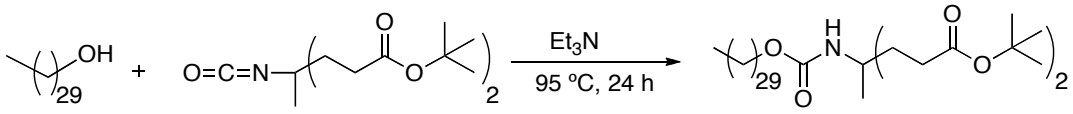

Isocyanatediester (**3**) (0.20 g, 0.61 mmol) and triacontan-1-ol (99%) (0.23 g, 0.53 mmol) were dissolved in Et_3N (9 mL). The clear solution was refluxed in an oil bath at 95 °C for 24 h. After cooling, Et_2O (100 mL) was added. The organic solution was concentrated to give a white solid (0.45 g, 100%). The white solid (0.45 g) was purified by flash column chromatography—4.2 cm ID, 4″ height, silica gel (71.48 g), 6:2.5:2.5 (v/v/v) hexane/Et_2O/MeOH, fraction size (10 mL), collecting and concentrating fractions 27 through 48—to get clear white solid (0.22 g, 49%): mp 57.5–57.9 °C; ^{1}H NMR (400 MHz, $CDCl_3$, δ): 0.88 (t, 3H), 1.25 (m, 57H), 1.44 (s, 18H), 1.57 (m, 2H), 1.85 (m, 2H), 2.03 (m, 2H), 2.24 (t, 4H), 3.97 (s, 2H), 4.68 (s, 1H); ^{13}C NMR (100.6 MHz, $CDCl_3$, δ): 14.1, 22.7, 23.9, 25.9, 28.1, 29.01, 29.34, 29.38, 29.58, 29.63, 29.67, 29.69, 29.70, 30.3, 32.0, 33.7, 54.3, 64.5, 80.5, 154.9, 172.9; IR: 3350, ~2900, 2848, 1725, 1525, 1147 cm^{-1}; HRMS–APCI (*m*/*z*): $[M + H]^+$ calcd for $C_{47}H_{92}O_6N$, 766.6919; found 766.6937. Anal. Calcd for $C_{47}H_{91}O_6N$: C, 73.67; H, 11.97; N, 1.83. Found: C, 73.77; H, 12.03; N, 1.82.

2.9.10 Experimental Procedure for Synthesis of Di-*tert*-butyl 4-(((3*S*,5*S*,8*R*,9*S*,10*S*,13*R*,14*S*,17*R*)-10,13-Dimethyl-17-((*R*)-6-methylheptan-2-yl)hexadecahydro-1*H*-cyclopenta[*a*]phenanthren-3-yloxy)carbonylamino)-4-methylheptanedioate, 2ECb5α-cholestan-3β-ol

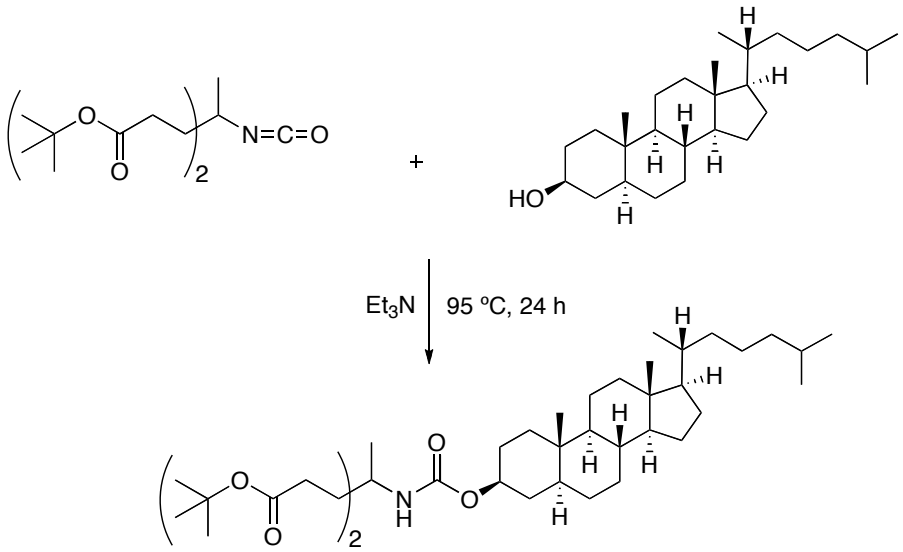

Isocyanatediester (**3**) (0.96 g, 2.93 mmol) and 5α-cholestan-3β-ol (1.00 g, 2.60 mmol) were dissolved in Et_3N (6 mL). The clear solution was refluxed in an oil bath at 95 °C for 24 h. After cooling, Et_2O (200 mL) was added. The organic solution was concentrated to get a white solid (2.08 g, 100%). Eluting with 6:2.5:2.5 (v/v/v) hexane/Et_2O/MeOH, the TLC showed two spots with R_f values of 0.16 and 0.07. The white solid (2.08 g) was purified by flash column chromatography—4.2 cm ID, 6″ height, silica gel (105.06 g), 6:2.5:2.5 (v/v/v) hexane/Et_2O/MeOH, fraction size (10 mL), collecting and concentrating fractions 43 through 77—to give white solid (1.28 g, 61%): mp 129.8–130.0 °C; ^{1}H NMR (400 MHz, $CDCl_3$, δ): 0.5–2.4 (m, 75H), 4.55 (m, 2H); ^{13}C NMR (100.6 MHz, $CDCl_3$, δ): 12.42, 12.58, 19.0, 21.5, 22.9, 23.2, 24.2, 24.6, 28.2, 28.36, 28.43, 28.6, 29.0, 30.7, 32.3, 34.1, 34.7, 35.78, 35.83, 36.15, 36.51, 37.1, 39.9,

40.4, 42.9, 45.0, 54.54, 54.65, 56.60, 56.75, 80.8, 155.3, 173.2; IR: 3349, ~2900, 2848, 1725, 1525, 1149 cm^{-1}; HRMS–ESI (*m*/*z*): $[M + Na]^+$ calcd for $C_{44}H_{77}O_6NNa$, 738.5643; found 738.5639. Anal. Calcd for $C_{44}H_{77}O_6N$: C, 73.80; H, 10.84; N, 1.96. Found: C, 73.89; H, 10.98; N, 1.98.

2.9.11 Experimental Procedure for Synthesis of 4-(Hexadecyloxycarbonylamino)-4-methylheptanedioic acid, 2CCb16

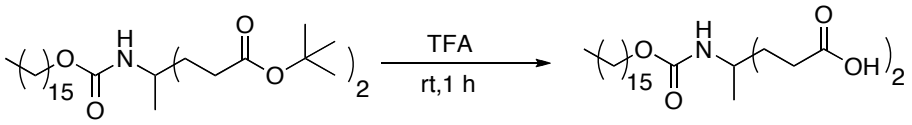

Diester **2ECb16** (0.600 g, 1.10 mmol) was dissolved in TFA (1.2 mL) and stirred at rt for 1 h. The solution was concentrated at 70 °C to give a viscous liquid. This liquid was dissolved in CH_2Cl_2 (20 mL), and the solution was concentrated; this process was repeated nine times to chase all traces of TFA to finally give a white solid. This solid was kept under high vacuum for 1 week to give a white solid (0.51 g, 100%): mp 100.0–100.5 °C; ^{1}H NMR (500 MHz, DMSO-d_6, δ): 0.89 (t, 3H), 1.10 (s, 3H), 1.27 (s, 26H), 1.54 (m, 2H), 1.71 (m, 2H), 1.97 (m, 2H), 2.16 (m, 4H), 3.91 (t, 2H), 6.78 (s, 1H), 12.06 (s, 2H); ^{13}C NMR (100.6 MHz, DMSO-d_6, δ): 14.9, 23.0, 24.2, 26.3, 29.59, 29.66, 29.928, 29.934, 29.961, 29.995, 32.3, 34.0, 54.2, 64.0, 155.8, 175.6; IR: 3425, 3177, 2915, 2847, 1725, 1671, 1518, 1202 cm^{-1}; HRMS–ESI (*m*/*z*): $[M + Na]^+$ calcd for $C_{25}H_{32}O_6NNa$, 480.3296; found 480.3300. Anal. Calcd for $C_{25}H_{32}O_6N$: C, 65.61; H, 10.35; N, 3.06. Found: C, 65.48; H, 10.28; N, 2.98.

2.9.12 Experimental Procedure for Synthesis of 4-(Octadecyloxycarbonylamino)-4-methylheptanedioic acid, 2CCb18

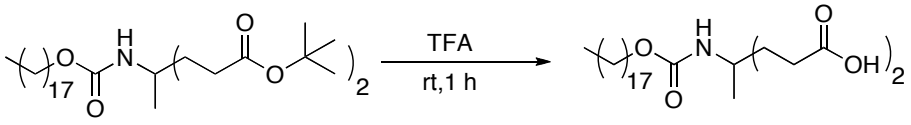

Diester **2ECb18** (0.52 g, 0.80 mmol) was dissolved in TFA (1.2 mL) and stirred at rt for 1 h. The solution was concentrated at 70 °C to give a viscous liquid. This liquid was dissolved in CH_2Cl_2 (20 mL), and the solution was concentrated; this process was repeated nine times to chase all traces of TFA to finally give a white solid. This solid was kept under high vacuum for 1 week to give a white solid (0.40 g, 95%): mp 102.6–102.8 °C; ^{1}H NMR (500 MHz, DMSO-d_6, δ): 0.89 (t, 3H), 1.10 (s, 3H), 1.27 (s, 30H), 1.54 (m, 2H), 1.72 (m, 2H), 1.98 (m, 2H), 2.16 (m, 4H), 3.91 (t, 2H), 6.78 (s, 1H), 12.06 (s, 2H); ^{13}C NMR (100.6 MHz, DMSO-d_6, δ): 14.6, 22.8, 23.8, 26.0, 29.28, 29.36, 29.37, 29.63, 29.64, 29.66, 29.68, 32.0, 33.6, 53.9, 63.7, 155.4, 175.3; IR: 3424, 3181, ~2900, 2847, 1725, 1673, 1519, 1228 cm^{-1}; HRMS–ESI (m/z): $[M + H]^+$ calcd for $C_{27}H_{37}O_6N$, 486.3789; found 486.3783. Anal. Calcd for $C_{27}H_{36}O_6N$: C, 66.77; H, 10.58; N, 2.88. Found: C, 67.04; H, 10.57; N, 2.83.

2.9.13 Experimental Procedure for Synthesis of 4-(Icosyloxycarbonylamino)-4-methylheptanedioic acid, **2CCb20**

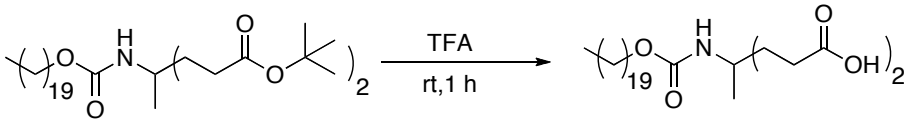

Diester **2ECb20** (1.96 g, 3.10 mmol) in TFA (3.6 mL), and stirred at rt for 1 h. The solution was concentrated at 70 °C to give a viscous liquid. This liquid was dissolved in CH_2Cl_2 (20 mL), and the solution was concentrated; this process was repeated nine

times to chase all traces of TFA to finally give a white solid. This solid was kept under high vacuum for 1 week to give a white solid (1.55 g, 97%): mp 100.6–101.1 °C; ^{1}H NMR (500 MHz, DMSO-d_6, δ): 0.89 (t, 3H), 1.10 (s, 3H), 1.27 (s, 34H), 1.54 (m, 2H), 1.72 (m, 2H), 1.98 (m, 2H), 2.16 (m, 4H), 3.91 (t, 2H), 6.77 (s, 1H), 12.06 (s, 2H); ^{13}C NMR (100.6 MHz, DMSO-d_6, δ): 14.9, 23.1, 24.2, 26.4, 28.7, 29.58, 29.680, 29.688, 29.981, 29.999, 32.9, 34.0, 54.3, 64.1, 155.7, 175.6; IR: 3425, ~2900, 2847, 1725, 1673, 1520, 1228 cm^{-1}; HRMS–ESI (*m*/*z*): $[M + H]^+$ calcd for $C_{29}H_{41}O_6N$, 514.4102; found 514.4099. Anal. Calcd for $C_{29}H_{40}O_6N$: C, 67.80; H, 10.79; N, 2.73. Found: C, 67.99; H, 10.60; N, 2.71.

2.9.14 Experimental Procedure for Synthesis of 4-(Docosyloxycarbonylamino)-4-methylheptanedioic acid, **2CCb22**

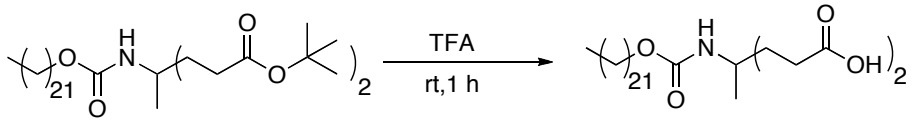

Diester **2ECb22** (4.16 g, 6.40 mmol) in TFA (7 mL), and stirred at rt for 1 h. The solution was concentrated at 70 °C to give a viscous liquid. This liquid was dissolved in CH_2Cl_2 (20 mL), and the solution was concentrated; this process was repeated nine times to chase all traces of TFA to finally give a white solid. This solid was kept under high vacuum for 1 week to give a white solid (3.44 g, 100%): mp 107.8–108.2 °C; ^{1}H NMR (500 MHz, DMSO-d_6, δ): 0.89 (t, 3H), 1.10 (s, 3H), 1.27 (s, 38H), 1.54 (m, 2H), 1.72 (m, 2H), 1.98 (m, 2H), 2.16 (m, 4H), 3.91 (t, 2H), 6.78 (s, 1H), 12.06 (s, 2H); ^{13}C NMR (125.8 MHz, DMSO-d_6, δ): 14.9, 23.0, 24.2, 26.3, 29.57, 29.65, 29.67, 29.94, 29.95, 29.96, 29.98, 32.2, 34.0, 54.2, 64.0, 65.9, 155.6, 175.6; IR: 3424, ~2900, 2847, 1725, 1673, 1520, 1229 cm^{-1}; HRMS–ESI (*m*/*z*): $[M + Na]^+$ calcd for $C_{31}H_{44}O_6NNa$, 564.4235;

found 564.4246. Anal. Calcd for $C_{31}H_{44}O_6N$: C, 68.72; H, 10.98; N, 2.59. Found: C, 68.58; H, 10.95; N, 2.54.

2.9.15 Experimental Procedure for Synthesis of 4-(Triacontyloxycarbonylamino)-4-methylheptanedioic acid, 2CCb30

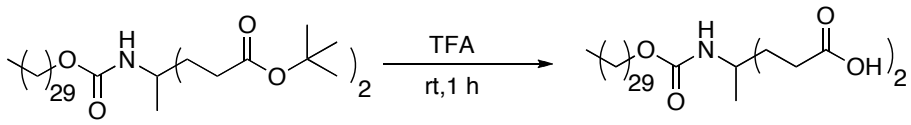

Diester **2ECb30** (0.19 g, 0.25 mmol) in TFA (2 mL), and stirred at rt for 1 h. The solution was concentrated at 70 °C to give a viscous liquid. This liquid was dissolved in CH_2Cl_2 (20 mL), and the solution was concentrated; this process was repeated nine times to chase all traces of TFA to finally give a white solid. This solid was kept under high vacuum for 1 week to give a white solid (0.16 g, 96%): mp 112.8–113.0 °C; ^{1}H NMR (400 MHz, THF-d_4, δ): 0.85 (t, 3H), 1.14 (s, 3H), 1.25 (s, 54H), 1.52 (m, 2H), 1.80 (m, 2H), 2.00 (m, 2H), 2.18 (m, 4H), 3.88 (t, 2H), 5.92 (s, 1H), 10.55 (s, 2H); ^{13}C NMR (125.8 MHz, THF-d_4, δ): 15.1, 24.3, 24.7, 25.71, 25.87, 26.03, 26.19, 26.35, 26.52, 27.7, 29.8, 30.9, 31.01, 31.07, 31.35, 33.6, 35.0, 55.1, 65.0, 156.4, 175.4; IR: 3425, ~2900, 2848, 1706, 1523, 1230 cm^{-1}; HRMS–APCI (*m*/*z*): $[M + H]^+$ calcd for $C_{39}H_{76}O_6N$, 654.5667; found 654.5726. Anal. Calcd for $C_{39}H_{75}O_6N$: C, 71.62; H, 11.56; N, 2.14. Found: C, 71.34; H, 11.63; N, 2.12.

2.9.16 Experimental Procedure for Synthesis of 4-(((3*S*,5*S*,8*R*,9*S*,10*S*,13*R*,14*S*,17*R*)-10,13-Dimethyl-17-((*R*)-6-methylheptan-2-yl)hexadecahydro-1*H*-cyclopenta[*a*]phenanthren-3-yloxy)carbonylamino)-4-methylheptanedioic acid, 2CCb5α-cholestan-3β-ol

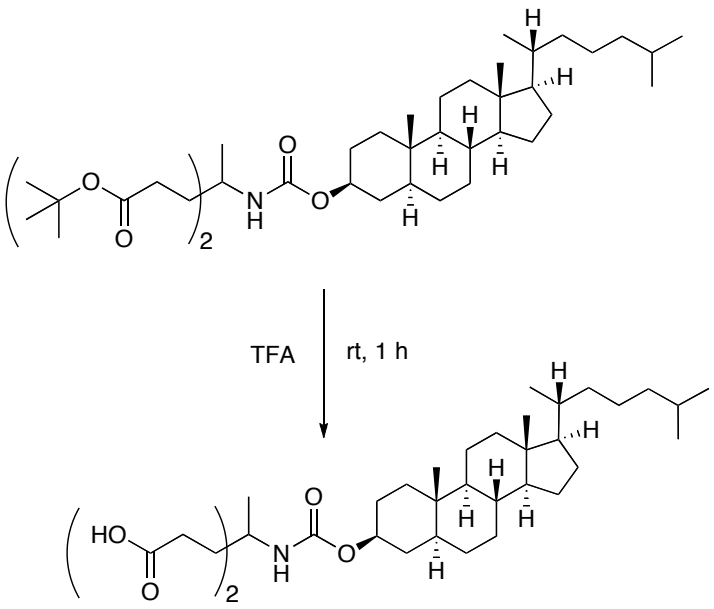

Diester **2ECb5α-cholestan-3β-ol** (1.28 g, 1.70 mmol) in TFA (2.5 mL), and stirred at rt for 1 h. The solution was concentrated at 70 °C to give a viscous liquid. This liquid was dissolved in CH_2Cl_2 (20 mL), and the solution was concentrated; this process was repeated nine times to chase all traces of TFA to finally give a white solid. This solid was kept under high vacuum for 1 week to give a white solid (1.04 g, 97%): mp 188.4–189.4 °C; ^{1}H NMR (500 MHz, DMSO-d_6, δ): 0.66-2.16 (m, 57H), 4.42 (m, 1H), 6.73 (s, 1H), 12.07 (s, 2H); ^{13}C NMR (125.8 MHz, DMSO-d_6, δ): 12.82, 12.88, 15.0, 21.69, 21.71, 23.3, 23.6, 24.2, 24.7, 28.3, 28.5, 28.7, 29.1, 29.6, 32.5, 33.9, 35.1, 35.91, 35.94, 36.15, 36.6, 37.2, 43.1, 45.1, 54.26, 54.49, 56.67, 56.86, 60.7, 72.0, 73.0, 155.1, 175.6; IR: 3571, 3319, 2930, 2865, ~1700, 1675, 1464, 1416, 1087 cm^{-1}; HRMS–ESI (*m*/*z*): [M

+ H]$^+$ calcd for $C_{36}H_{62}O_6N$, 604.4572; found 604.4573. Anal. Calcd for $C_{36}H_{61}O_6N$: C, 71.60; H, 10.18; N, 2.32. Found: C, 71.79; H, 10.28; N, 2.36.

2.10 References for Chapter 2

1. Newkome, G. R., He, E., Godinez, L. A., Baker, G. R., Electroactive metallomacromolecules via Tetrabis (2, 2':6',2"-terpyridine) ruthenium (II) Complex, Dendritic Nanonetworks towards Constitutinal Isomers and Neutral Species withour External Counterions. *J. Am. Chem. Soc.* **2000,** *122*, 9993-10006.
2. Newkome, G. R., Kim, H. J., Moorfield, C. N., Maddi, H., Yoo, K., Synthesis of New 1→(2+1) C-Branched Monomers for the Construction of Multifunctional Dendrimers. *Macromolecules* **2003,** *36*, 4345–4354.
3. Newkome, G. R.; Behera, R. K.; Moorefield, C. N.; Baker, G. R., Chemistry of micelles. 18. Cascade polymers: syntheses and characterization of one-directional arborols based on adamantane. *J. Org. Chem.* **1991,** *56* (25), 7162–7167.
4. Actis, M. L. Synthesis, Characterization, Critical Micelle Concentration and Biological Acitivity of two-Headed Amphiphiles: Master of Science Thesis. Virginia Tech, Blacksburg, VA, November 6, 2008.
5. Tishkov, A. A.; Smirnov, V., O.; Nefed'eva, M. V.; Lyapkalo, I. M.; Semenov, S. E.; Ioffe, S. L.; Strelenko, Y. A.; Tartakovskii, V. A., General Synthesis γ-Functionalized ß-Aryl-Substituted Primary Nitro Compounds. *Russ. J. Org. Chem.* **2001,** *37* (3), 390–394.
6. Akpo, C.; Weber, E.; Reiche, J., Synthesis, Langmuir and Langmuir–Blodgett film behaviour of new dendritic amphiphiles. *New J. Chem.* **2006,** *30* (12), 1820–1833.
7. Newkome, G. R.; Weis, C. D.; Moorefield, C. N.; Fronczek, F. R., A useful dendritic building block: Di-*tert*-butyl 4-[(2-*tert*-butoxycarbonyl)ethyl]-4-isocyanato-1,7-heptanedicarboxylate. *Tetrahedron Lett.* **1997,** *38* (40), 7053–7056.
8. Newkome, G. R., Weis, C. D., Childs, B. J., Synthesis of 1→3 Branched Isocyanate Monomers for Dendritic Construction. *Des. Monomers Polym.* **1998,** *1*, 3–14.
9. Basel, Y.; Hassner, A., Di-*tert*-butyl Dicarbonate and 4-(Dimethylamino)pyridine Revisited. Their Reactions with Amines and Alcohols. *J. Org. Chem.* **2000,** *65* (20), 6368–6380.
10. Schwetlick K, N. R., Stebner F., 3 Fundamental mechanisms of base-catalyzed reactions of isocyanates with hydrogen-acidic compounds. *J. Chem. Soc., Perkin Trans. 2* **1994**, 599–608.
11. Ault, A., Test for Chemical Shift and Magnetic Equivalence in NMR. *J. Chem. Educ.* **1974,** *51* (11), 729–731.
12. Silverstein, R. M.; LaLonde, R. T., Chemical Shift Equivalence and Magnetic Equivalence in Conformationally Mobile Molecules. *J. Chem. Educ.* **1980,** *57* (5), 343–344.
13. ChemBioDraw *Ultra,1986–2007,ChemNMR ^{1}H Estimation*, 11.0.1; CambridgeSoft.
14. Silverstein, R. M.; Webster, F. X.; Kiemle, D., J., *SPECTROMETRIC IDENTIFICATION OF ORGANIC COMPOUNDS*. 7th ed.; John Wiley & Sons, Inc.: Hoboken, 2005; p 143–150.

Chapter 3: Critical Micelle Concentration (CMC) for the 2CCbn Series

3.1 Introduction to CMC

The CMCs of dendritic amphiphiles were measured by three different methods—a surface tension method method, a conductivity method, and a pyrene-base fluorescent probe method.[1] The CMCs of the **3CAmn**, and **3CUrn** were measured by all three methods; and the CMCs of the **3CCbn** series were measured by the surface tension and the fluorescence methods. Triethanolammonium was the counterion in both the surface tension method and fluorescence methods, while potassium was the counterion in the conductivity method. The counterion and pH affected the CMCs. The CMCs for three-headed amphiphiles were lower with the potassium counterion than the triethanolammonium counterion. In the conductivity method, the CMCs for the **3CAmn** series, decreased by an average of 12-fold, compared to the surface tension method. Similarly, the CMCs for the **3CUrn** series, decreased in ranges of 3- to 13-fold as the chain length increased. The fluorescence method gave a more accurate result than the surface tension method because the inflection point was clearer.

The CMCs of the **2CAmn** series were already measured by Marcelo Actis,[2] who used the surface tension method. The CMCs of all three-headed series were measured by the more accurate fluorescence method, the CMCs of the **2CCbn** and the **2CAmn** series are measured here similarly. Furthermore, the CMCs are measured at pH ~ 9.2 and 7.4; the latter is the pH of the antimicrobial assays. We expect the CMCs to be lower at this pH because the CMCs at pH 9.2 and 7.4 for **3CUr16** and **3CAm21** were decreased by 2-

fold and 4-fold, respectively. Before reporting the results, a brief review of fluorescence method follows.

3.2 The Pyrene-Based Fluorescent Probe Method

The pyrene-based fluorescent probe method is used here to measure CMC.[3, 4] Under the influence of light at 334 nm, pyrene is excited and fluoresces with maxima at λ_{max} = 373 nm (I_1) and 385 nm (I_3). Pyrene excites from $S_0 \rightarrow S_2$ and emits at $S_1^{v=0} \rightarrow S_0^{v=0}$ (I_1) and $S_1^{v=0} \rightarrow S_0^{v=1}$ (I_3).[5] The emission properties of pyrene are sensitive to the polarity of the local environment. In an aqueous environment, I_1 is higher than I_3. In a hydrocarbon environment, I_1 is lower than it is in water. Further, I_1 is more sensitive than I_3 to solvent polarity. The CMC can be measured by the ratio, I_1/I_3. At low amphiphile concentration, there is no micelle formation. Both I_1 and I_3 are low, but the I_1/I_3 ratio is much greater than one. As amphiphile concentrations increases, both I_1 and I_3 increase. When micelles form, the pyrene gets absorbed inside the micelle. Then, I_1 decreases and the I_1/I_3 ratio gets closer to one.

3.3 CMC Data for the 2CAmn Series by the Surface Tension and the Pyrene Fluorescence Methods

The CMCs of all three-headed amphiphile series were measured[1] first by the surface tension method and then verified with the fluorescence method. The study demonstrated that the fluorescence method gave sharper breaks in plots to determine the CMCs. Further, the fluorescence method required less time. Marcelo Actis[2] used a pendant-drop analyzer to measure the surface tension of individual amphiphiles of the **2CAmn** series. The CMCs were measured by finding the inflection point in interfacial tension (IFT) versus log [amphiphile] plot. In order to verify the CMCs measured by the

surface tension method, the fluorescence method was used here to measure the CMCs of the **2CAmn** series. Intensity ratio (I_1 /I_3) versus log [amphiphile] was used to measure the CMCs.

3.3.1 CMC for 2CAm13 at pH ~9.2

With the surface tension method, the CMC for **2CAm13** was 12000 mg/L or 30000 µM (vertical dashed line on Figure 3.1), while with the fluorescence method; it was 9000 mg/L or 22525 µM (vertical dashed line on Figure 3.2). The reason for picking this point as the CMC is discussed below (See Section 3.6).

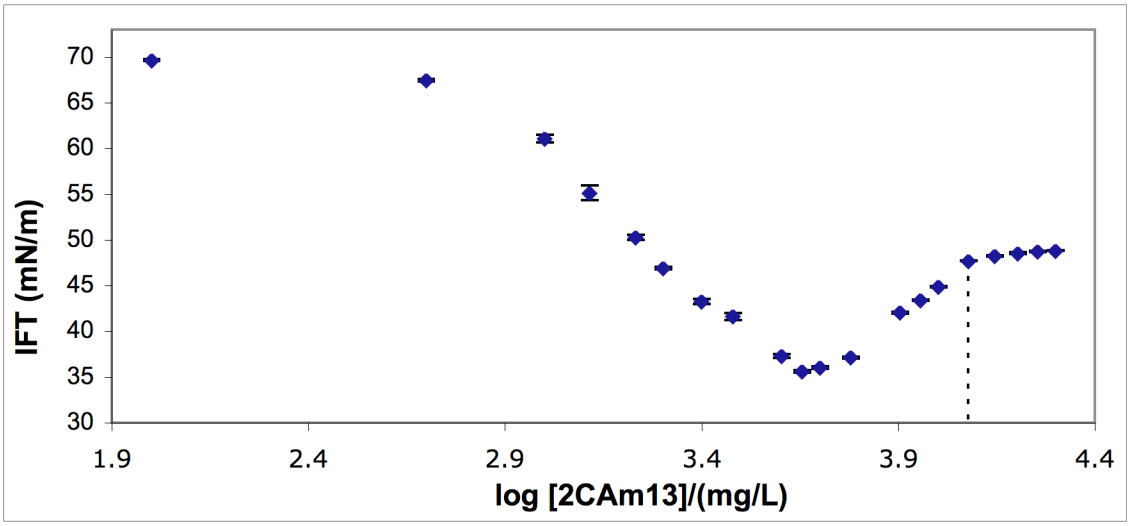

Figure 3.1 IFT versus log [**2CAm13**] at pH ~9.2

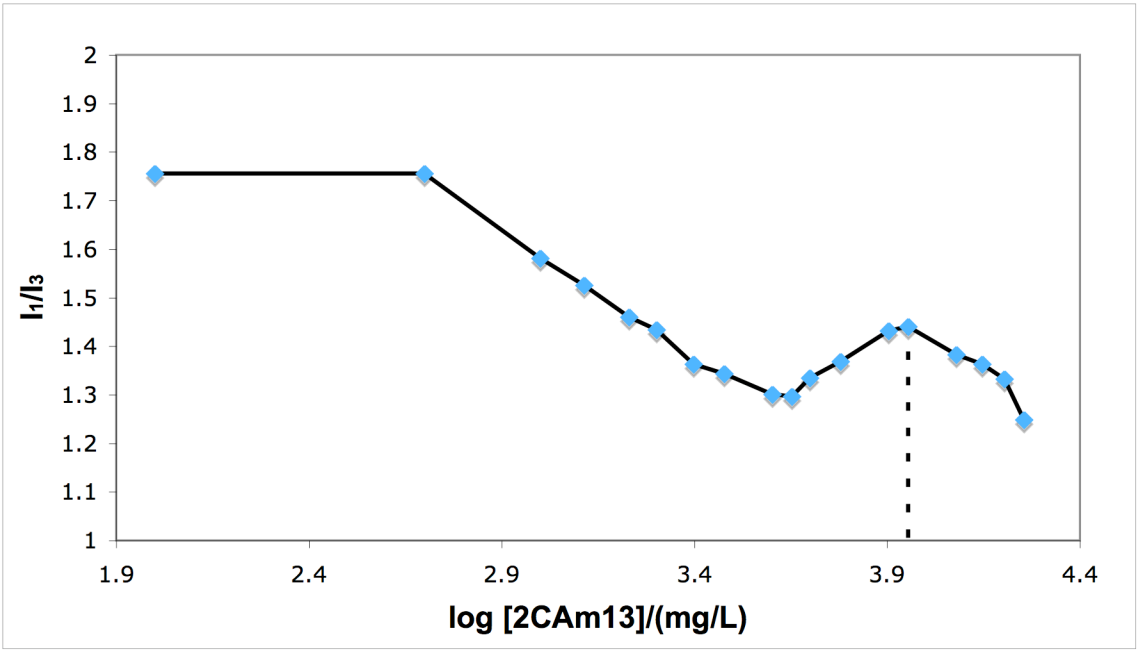

Figure 3.2 I_1/I_3 versus log **[2CAm13]** at pH ~9.2

3.3.2 CMC for 2CAm15 at pH ~9.2

With the surface tension method, the CMC for **2CAm15** was 4100 mg/L or 9600 µM (vertical dashed line on Figure 3.3), while with the fluorescence method; it was 2700 mg/L or 6300 µM (vertical dashed line on Figure 3.4). The reason for picking this point as the CMC is discussed below (See Section 3.6).

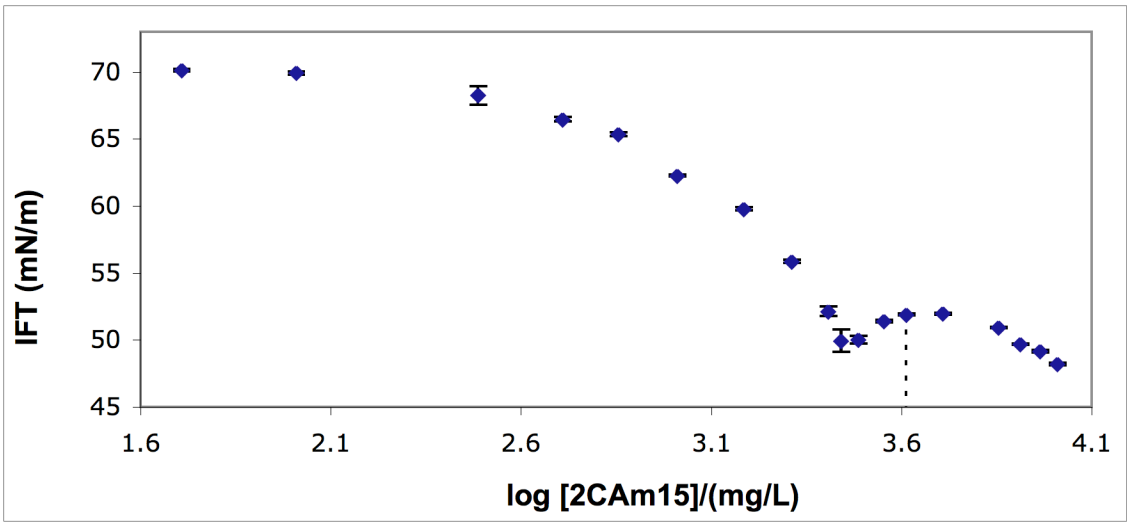

Figure 3.3 IFT versus log [**2CAm15]** at pH ~9.2

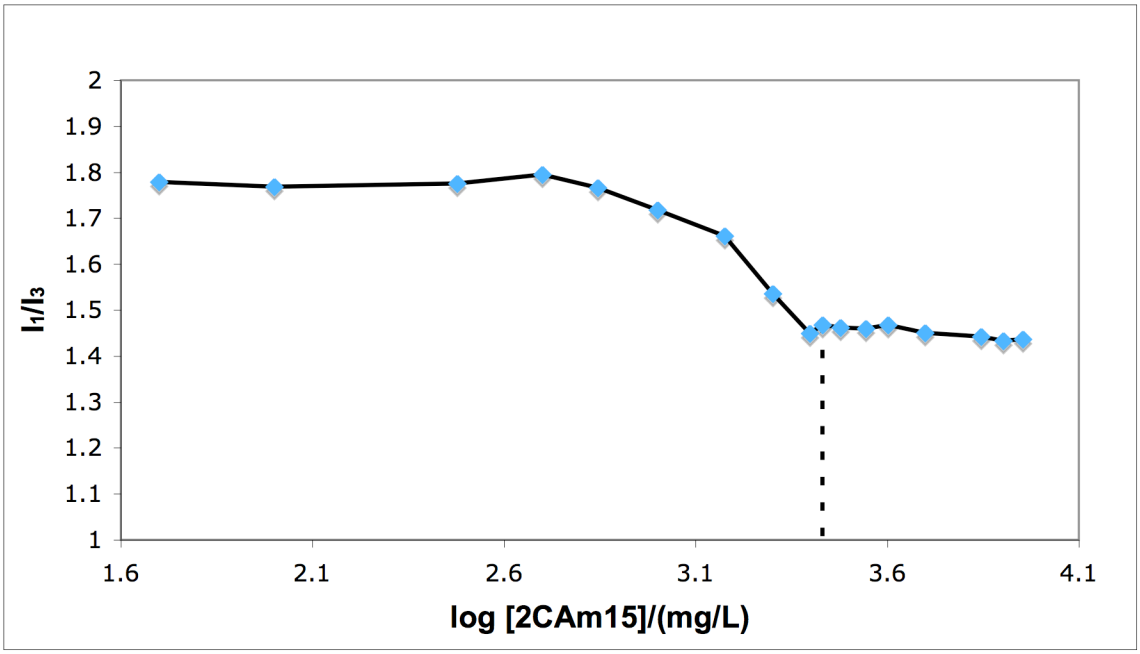

Figure 3.4 I_1/I_3 versus log [**2CAm15**] at pH ~9.2

3.3.3 CMC for 2CAm17 at pH ~9.2

With the surface tension method, the CMC for **2CAm17** was 1000 mg/L or 2200 µM (vertical dashed line on Figure 3.5), while with the fluorescence method; it was 1000 mg/L or 2200 µM (vertical dashed line on Figure 3.6).

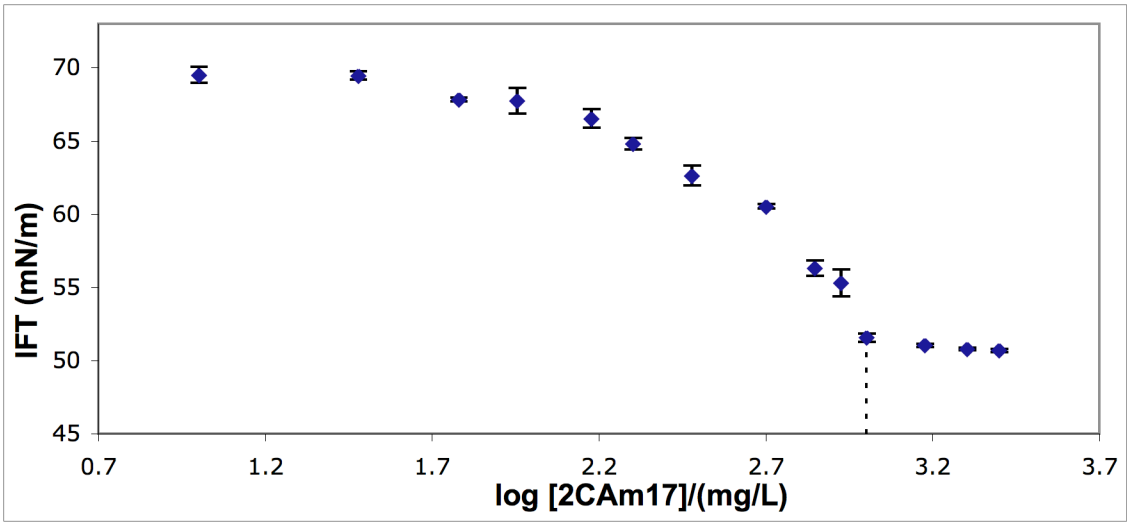

Figure 3.5 IFT versus log [**2CAm17]** at pH ~9.2

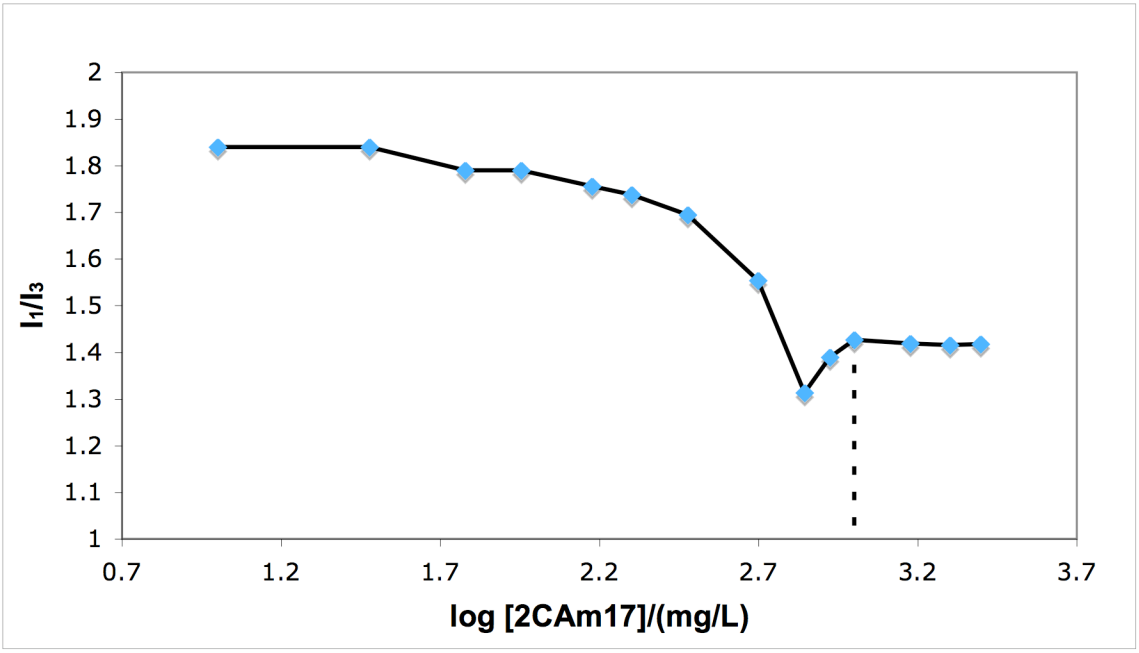

Figure 3.6 I_1/I_3 versus log [**2CAm17**] at pH ~9.2

3.3.4 CMC for 2CAm19 at pH ~9.2

With the surface tension method, the CMC for **2CAm19** was 360 mg/L or 740 µM (vertical dashed line on Figure 3.7), while with the fluorescence method; it was 500

mg/L or 1033 µM (vertical dashed line on Figure 3.9).

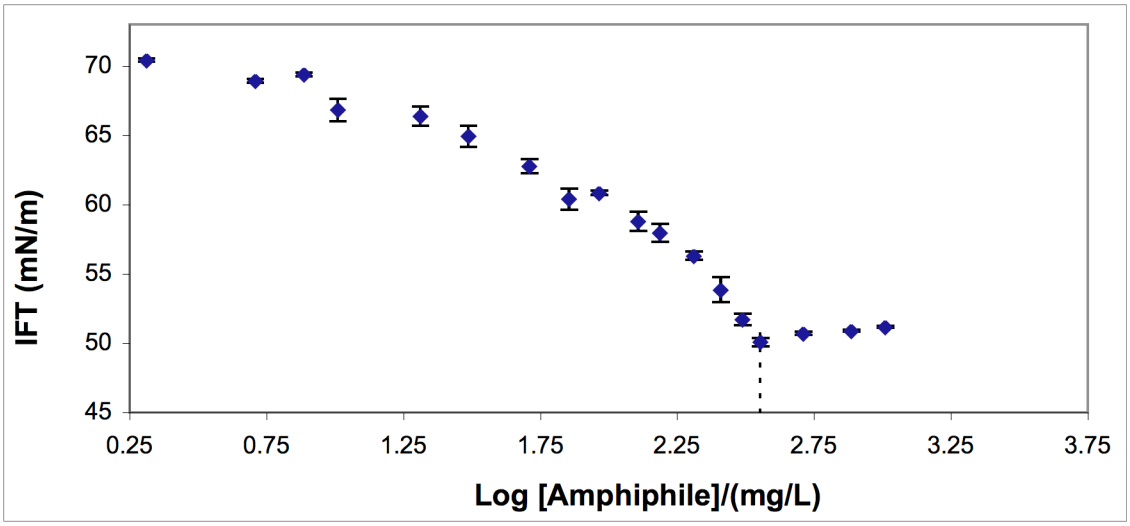

Figure 3.7 IFT versus log [**2CAm19]** at pH ~9.2

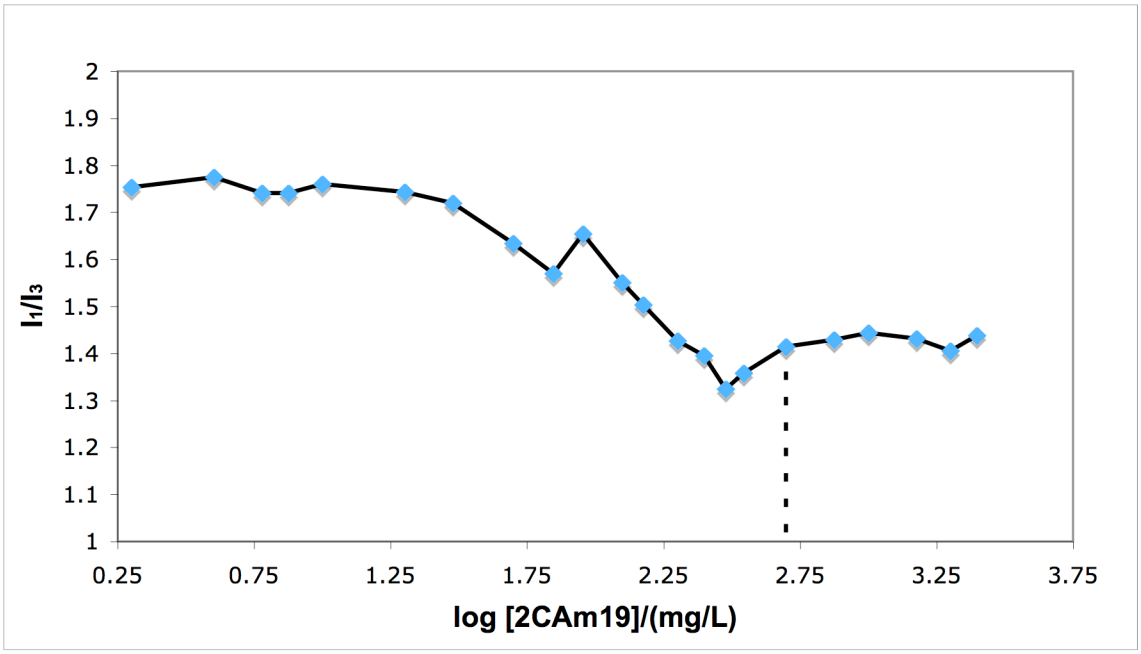

Figure 3.8 I_1/I_3 versus log [**2CAm19**] at pH ~9.2

3.3.5 CMC for 2CAm21 at pH ~9.2

With the surface tension method, the CMC for **2CAm21** was 85 mg/L or 170 µM (vertical dashed line on Figure 3.9), while with the fluorescence method; it was 90 mg/L or 175 µM (vertical dashed line on Figure 3.10).

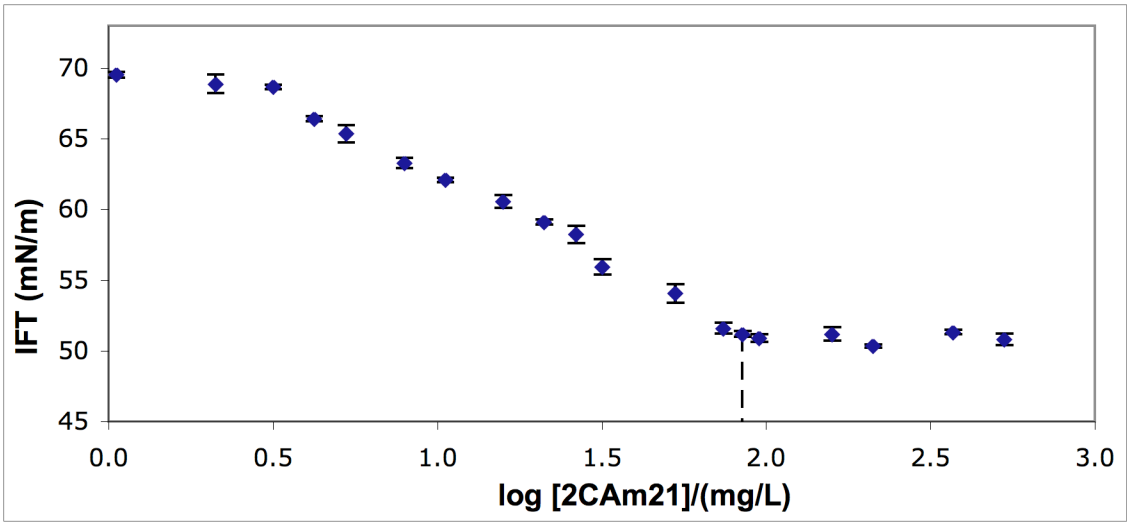

Figure 3.9 IFT versus log [**2CAm21**] at pH ~9.2

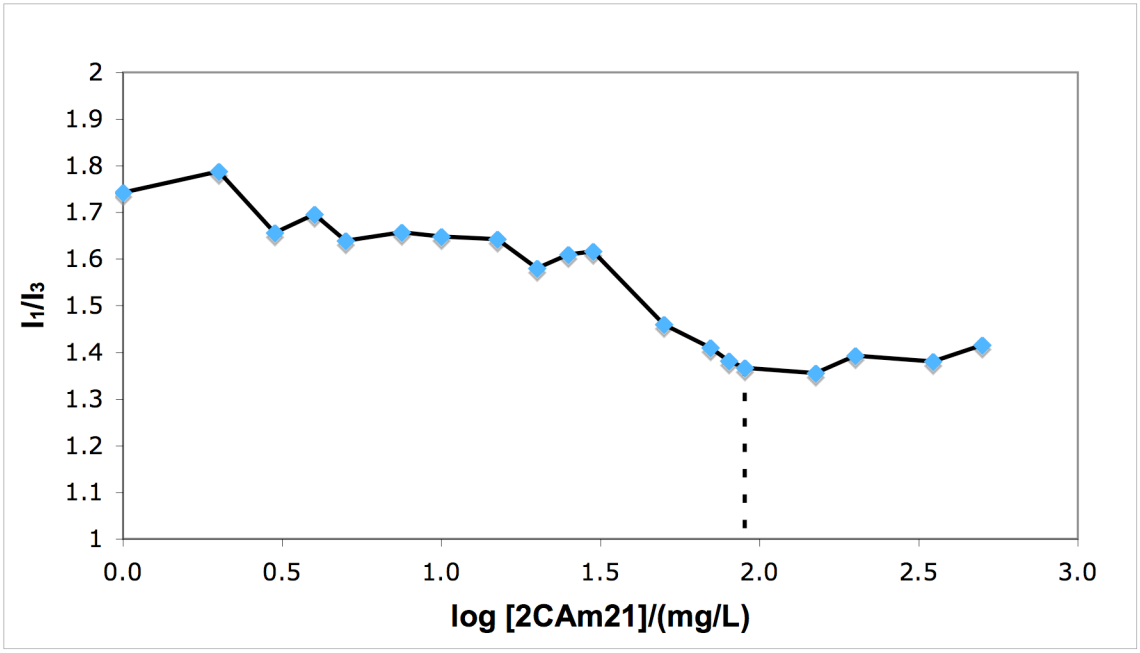

Figure 3.10 I_1/I_3 versus log [**2CAm21**] at pH ~9.2

3.4 CMC Data for the 2CCbn Series by the Pyrene Fluorescence Method at pH ~9.2

The **2CCbn** series were measured by the fluorescence method. Plots of intensity ratio (I_1/I_3) versus log [amphiphile] were prepared for each amphiphile. A few compounds were measured in duplicate. The I_1/I_3 value decreased with increasing concentration, and then leveled off. The point where it started to level off is the actual CMC value.

3.4.1 CMC for 2CCb16 at pH ~9.2

With the fluorescence method, the CMC for **2CCb16** was 1500 mg/L or 3280 µM (vertical dashed line on Figure 3.11).

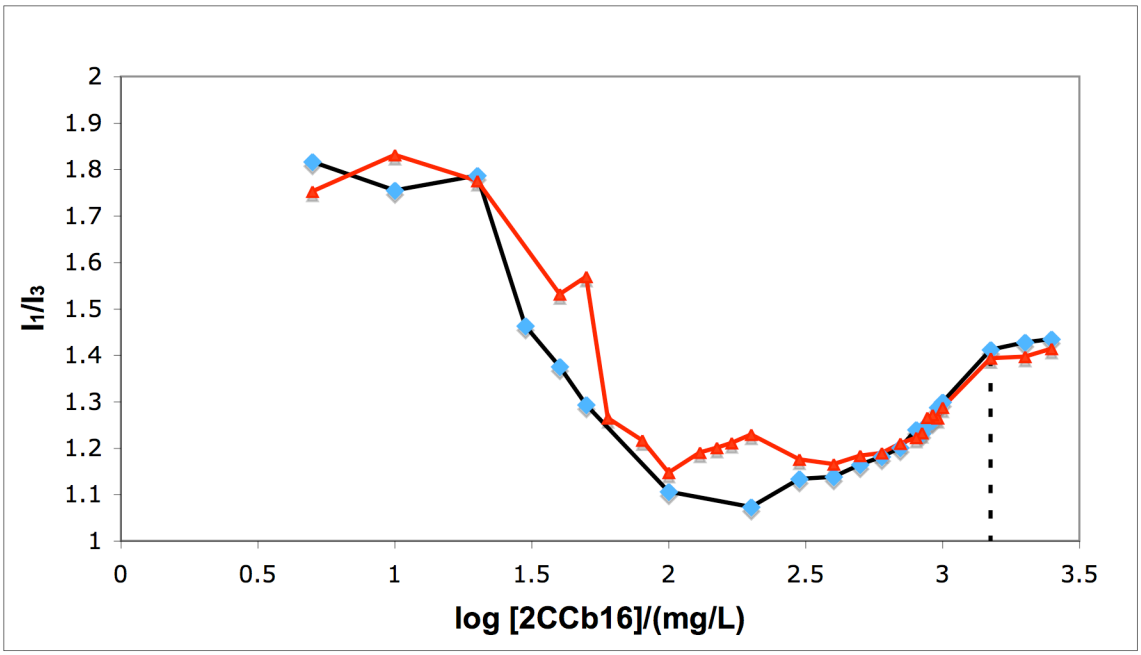

Figure 3.11 I_1/I_3 versus log [**2CCb16**] at pH ~9.2

3.4.2 CMC for 2CCb18 at pH ~9.2

With the fluorescence method, the CMC for **2CCb18** was 600 mg/L or 1235 µM (vertical dashed line in Figure 3.12).

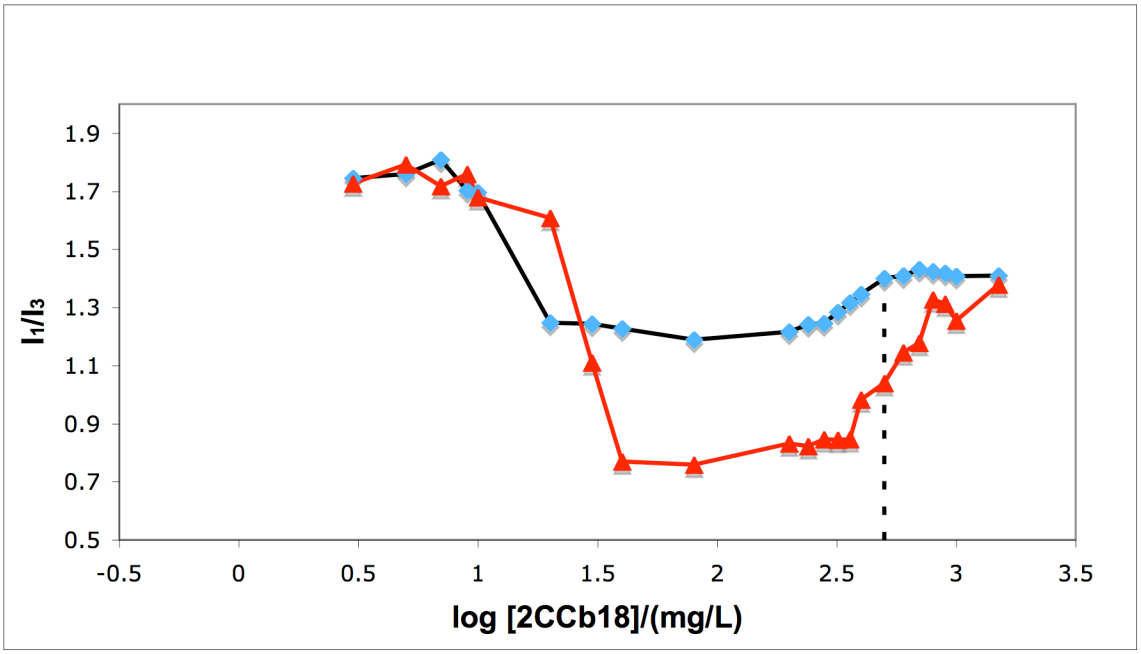

Figure 3.12 I_1/I_3 versus log [**2CCb18**] at pH ~9.2

3.4.3 CMC for 2CCb20 at pH ~9.2

With the fluorescence method, the CMC for **2CCb20** was 80 mg/L or 155 µM (vertical dashed line in Figure 3.13).

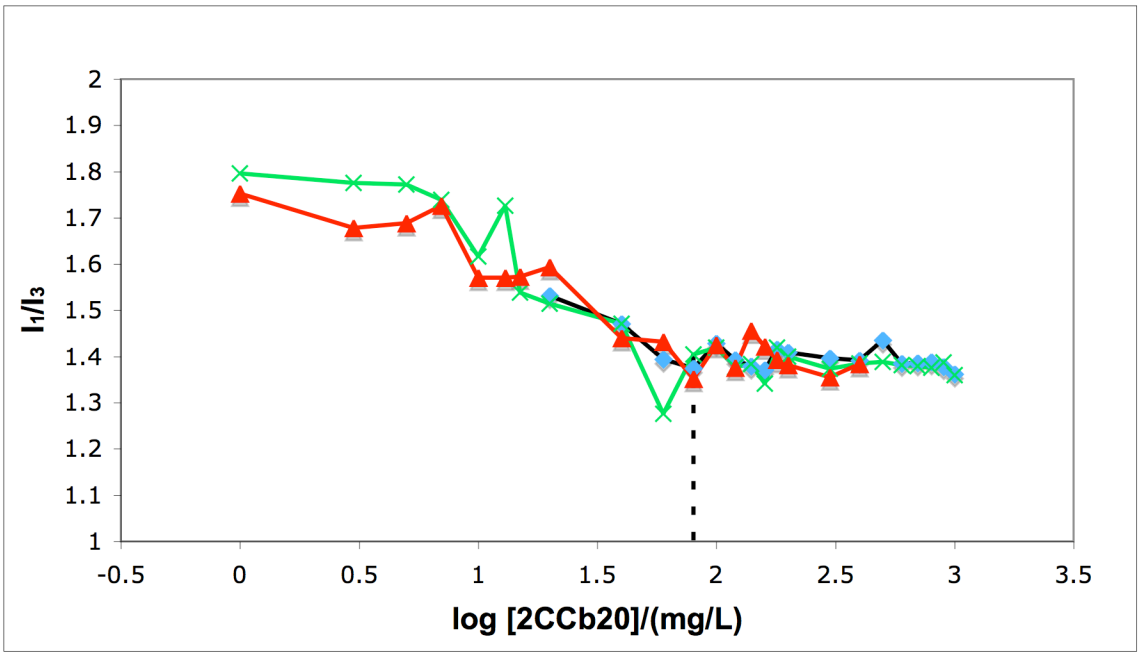

Figure 3.13 I_1/I_3 versus log [**2CCb20**] at pH ~9.2

3.4.4 CMC for 2CCb22 at pH ~9.2

With the fluorescence method, the CMC for **2CCb22** was 20 mg/L or 37 µM (vertical dashed line in Figure 3.14).

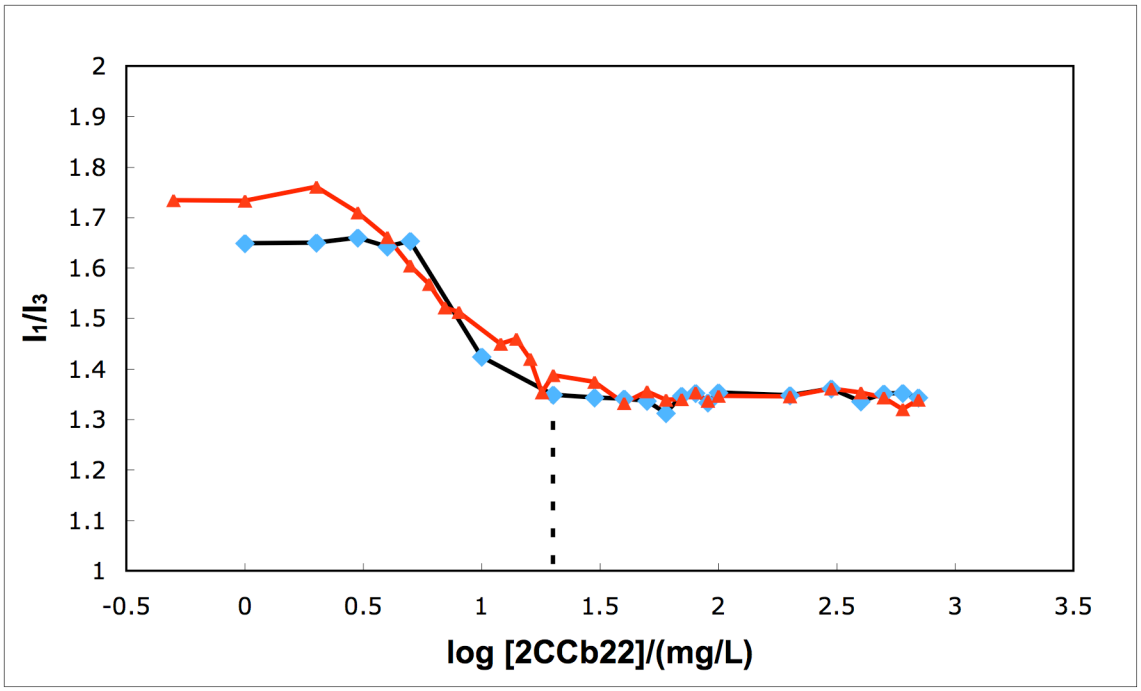

Figure 3.14 I_1/I_3 versus log [**2CCb22**] at pH ~9.2

3.4.5 CMC for 2CCb30 at pH ~9.2

With the fluorescence method, the CMC for **2CCb30** was not determined due to very poor aqueous solubility (Figure 3.15).

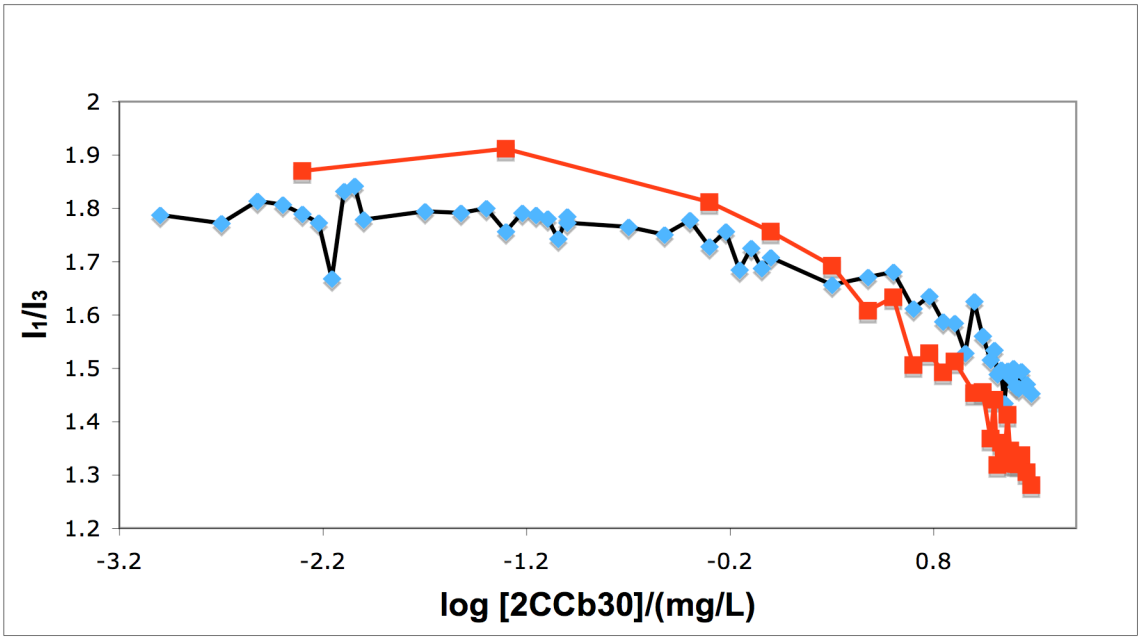

Figure 3.15 I_1/I_3 versus log [**2CCb30**] at pH ~9.2

3.4.6 CMC for 2CCb5α–cholestan-3ß-ol at pH ~9.2

With the fluorescence method, the CMC for **2CCb5α–cholestan-3ß-ol** was 700 mg/L or 1160 µM (vertical dashed line in Figure 3.16).

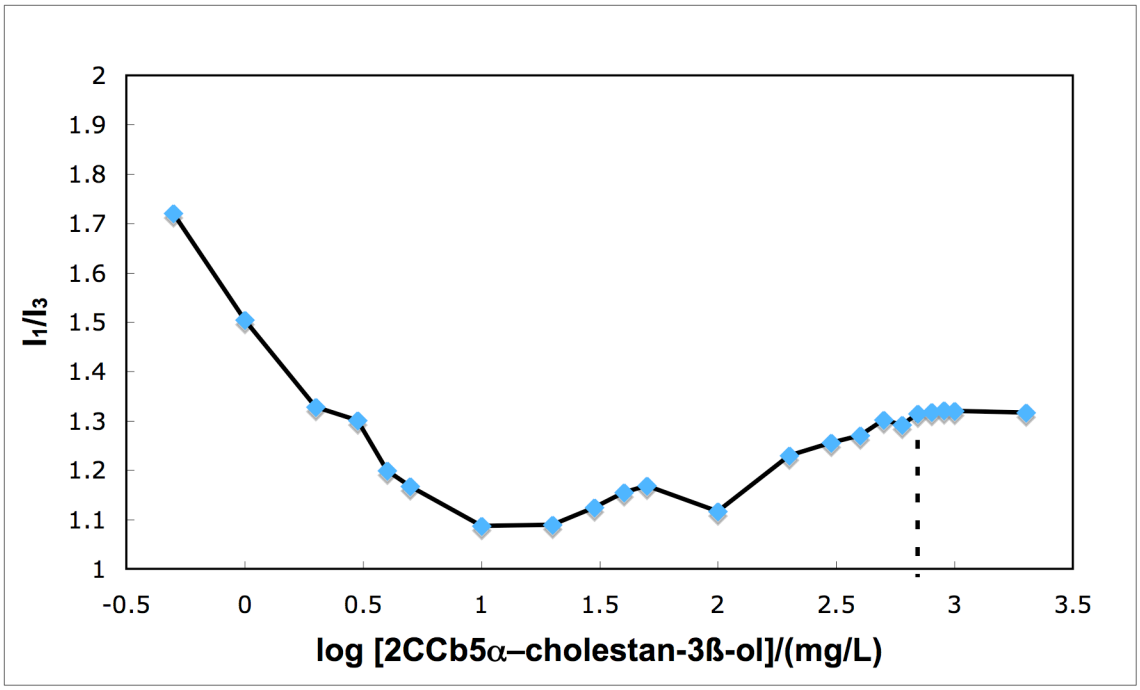

Figure 3.16 I_1/I_3 versus log [**2CCb5α–cholestan-3ß-ol**] at pH ~9.2

3.5 CMCs of the 2CAmn Series and the 2CCbn Series Measured at pH 7.4 by the Pyrene Fluorescence Method

The fluorescence method was used to measure the CMCs at pH 7.4 for the **2CAmn** and the **2CCbn** series. The I_1/I_3 versus log [amphiphile] were used to determine the CMCs. The CMCs were not determined due to steady decrease in I_1/I_3. Only, the clear solutions were used to determine the CMCs (See Section 3.10).

3.5.1 CMC for 2CAm13 at pH 7.4

With the fluorescence method, the CMC for **2CAm13** was 2930 mg/L or 7333 µM (vertical dashed line in Figure 3.17).

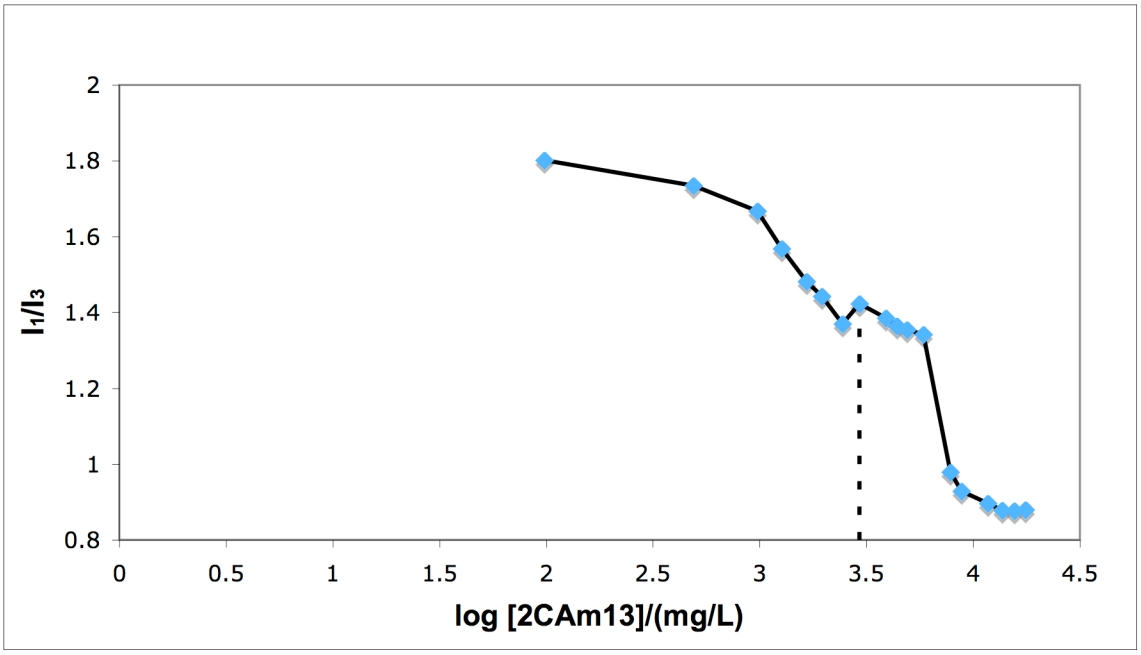

Figure 3.17 I_1/I_3 versus log [**2CAm13**] at pH 7.4

3.5.2 CMC for 2CAm15 at pH 7.4

With the fluorescence method, the CMC for **2CAm15** was 977 mg/L or 2285 µM (vertical dashed line in Figure 3.18).

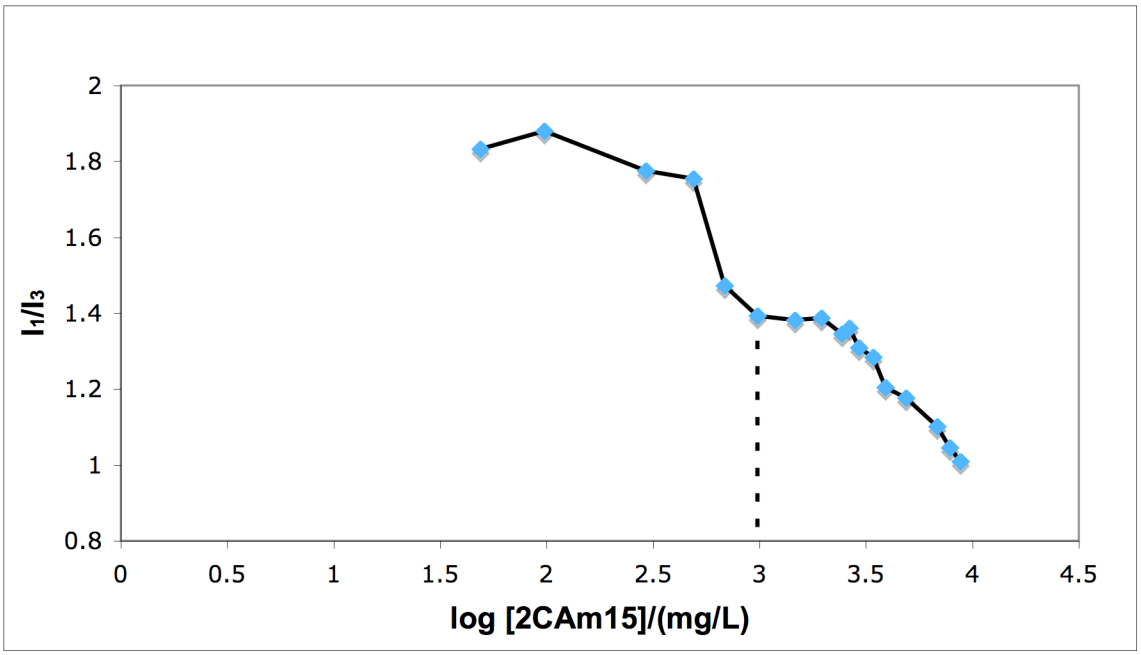

Figure 3.18 I_1/I_3 versus log [**2CAm15**] at pH 7.4

3.5.3 CMC for 2CAm17 at pH 7.4

With the fluorescence method, the CMC for **2CAm17** was 59 mg/L or 130 μM (vertical dashed line in Figure 3.19).

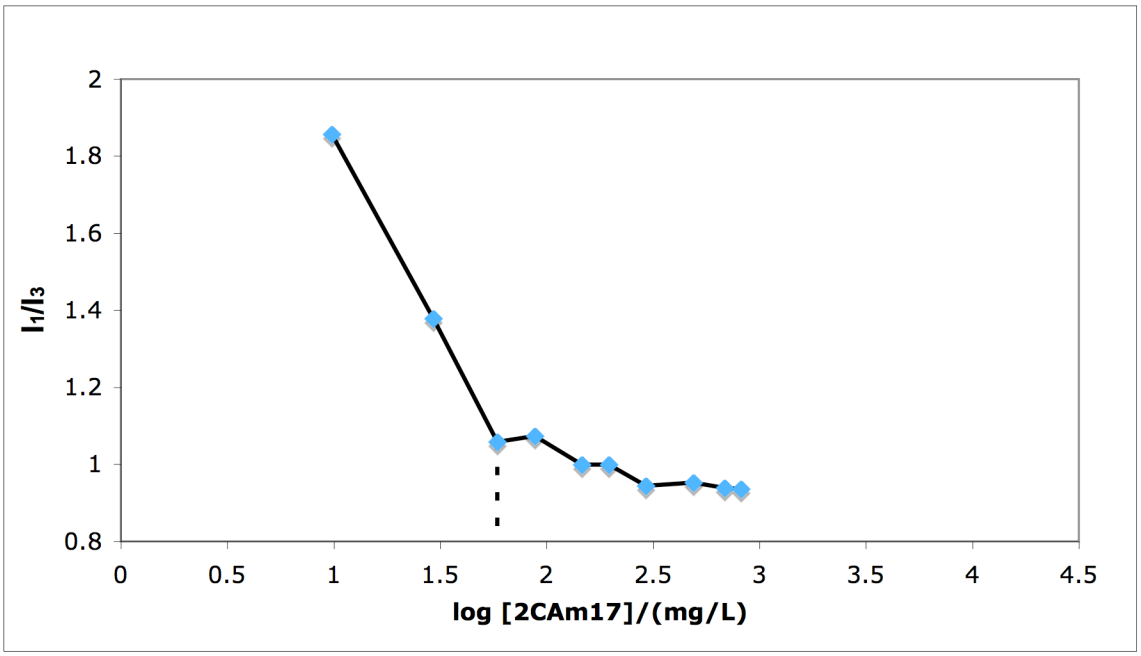

Figure 3.19 I_1/I_3 versus log [**2CAm17**] at pH 7.4

3.5.4 CMC for 2CAm19 at pH 7.4

With the fluorescence method, the CMC for **2CAm19** was 20 mg/L or 40 µM (vertical dashed line in Figure 3.20).

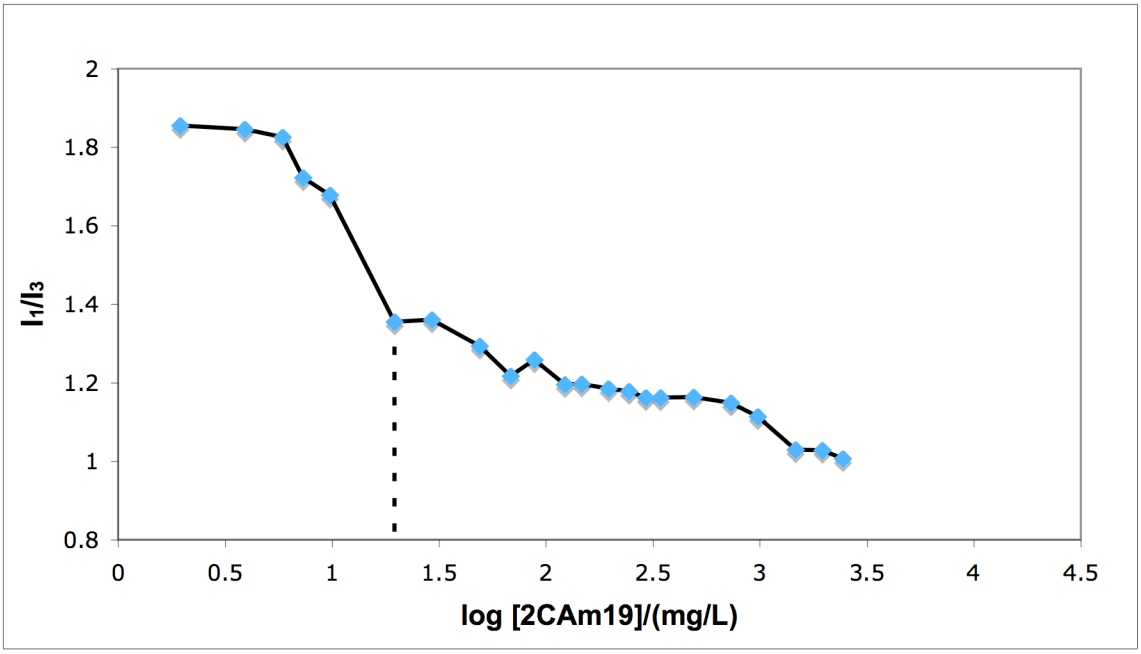

Figure 3.20 I_1/I_3 versus log [**2CAm19**] at pH 7.4

3.5.5 CMC for 2CAm21 at pH 7.4

With the fluorescence method, the CMC for **2CAm21** was 10 mg/L or 19 µM (vertical dashed line in Figure 3.21). The CMC determination was hard due to poor solubility.

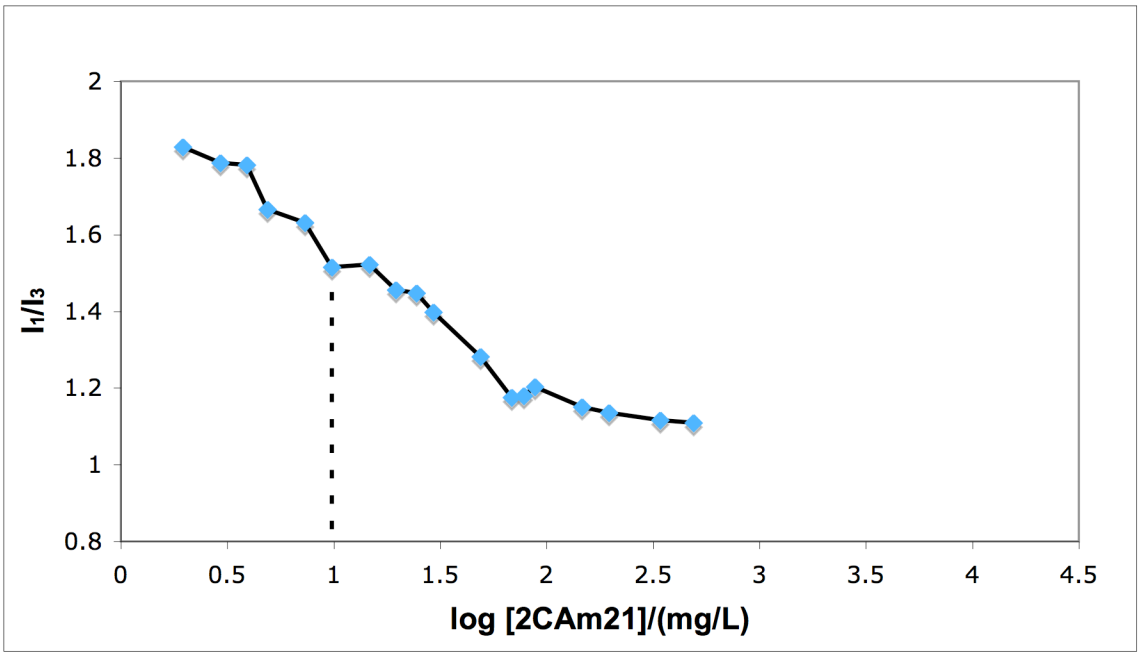

Figure 3.21 I_1/I_3 versus log [**2CAm21**] at pH 7.4

3.5.6 CMC for 2CCb16 at pH 7.4

With the fluorescence method, the CMC for **2CCb16** was 98 mg/L or 215 µM (vertical dashed line in Figure 3.22).

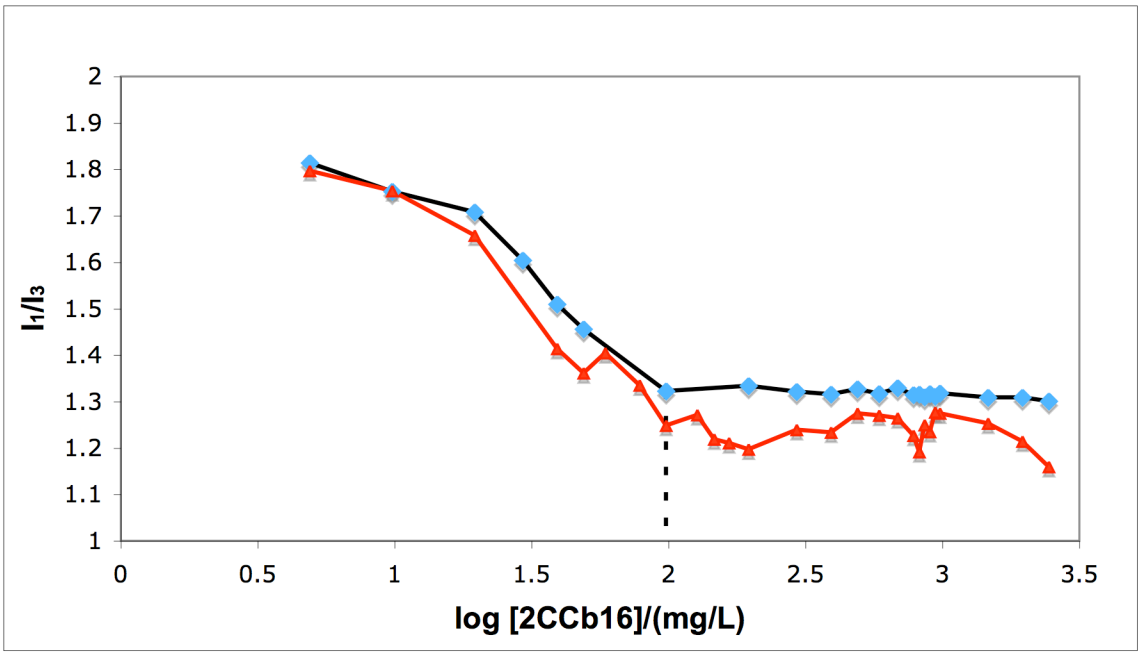

Figure 3.22 I_1/I_3 versus log [**2CCb16**] at pH 7.4

3.5.7 CMC for 2CCb18 at pH 7.4

With the fluorescence method, the CMC for **2CCb18** was 39 mg/L or 80 μM (vertical dashed line in Figure 3.23).

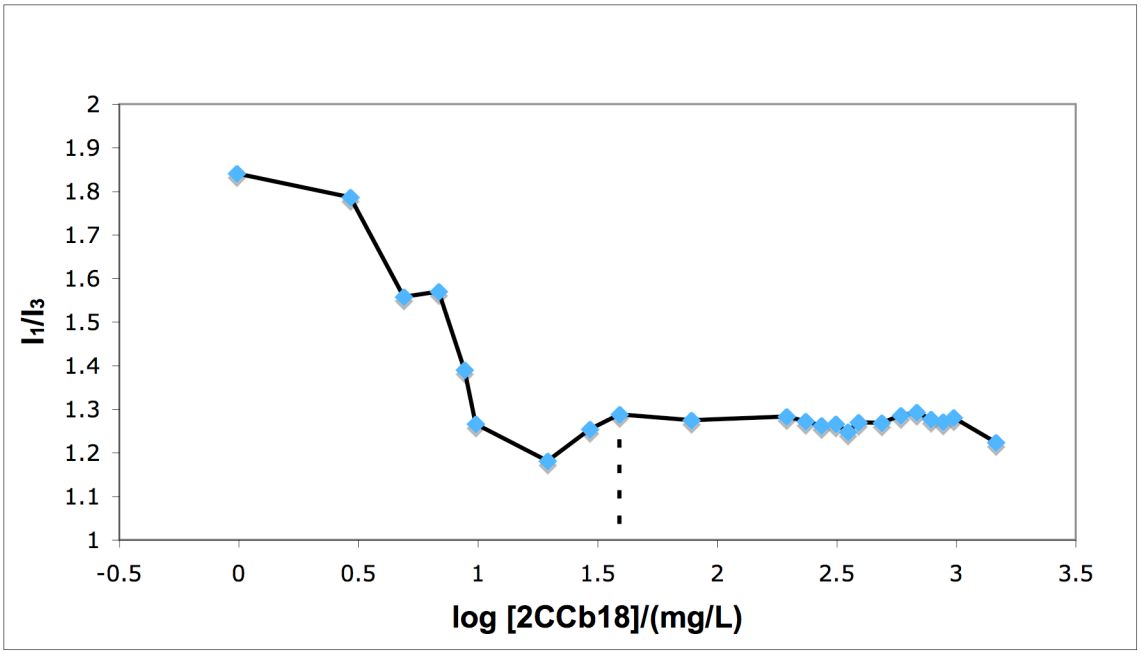

Figure 3.23 I_1/I_3 versus log [**2CCb18**] at pH 7.4

3.5.8 CMC for 2CCb20 at pH 7.4

With the fluorescence method, the CMC for **2CCb20** was 10 mg/L or 19 μM (vertical dashed line in Figure 3.24).

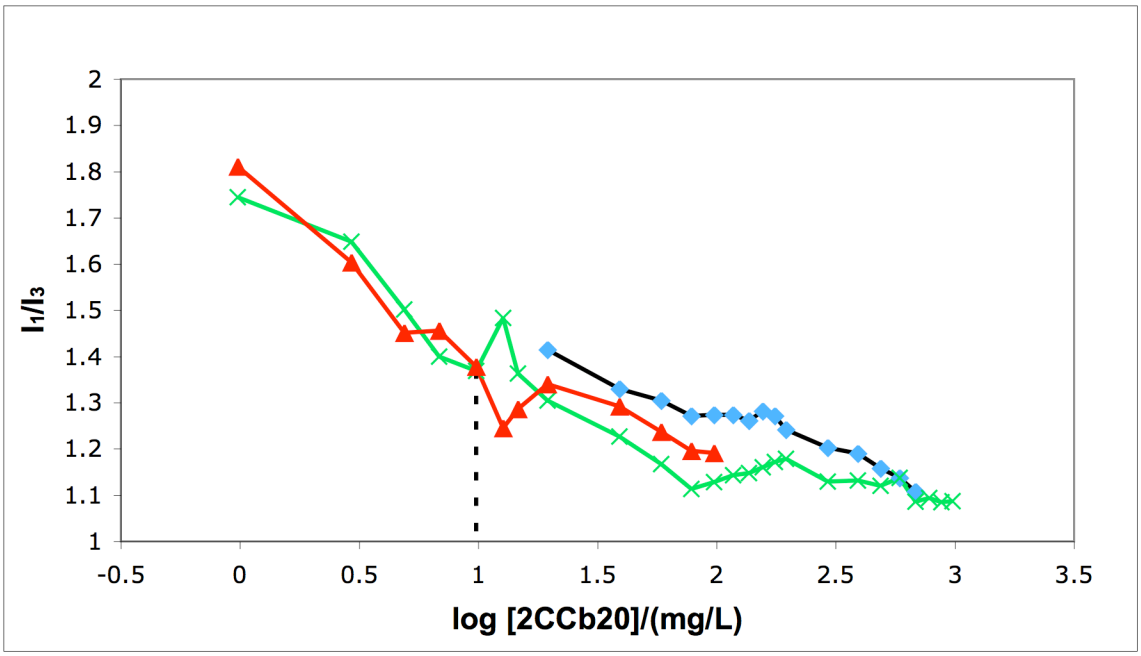

Figure 3.24 I_1/I_3 versus log [**2CCb20**] at pH 7.4

3.5.9 CMC for 2CCb22 at pH 7.4

With the fluorescence method, the CMC for **2CCb22** was 10 mg/L or 18 µM (vertical dashed line in Figure 3.25).

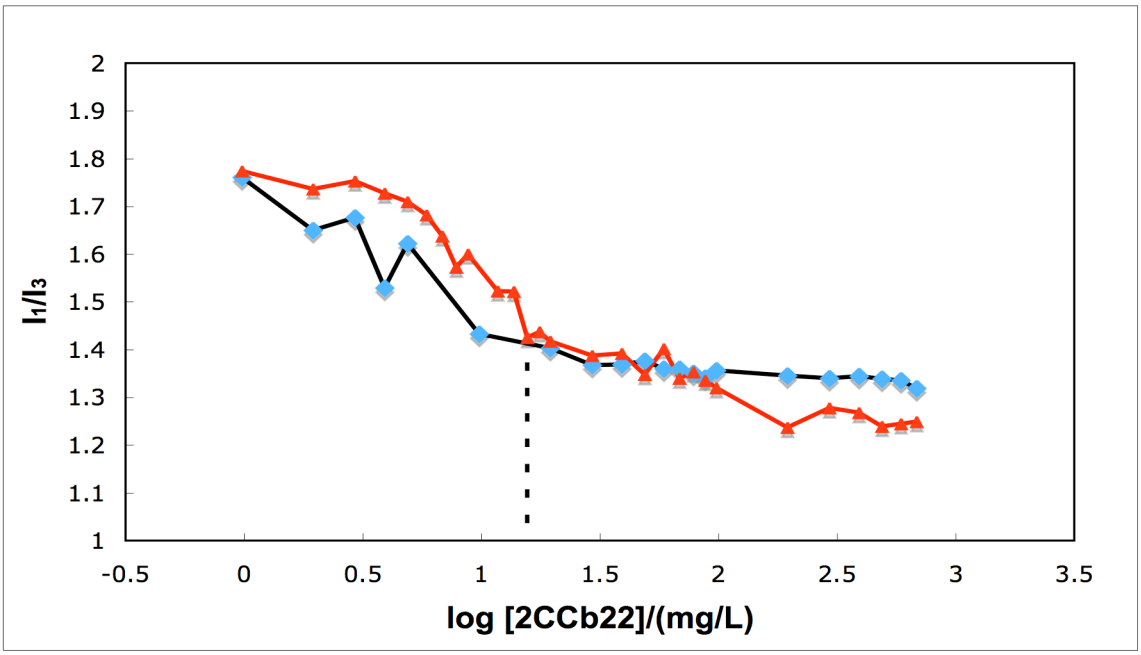

Figure 3.25 I_1/I_3 versus log [**2CCb22**] at pH 7.4

3.5.10 CMC for 2CCb30 at pH 7.4

With the fluorescence method, the CMC for **2CCb30** was not determined (Figure 3.16).

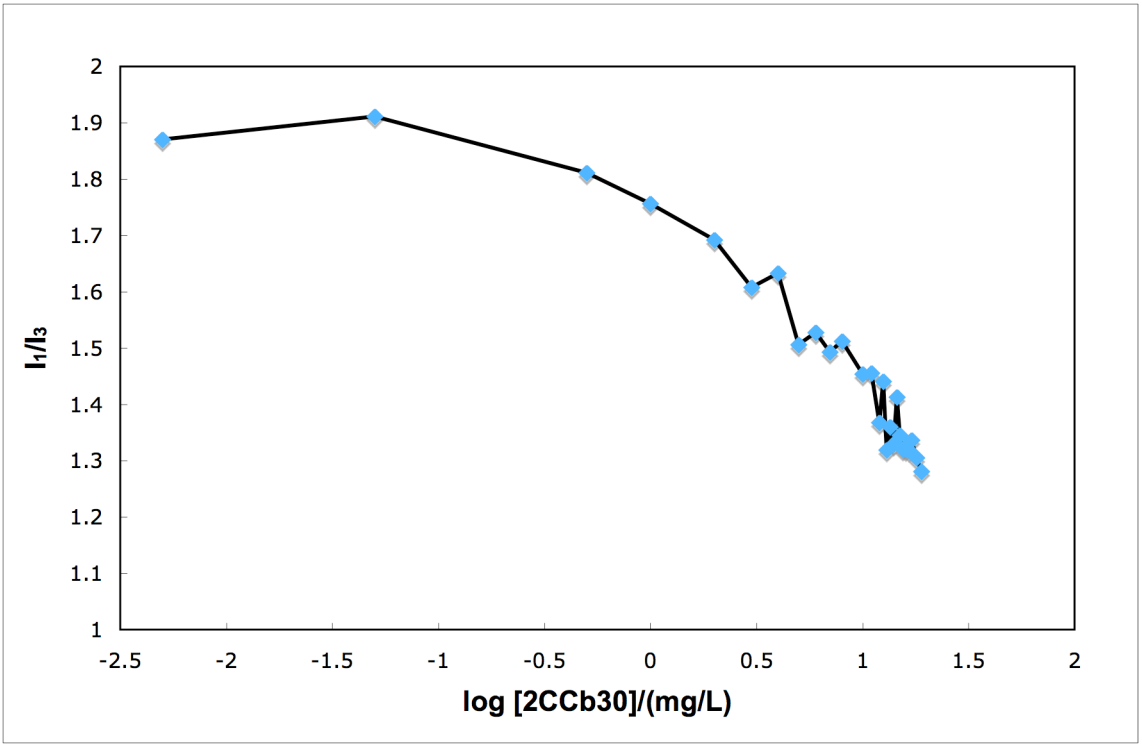

Figure 3.26 I_1/I_3 versus log [**2CCb30**] at pH 7.4

3.5.11 CMC for 2CCb5α–cholestan-3ß-ol at pH 7.4

With the fluorescence method, the CMC for **2CCb5α–cholestan-3ß-ol** was 39 mg/L or 65 µM (vertical dashed line in Figure 3.27).

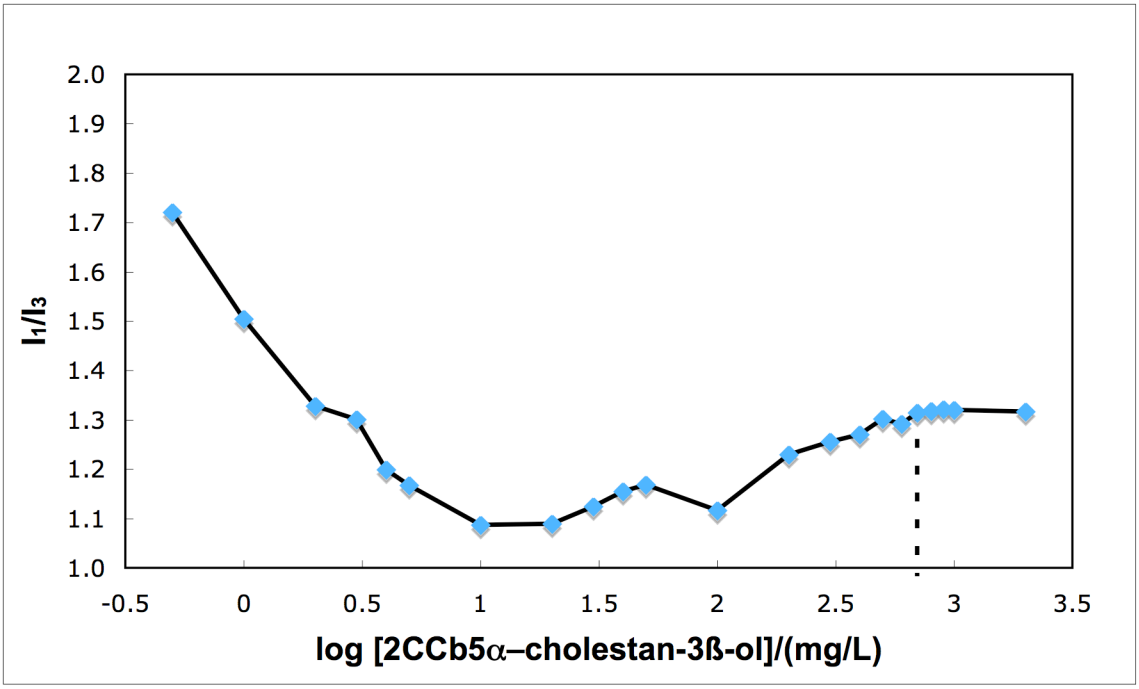

Figure 3.27 I_1/I_3 versus log [**2CCb5α–cholestan-3ß-ol**] at pH 7.4

3.6 The Effect of Impurities in CMC Measurements for the 2CAmn Series and the 2CCbn Series

Lin et al.[6] have observed the minimum in the curve for sodium dodecyl sulfate (SDS) by the surface tension method. They described that lauryl alcohol, a product obtained by SDS hydrolysis, is an impurity. Lauryl alcohol can lower the surface tension at low SDS concentrations. As the concentrations of SDS and lauryl alcohol increase, the surface tension decreases sharply because the impurity is more surface active than SDS. When mixed micelles form, the surface tension stops decreasing. This mixed micelle formation lowers the concentration of the impurity into the SDS solution. Eventually, the surface tension increases and levels off because all of the impurity is in the micelles. It was hard to determine the CMC for SDS by the surface tension method because of the shape of the curve.

To determine the CMC for the same SDS solution, the conductivity method was used because it gave a good inflection point. The conductivity method depends on the velocity of the ions of the electrolyte (SDS). As the concentration of SDS increases, the conductivity increases due to the increase in the number of charged SDS ions. Further increase in the SDS concentration causes micelles to form, which are large and have a low velocity. Thus, the conductivity does not increase further and starts to level off. There was no impact of the impurity on the curve because lauryl alcohol does not have any charge. To find the actual CMC value for SDS solution in the surface tension method, they compared the curves obtained by the two methods. In the surface tension method, the point at which the surface tension levels off was the same as the point at which it gave inflection point in the conductivity method.

Marcelo Actis[2] has also observed the minimum in the curve by the surface tension method for **2CAm13** (Figure 3.1, from 2.7 to 4.0 mg/L) and **2CAm15** (Figure 3.3, from 2.5 to 3.6 mg/L). The same behavior was observed for **2CAm13** (Figure 3.2, from 2.7 to 4.0 mg/L), for **2CAm15** (Figure 3.4, from 2.7 to 3.4 mg/L), for **2CCb16** (Figure 3.11, from 1.3 to 3.2 mg/L), and for **2CCb18** (Figure 3.12, from 0.8 to 2.8 mg/L) by the fluorescence method. Samples were made in excess TEA (0.0005–0.002 mole). Two moles of triethanolamine (TEA) were required to deprotonate one mole of a two-headed amphiphile. This excess TEA may be combining with the amphiphile to form going inside the micelle and loosening the micelle and thus causing the minimum in the curve (Figure 3.28). The increasing concentration of amphiphile increases the number of micelles; the neutral TEAs get solubilized into the micelles. The curve increases and levels off; this point was chosen as the CMC for two-headed amphiphiles.

The data at pH 7.4 support the suggestion that neutral excess TEA is causing the minimum in the curve. The minimum in the curve for **2CAm13** by the surface tension (Figures 3.1) and by the fluorescence method (Figure 3.2) at pH ~9.2, was observed from 2.7 to 4.0 mg/L and from 2.7 to 4.0 mg/L, respectively. Adjusting the pH by 1M H_3PO_4 greatly reduce the minimum in the curve (Figure 3.17). One possible reason is that the phosphoric acid is protonating the excess neutral TEA (pKa = 7.76), which reduces the amount of TEA. Another possible reason is that adjusting the pH 7.4 changes the amount of monoanion and dianion of the two-headed amphiphile.

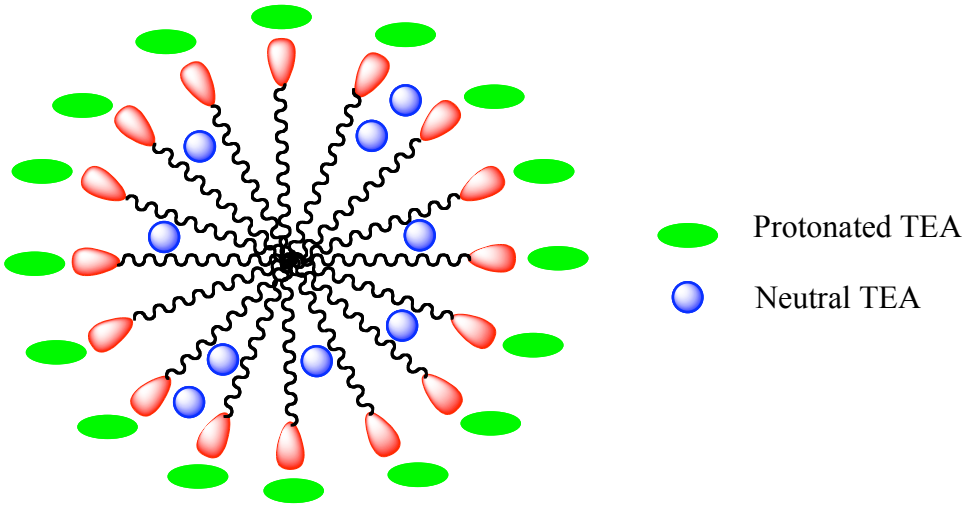

Figure 3.28 TEA as an impurity in the micelle structure.

3.7 Comparison Between the Surface Tension Method and the Pyrene Fluorescence Method at pH ~9.2 and 7.4 for the 2CAmn Series and the 2CCbn Series

At pH ~9.2, the CMCs decreased with increasing chain length for both the **2CAmn** series and the **2CCbn** series. The CMCs for the **2CAmn** series measured by the surface tension method and the fluorescence method were similar (Figure 3.29). The **2CCb16**, **2CCb18**, and **2CCb20** are classical isosteres to **2CAm17**, **2CAm19**, and **2CAm21**, respectively. At pH ~9.2, the CMCs observed for **2CCb16**, **2CCb18**, and

2CCb20 were almost same as the CMCs observed for **2CAm17**, **2CAm19**, and **2CAm21** (Figure 3.29). At pH ~9.2, the CMCs for **2CAm19**, **2CAm21**, and **2CCb18** deviated the most from their respective linear regressions.

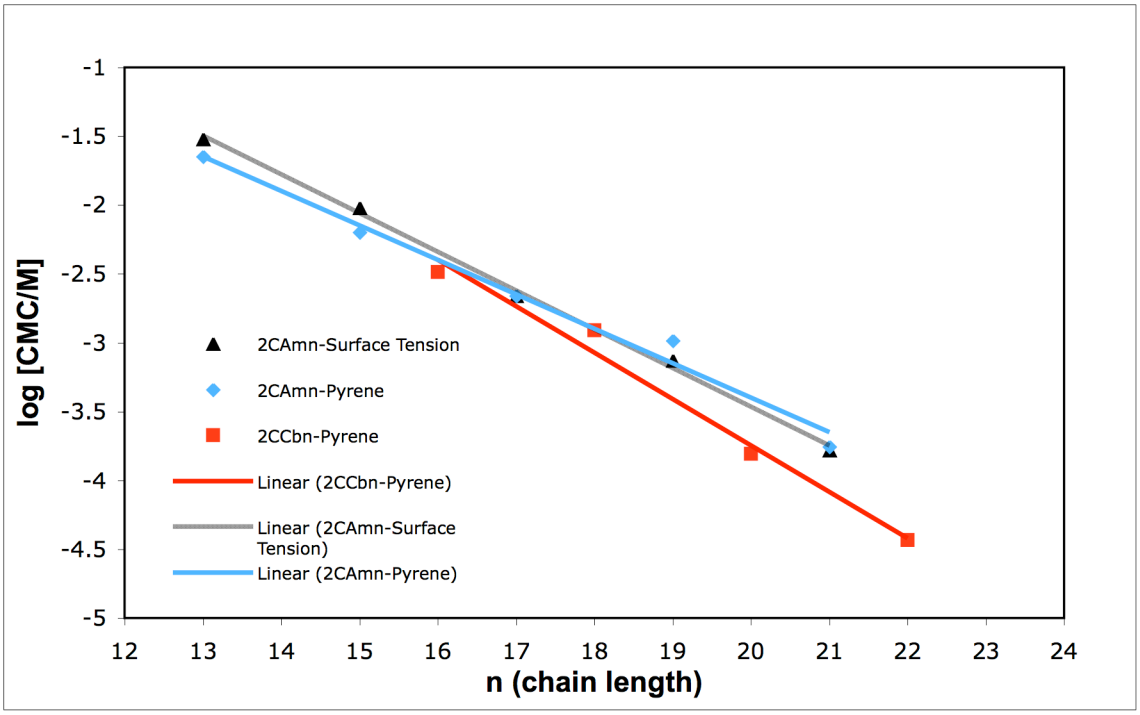

Figure 3.29 Comparison of CMCs between the **2CAmn** series (measured by the surface tension and the fluorescence methods) and the **2CCbn** series (measured by the fluorescence method) at pH ~9.2. M = Molar. The solid lines are linear-regression analyses, where log CMC = for the **2CAmn** series, the surface tension method: (–0.28 ± 0.01) × **n** + 2.2 ± 0.1; for the **2CAmn** series, the fluorescence method: (–0.25 ± 0.02) × **n** + 1.6 ± 0.3; for the **2CCbn** series, the fluorescence method: (–0.34 ± 0.03) × **n** + 3.0 ± 0.6.

At pH 7.4, the CMC measurements for the **2CAmn** series and the **2CCbn** series were done only by the fluorescence method (Figure 3.30).

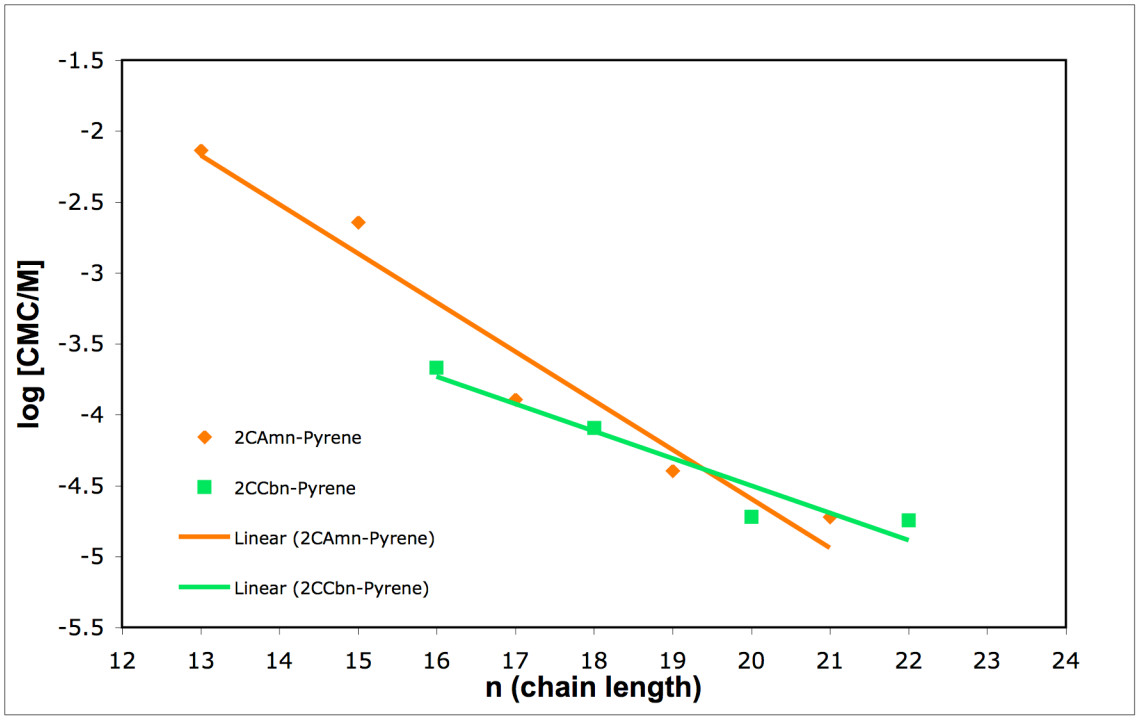

Figure 3.30 Comparison of CMCs between the **2CAmn** series and the **2CCbn** series (both measured by the fluorescence method) at pH 7.4. M = Molar. Solid lines are linear-regression analyses, where log CMC = for the **2CAmn** series, the fluorescence method: (–0.35 ± 0.04) × **n** + 2.3 ± 0.8; for the **2CCbn** series, the fluorescence method: (–0.19 ± 0.04) × **n** + (–0.7 ± 0.8).

At pH 7.4, the CMCs of the **2CAmn** series decreased with increasing chain length (Figure 3.31). The CMCs measured at pH ~9.2 were higher than the CMCs measured at pH 7.4. The gap between the CMCs measured at pH ~9.2 and 7.4 for the **2CAmn** series was increasing with increasing chain-length except **2CAm21** amphiphile. At pH 7.4, the CMCs of **2CAm15**, **2CAm17**, and **2CAm19** deviated from the line. The CMCs measured at pH 7.4 for the **2CAm13**, **2CAm15**, **2CAm17**, **2CAm19**, and **2CAm21** were 3, 3, 17, 26, 9-fold lower than the CMCs measured at pH ~9.2.

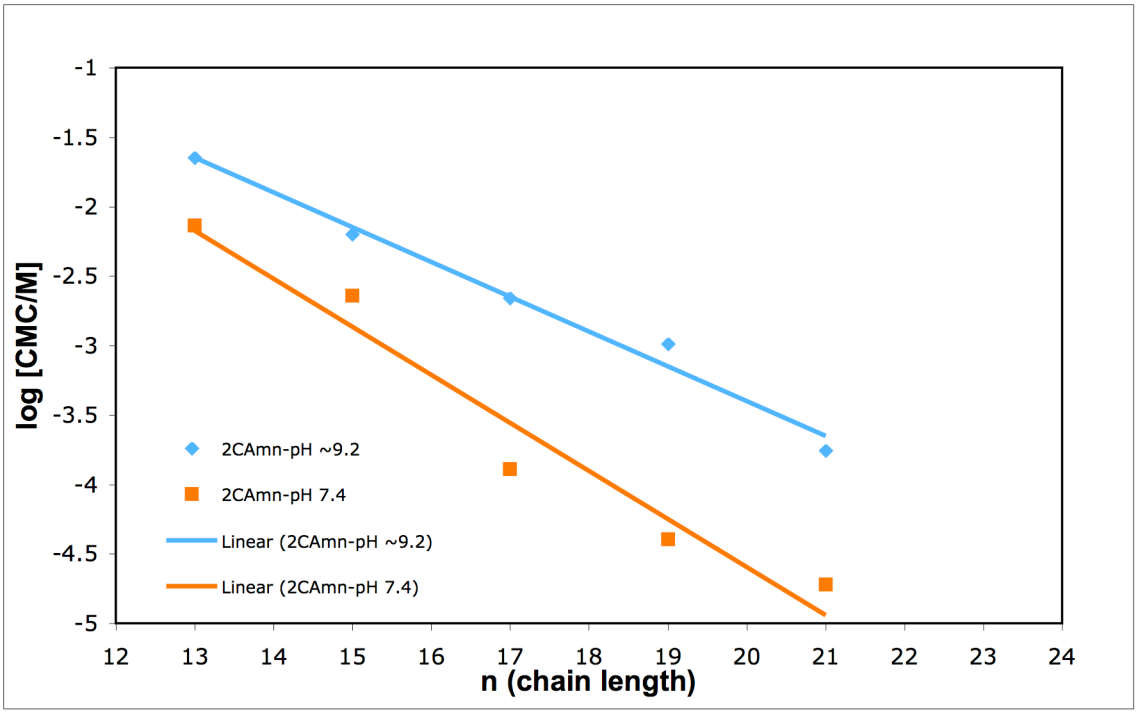

Figure 3.31 CMCs comparison for the **2CAmn** series at pH ~9.2 and 7.4. M = Molar. The solid lines are linear-regression analyses, where log CMC = for the **2CAmn** series at pH ~9.2, the fluorescence method: (–0.25 ± 0.02) × **n** + 1.6 ± 0.3; for the **2CAmn** series at pH 7.4, the fluorescence method: (–0.35 ± 0.04) × **n** + 2.3 ± 0.8.

At pH 7.4, the CMCs of the **2CCbn** series decreased with increasing chain length (Figure 3.32). The CMCs measured at pH ~9.2 were higher than the CMCs measured at pH 7.4. The gap between the CMCs measured at pH ~9.2 and 7.4 for the **2CCbn** series was decreasing with increasing chain-length. At pH 7.4, the CMCs of **2CCb20** and **2CCb22** were not linear. The CMCs measured at pH 7.4 for the **2CCb16**, **2CCb18**, **2CCb20**, and **2CCb22** were 15, 15, 8, and 2-fold lower than the CMCs measured at pH ~9.2.

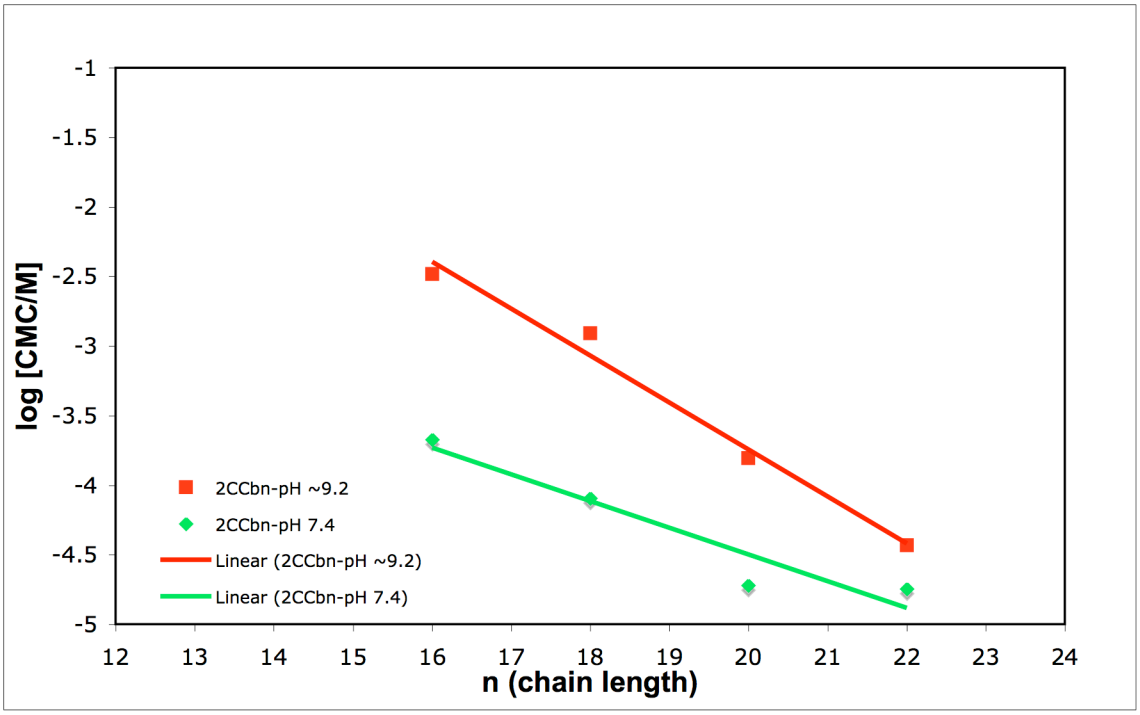

Figure 3.32 CMCs comparison for the **2CCbn** series at pH ~9.2 and 7.4. M = Molar. The solid lines are linear-regression analyses, where log CMC = for the **2CCbn** series at pH ~9.2, the fluorescence method: (–0.34 ± 0.03) × **n** + 3.0 ± 0.6; for the **2CCbn** series at pH 7.4, the fluorescence method: (–0.19 ± 0.04) × **n** + (–0.7 ± 0.8).

3.8 CMCs Comparison

The three-headed amphiphiles have higher CMCs than the two-headed amphiphiles (also for iminodiacetic acid **4**) followed by the fatty acids (FA) **1** (Figure 3.33, 3.34).

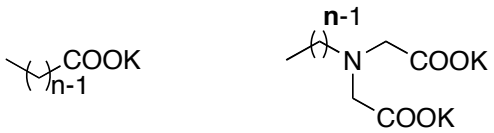

1 **4**

n= 8–18 **n**= 12, 16, 18

Figure 3.33 Structures of fatty acids (**1**) by Shinoda[8] and iminodiacetic acids (**4**) by Paleos et al.[7]

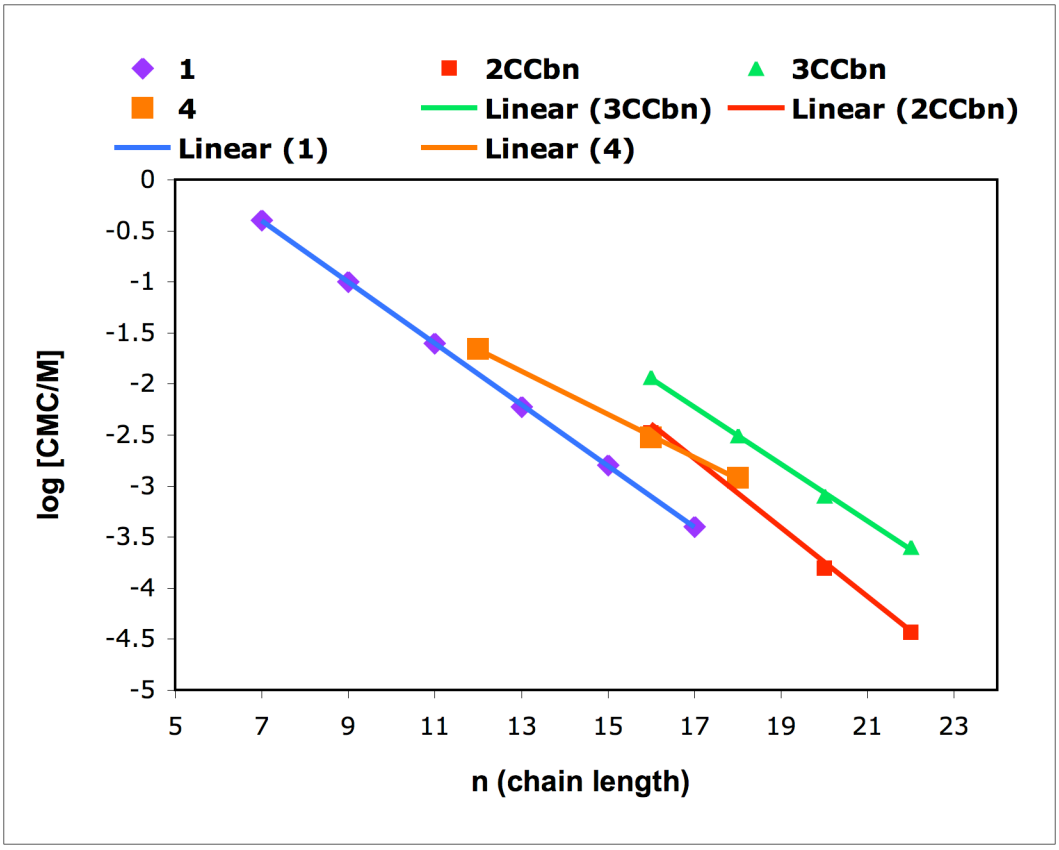

Figure 3.34 CMCs comparison between fatty acids and two- and three-headed amphiphiles. M = Molar. The solid lines are linear-regression analyses, where log CMC = for **1**, the solubilization method: (–0.3 ± 0.001) × **n** + 1.7 ± 0.02; for **4**, the electroconductometry and the fluorescence method: (-0.21 ± 0.0) × **n** + 0.87 ± 0.06; for the **2CCbn** series, the fluorescence method: (–0.34 ± 0.03) × **n** + (3.0 ± 0.6); for the **3CCbn** series, the surface tension method: (–0.28 ± 0.01) × **n** + 2.5 ± 0.1.

The CMCs of the **3CCbn** series are higher in respect to the **2CCbn** series (Figure 3.35). As chain length increases, the CMC decreases more for the **2CCbn** series than the **3CCbn** series. The two-headed amphiphiles have one carboxyl group fewer than the three-headed amphiphiles, and one carboxyl group more than the FAs. Due to hydrophilic headgroups, the repulsion into the micelle formation is more for three-headed than the

two-headed amphiphiles followed by the FAs. The hydrophobic interaction in the **2CCbn** series and the **3CCbn** series is same for same chain length.

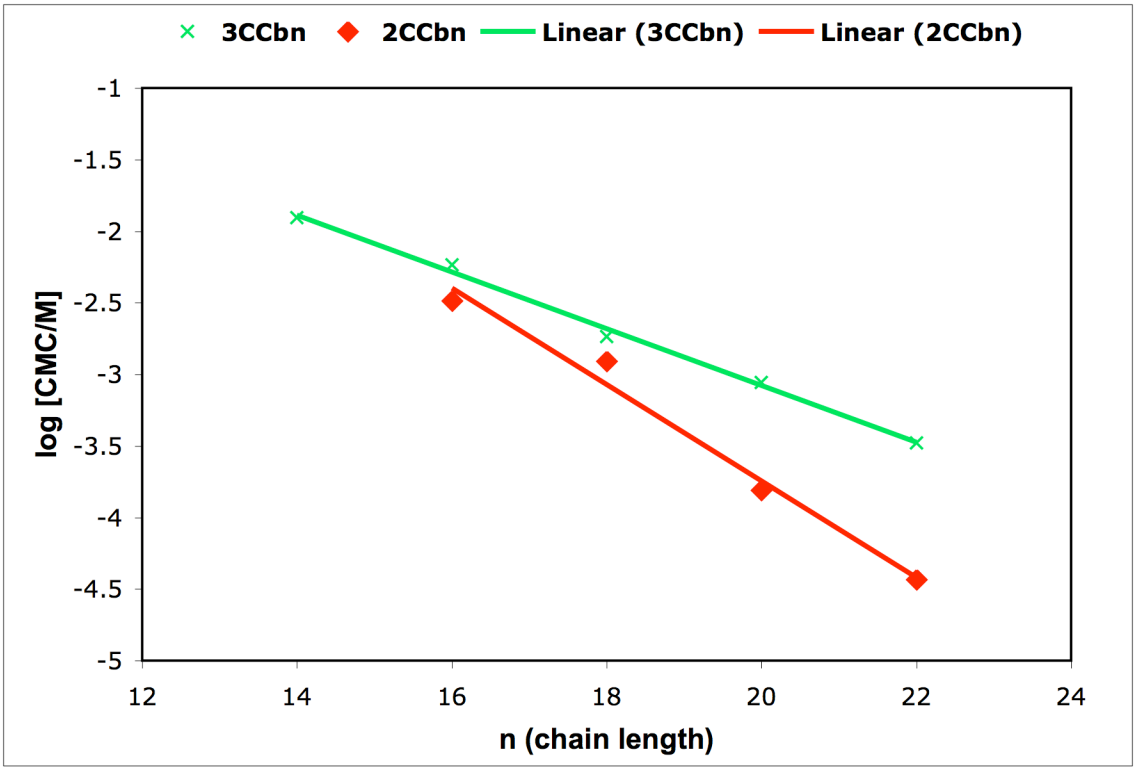

Figure 3.35 CMCs comparison between the **2CCbn** series and the **3CCbn** series. M = Molar. The solid lines are linear-regression analyses, where log CMC = for the **3CCbn** series, the fluorescence method: (–0.0015 ± 0.0004) × **n** + 0.03 ± 0.007; for the **2CCbn** series, the fluorescence method: (–0.34 ± 0.03) × **n** + 3.0 ± 0.6.

3.9 Summary

In the Gandour group, three different CMC measurement methods (the surface tension method, the fluorescence method, and the conductivity method) have been used. The fluorescence method was better than the other two methods because it required less time, less sample, and gave a good inflection point. The CMC measurements for the **2CAmn** series were done by the surface tension method at pH ~9.2 and by the

fluorescence method at two different pH ~9.2 and 7.4. The CMC measurements for the **2CCbn** series were done only by the fluorescence method at two different pH ~9.2 and 7.4. The CMC data for the **2CAmn** series measured by the surface tension method are similar to those measured by the fluorescence method. The three-headed amphiphiles have higher CMCs than two-headed amphiphiles followed by the FAs. The CMCs decreased with increasing chain length at both pH ~9.2 and 7.4. The CMCs were lower at pH 7.4 than the pH ~9.2. The **2CAmn** series and the **2CCbn** series are bioisosteres, which gave almost similar CMC data. The amphiphiles with the shorter chain length have a higher CMC (**2CAm13**, CMC = 6300 μM; **2CCb16**, CMC = 3280 μM) than one with the longer chain length (**2CAm21**, CMC = 175 μM; **2CCb22**, CMC = 37 μM).

The impurities have been observed in the CMC measurement by the surface tension method and the fluorescence method, which gave a minimum in the curve. If we could do this experiment by the conductivity method, we might not have seen any impact of the impurity in the curve.

3.10 CMC General Methods

The 0.01 M pyrene stock solution was prepared by dissolving solid pyrene (0.51 g) into methanol (250 mL). Diluting 0.01 M stock solution (0.5 mL) into methanol (50 mL) gave 1×10^{-4} M pyrene solution. The 1×10^{-4} M pyrene solution (10 μL) was taken into each scintillation vial (capacity 10.00 mL) and methanol was removed by placing it in the oven at 60 °C for ten minutes.

The stock solutions of each **2CCbn** series amphiphile were prepared in a 0.9% (w/v) TEA solution. The dilution series were made in those dry pyrene scintillation vials by using the stock solution and fresh TEA. The CMC measurements require solution

(3000 μL) for each dilution. The pH of each vial was around ~9.2. All scintillation vials had been vortexed and placed on a rocker at normal speed in an incubator at 30 °C for overnight.

The experiments were made at pH 7.4 also by using same samples. The pH 7.4 was adjusted by adding 1.0 M H_3PO_4 (70 μL) into each vial. Each vial was vortexed and kept in an incubator at 30 ºC for overnight.

A Perkin Elmer Luminescence Spectrometer LS50B was used to determine the CMCs for the sample made at pH ~9.2 and 7.4; plastic cuvette (capacity of 4000 μL) was used. The pyrene was excited at 334 nm and fluoresces maxima at 373 nm (I_1) and 385 nm (I_3). The excitation and emission slit were kept at 5 and 2.5 nm, respectively; the scan speed was 40 nm/min. The fluorescence of pyrene was recorded from 365 to 450 nm. I_1/I_3 versus log [amphiphile] plot was made to determine the CMCs.

3.10.1 CMC Determination of 2CCb16

The amphiphile **2CCb16** (46.3 mg) was dissolved in 0.9 % (w/v) TEA (10 mL) and sonicated for 15 minutes to give stock solution (4630 mg/L). Only 1 x 10^{-4} M pyrene (10 μL) was taken into scintillation vial and the methanol was removed by keeping it in the oven for 10 minutes. The stock solution (4630 mg/L) and 0.9 % TEA were dispensed by using an autopipettor into the scintillation vials to get the desired concentration as mentioned in Table 3.1. The results are shown in Table 3.2. The CMC was determined to be 1500 mg/L or 3280 μM at pH ~9.2 and 98 mg/L or 215 μM at pH 7.4.

Table 3.1 Preparation of dilutions for the **2CCb16**

Dilution from 4630 mg/L	Pyrene (μL)	Total volume = 3000 μL	
Desired solutions (mg/L)		Volume of stock used (μL)	Volume of TEA used (μL)

2500	10	1619.87	1380.13
2000	10	1295.90	1704.10
1500	10	971.92	2028.08
1000	10	647.95	2352.05
960	10	622.03	2377.97
920	10	596.11	2403.89
880	10	570.19	2429.81
840	10	544.28	2455.72
800	10	518.36	2481.64
700	10	453.56	2546.44
600	10	388.77	2611.23
500	10	323.97	2676.03
400	10	259.18	2740.82
300	10	194.38	2805.62
200	10	129.59	2870.41
100	10	64.79	2935.21
50	10	32.40	2967.60
40	10	25.92	2974.08
30	10	19.44	2980.56
20	10	12.96	2987.04
10	10	6.48	2993.52
5	10	3.24	2996.76

Table 3.2 CMC data for **2CCb16**

pH ~9.2		pH 7.4		
Amphiphile Concentration (mg/L)	I_1/I_3	Amphiphile Concentration (mg/L)	I_1/I_3	Visibility
2500	1.4347	2443.00	1.3016	Clear
2000	1.4275	1954.40	1.3093	Clear
1500	1.4111	1465.80	1.3091	Clear
1000	1.2990	977.20	1.3181	Clear
960	1.2868	938.11	1.3116	Clear
920	1.2588	899.02	1.3173	Clear
880	1.2508	859.93	1.3104	Clear
840	1.2311	820.85	1.3159	Clear
800	1.2390	781.76	1.3146	Clear
700	1.2010	684.04	1.3293	Clear
600	1.1809	586.32	1.3168	Clear
500	1.1648	488.60	1.3267	Clear
400	1.1383	390.88	1.3156	Clear
300	1.1339	293.16	1.3220	Clear
200	1.0734	195.44	1.3342	Clear

100	1.1066	97.72	1.3223	Clear
50	1.2925	48.86	1.4565	Clear
40	1.3748	39.09	1.5102	Clear
30	1.4630	29.32	1.6045	Clear
20	1.7873	19.54	1.7078	Clear
10	1.7552	9.77	1.7523	Clear
5	1.8168	4.89	1.8139	Clear

3.10.2 CMC Determination of 2CCb18

The amphiphile **2CCb18** (24.1 mg) was dissolved in 0.9 % (w/v) TEA (2 mL) and sonicated for 15 minutes to give a stock solution (12050 mg/L). Only 1 x 10^{-4} M pyrene (10 µL) was taken into scintillation vial and the methanol was removed by keeping it in the oven for 10 minutes. The stock solution (12050 mg/L) and 0.9 % TEA were dispensed by using an autopipettor into these scintillation vials to get the desired concentration as mentioned in Table 3.3. The results are shown in Table 3.4. The CMC was determined to be 600 mg/L or 1235 µM at pH ~9.2 and 39 mg/L or 80 µM at pH 7.4.

Table 3.3 Preparation of dilutions for the **2CCb18**

Dilution from 12050 mg/L	Pyrene (µL)	Total volume = 3000 µL	
Desired solutions (mg/L)		Volume of stock used (µL)	Volume of TEA used (µL)
1500	25	373.44	2626.56
1000	25	248.96	2751.04
900	25	224.07	2775.93
800	25	199.17	2800.83
700	25	174.27	2825.73
600	25	149.38	2850.62
500	25	124.48	2875.52
400	25	99.59	2900.41
360	25	89.63	2910.37
320	25	79.67	2920.33
280	25	69.71	2930.29
240	25	59.75	2940.25
200	25	49.79	2950.21
160	25	39.83	2960.17
120	25	29.88	2970.12

80	25	19.92	2980.08
40	25	9.96	2990.04

Table 3.4 CMC data for **2CCb18**

pH ~9.2		pH 7.4		
Amphiphile Concentration (mg/L)	I_1/I_3	Amphiphile Concentration (mg/L)	I_1/I_3	Visibility
1500	1.4090	1465.80	1.2240	Cloudy
1000	1.4080	977.20	1.2804	Cloudy
900	1.4189	879.48	1.2715	Cloudy
800	1.4243	781.76	1.2770	Cloudy
700	1.4308	684.04	1.2924	Cloudy
600	1.4103	586.32	1.2857	Cloudy
500	1.4000	488.60	1.2687	Cloudy
400	1.3453	390.88	1.2697	Cloudy
360	1.3170	351.79	1.2475	Cloudy
320	1.2830	312.70	1.2663	Cloudy
280	1.2455	273.62	1.2626	Cloudy
240	1.2415	234.53	1.2721	Cloudy
200	1.2156	195.44	1.2836	Cloudy
80	1.1881	78.18	1.2740	Clear
40	1.2277	39.09	1.2885	Clear
30	1.2444	29.32	1.2534	Clear
20	1.2464	19.54	1.1814	Clear
10	1.6954	9.77	1.2662	Clear
9	1.7024	8.79	1.3905	Clear
7	1.8084	6.84	1.5700	Clear
5	1.7594	4.89	1.5580	Clear
3	1.7448	2.93	1.7859	Clear
1	1.7091	0.98	1.8413	Clear

3.10.3 CMC Determination of 2CCb20

The amphiphile **2CCb20** (26.0 mg) was dissolved in 0.9 % (w/v) TEA (15 mL) and sonicated for 15 minutes to give a stock solution (1733.33 mg/L). Only 1 x 10^{-4} M pyrene (10 µL) was taken into scintillation vial and the methanol was removed by keeping it in the oven for 10 minutes. The stock solution (1733.33 mg/L) and 0.9 % TEA

were dispensed by using an autopipettor into these scintillation vials to get the desired concentration as mentioned in Table 3.5. The results are shown in Table 3.6. The CMC was determined to be 80 mg/L or 155 μM at pH ~9.2 and 10 mg/L or 19 μM at pH 7.4.

Table 3.5 Preparation of dilutions for the **2CCb20**

Dilution from 1733.33 mg/L	Pyrene (μL)	Total Volume = 3000 μL	
Desired solutions (mg/L)		Volume of stock used (μL)	Volume of TEA used (μL)
1000	10	1730.77	1269.23
900	10	1557.69	1442.31
800	10	1384.62	1615.38
700	10	1211.54	1788.46
600	10	1038.46	1961.54
500	10	865.38	2134.62
400	10	692.31	2307.69
300	10	519.23	2480.77
200	10	346.15	2653.85
180	10	311.54	2688.46
160	10	276.92	2723.08
140	10	242.31	2757.69
120	10	207.69	2792.31
100	10	173.08	2826.92
80	10	138.46	2861.54
60	10	103.85	2896.15
40	10	69.23	2930.77
20	10	34.62	2965.38
15	10	25.96	2974.04
13	10	22.50	2977.50
10	10	17.31	2982.69
7	10	12.12	2987.88
5	10	8.65	2991.35
3	10	5.19	2994.81
1	10	1.73	2998.27

Table 3.6 CMC data for **2CCb20**

pH ~9.2		pH 7.4		
Amphiphile Concentration (mg/L)	I_1/I_3	Amphiphile Concentration (mg/L)	I_1/I_3	Visibility

1000	1.3595	977.20	1.0873	Cloudy
900	1.3867	879.48	1.0843	Cloudy
800	1.3756	781.76	1.0938	Cloudy
700	1.3790	684.04	1.0865	Cloudy
600	1.3819	586.32	1.1374	Cloudy
500	1.3881	488.60	1.1205	Cloudy
400	1.3851	390.88	1.1317	Cloudy
300	1.3732	293.16	1.1289	Cloudy
200	1.3994	195.44	1.1790	Cloudy
180	1.4192	175.90	1.1720	Cloudy
160	1.3417	156.35	1.1602	Cloudy
140	1.3836	136.81	1.1482	Cloudy
120	1.3767	117.26	1.1427	Cloudy
100	1.4197	97.72	1.1283	Cloudy
80	1.4042	78.18	1.1139	Cloudy
60	1.2759	58.63	1.1674	Clear
40	1.4705	39.09	1.2264	Clear
20	1.5139	19.54	1.3052	Clear
15	1.5382	14.66	1.3635	Clear
13	1.7267	12.70	1.4837	Clear
10	1.6165	9.77	1.3685	Clear
7	1.7387	6.84	1.3995	Clear
5	1.7724	4.89	1.5018	Clear
3	1.7753	2.93	1.6485	Clear
1	1.7966	0.98	1.7441	Clear

3.10.4 CMC Determination of 2CCb22

The amphiphile **2CCb22** (11.3 mg) was dissolved in 0.9 % (w/v) TEA (15 mL) and sonicated for 15 minutes to give a stock solution (753.33 mg/L). Only 1 x 10^{-4} M pyrene (10 μL) was taken into scintillation vial and the methanol was removed by keeping it in the oven for 10 minutes. The stock solution (753.33 mg/L) and 0.9 % TEA were dispensed by using an autopipettor into these scintillation vials to get the desired concentration as mentioned in Table 3.7. The results are shown in Table 3.8. The CMC was determined to be 20 mg/L or 37 μM at pH ~9.2 and 10 mg/L or 18 μM at pH 7.4.

Table 3.7 Preparation of dilutions for the **2CCb22**

Dilution from 753.33 mg/L	Pyrene (μL)	Total volume = 3000 μL	
Desired solution (mg/L)		Volume of stock used (μL)	Volume of TEA used (μL)
700	10	2787.61	212.39
600	10	2389.38	610.62
500	10	1991.15	1008.85
400	10	1592.92	1407.08
300	10	1194.69	1805.31
200	10	796.46	2203.54
100	10	398.23	2601.77
90	10	358.41	2641.59
80	10	318.58	2681.42
70	10	278.76	2721.24
60	10	238.94	2761.06
50	10	199.12	2800.88
40	10	159.29	2840.71
30	10	119.47	2880.53
20	10	79.65	2920.35
10	10	39.82	2960.18
5	10	19.91	2980.09
4	10	15.93	2984.07
3	10	11.95	2988.05
2	10	7.96	2992.04
1	10	3.98	2996.02

Table 3.8 CMC data for **2CCb22**

pH ~9.2		pH 7.4		
Amphiphile Concentration (mg/L)	I_1/I_3	Amphiphile Concentration (mg/L)	I_1/I_3	Visibility
700	1.3428	684.04	1.3189	Cloudy
600	1.3524	586.32	1.3351	Cloudy
500	1.3508	488.60	1.3384	Cloudy
400	1.3354	390.88	1.3449	Cloudy
300	1.3610	293.16	1.3404	Cloudy
200	1.3479	195.44	1.3458	Cloudy
100	1.3536	97.72	1.3567	Cloudy
90	1.3329	87.95	1.3410	Cloudy
80	1.3516	78.18	1.3508	Cloudy
70	1.3462	68.40	1.3596	Cloudy
60	1.3121	58.63	1.3604	Cloudy
50	1.3365	48.86	1.3763	Clear

40	1.3411	39.09	1.3689	Clear
30	1.3437	29.32	1.3679	Clear
20	1.3489	19.54	1.4033	Clear
10	1.4244	9.77	1.4328	Clear
5	1.6530	4.89	1.6228	Clear
4	1.6424	3.91	1.5294	Clear
3	1.6598	2.93	1.6766	Clear
2	1.6504	1.95	1.6506	Clear
1	1.6492	0.98	1.7604	Clear

3.10.5 CMC Determination of 2CCb30

The amphiphile **2CCb30** (1 mg) was dissolved in 0.9 % (w/v) TEA (35 mL) and sonicated for 15 minutes to give a stock solution (28.57 mg/L). Only 1 x 10^{-4} M pyrene (10 µL) was taken into scintillation vial and the methanol was removed by keeping it in the oven for 10 minutes. The stock solution (28.57 mg/L) and 0.9 % TEA were dispensed by using an autopipettor into these scintillation vials to get the desired concentration as mentioned in Table 3.9. The results are shown in Table 3.10. The CMC was not determined easily for pH ~9.2 and for pH 7.4.

Table 3.9 Preparation of dilutions for the **2CCb30**

Dilution from 28.57 mg/L	Pyrene (µL)	Total volume = 3000 µL	
Desired solution (mg/L)		Volume of stock used (µL)	Volume of TEA used (µL)
23	10	2415.00	585.00
22	10	2310.00	690.00
21	10	2205.00	795.00
20	10	2100.00	900.00
19	10	1995.00	1005.00
18	10	1890.00	1110.00
17	10	1785.00	1215.00
16	10	1680.00	1320.00
15	10	1575.00	1425.00
14	10	1470.00	1530.00
13	10	1365.00	1635.00
12	10	1260.00	1740.00
11	10	1155.00	1845.00

10	10	1050.00	1950.00
9	10	945.00	2055.00
8	10	840.00	2160.00
7	10	735.00	2265.00
6	10	630.00	2370.00
5	10	525.00	2475.00
4	10	420.00	2580.00
3	10	315.00	2685.00
2	10	210.00	2790.00
1	10	105.00	2895.00
0.5	10	52.50	2947.50
0.05	10	5.25	2994.75
0.005	10	0.53	2999.48

Table 3.10 CMC data for **2CCb30**

pH ~9.2		pH 7.4		
Amphiphile Concentration (mg/L)	I_1/I_3	Amphiphile Concentration (mg/L)	I_1/I_3	Visibility
23	1.2807	22.48	0.6056	Clear
22	1.3050	21.50	0.7356	Clear
21	1.3369	20.52	0.6910	Clear
20	1.3192	19.54	0.6856	Clear
19	1.3204	18.57	0.6922	Clear
18	1.3209	17.59	0.7399	Clear
17	1.3453	16.61	0.7270	Clear
16	1.4126	15.64	0.7658	Clear
15	1.3295	14.66	0.6928	Clear
14	1.3601	13.68	0.6999	Clear
13	1.3188	12.70	0.7681	Clear
12	1.4412	11.73	0.7281	Clear
11	1.3678	10.75	0.6789	Clear
10	1.4555	9.77	0.7030	Clear
9	1.4537	8.79	0.6780	Clear
8	1.5122	7.82	0.7759	Clear
7	1.4927	6.84	0.8533	Clear
6	1.5280	5.86	0.8854	Clear
5	1.5063	4.89	0.7693	Clear
4	1.6329	3.91	0.7631	Clear
3	1.6078	2.93	0.8149	Clear
2	1.6918	1.95	0.8941	Clear
1	1.7563	0.98	0.8819	Clear
0.5	1.8116	0.49	0.9043	Clear

0.05	1.9113	0.05	0.9294	Clear
0.005	1.8700	0.00	0.8588	Clear

3.10.6 CMC Determination of 2CCb5α–cholestan-3ß-ol

The amphiphile **2CCb5α–cholestan-3ß-ol** (25.3 mg) was dissolved in 0.9 % (w/v) TEA (2 mL) and sonicated for 15 minutes to give a stock solution (12650 mg/L). Only 1 x 10^{-4} M pyrene (10 µL) was taken into scintillation vial and the methanol was removed by keeping it in the oven for 10 minutes. The stock solution (12650 mg/L) and 0.9 % TEA were dispensed by using an autopipettor into these scintillation vials to get the desired concentration as mentioned in Table 3.11. The results are shown in Table 3.12. The CMC was determined to be 700 mg/L or 1160 µM at pH ~9.2 and 39 mg/L or 65 µM at pH 7.4.

Table 3.11 Preparation of dilutions for the **2CCb5α–cholestan-3ß-ol**

Dilution from 12650 mg/L	Pyrene (µL)	Total volume = 3000 µL	
Desired solution (mg/L)		Volume of stock used (µL)	Volume of TEA used (µL)
2000	10	474.31	2525.69
1000	10	237.15	2762.85
900	10	213.44	2786.56
800	10	189.72	2810.28
700	10	166.01	2833.99
600	10	142.29	2857.71
500	10	118.58	2881.42
400	10	94.86	2905.14
300	10	71.15	2928.85
200	10	47.43	2952.57
100	10	23.72	2976.28
50	10	11.86	2988.14
40	10	9.49	2990.51
30	10	7.11	2992.89
20	10	4.74	2995.26
10	10	2.37	2997.63
5	10	1.19	2998.81

4	10	0.95	2999.05
3	10	0.71	2999.29
2	10	0.47	2999.53
1	10	0.24	2999.76
0.5	10	0.12	2999.88

Table 3.12 CMC data for **2CCb5α–cholestan-3ß-ol**

pH ~9.2		pH 7.4		
Amphiphile Concentration (mg/L)	I_1/I_3	Amphiphile Concentration (mg/L)	I_1/I_3	Visibility
2000	1.3170	1954.40	1.0747	Cloudy
1000	1.3206	977.20	1.0686	Cloudy
900	1.3212	879.48	1.0757	Cloudy
800	1.3179	781.76	1.0754	Cloudy
700	1.3140	684.04	1.0646	Cloudy
600	1.2921	586.32	1.0650	Cloudy
500	1.3023	488.60	1.0613	Cloudy
400	1.2700	390.88	1.0618	Cloudy
300	1.2560	293.16	1.0604	Cloudy
200	1.2300	195.44	1.0508	Cloudy
100	1.1165	97.72	1.0506	Cloudy
50	1.1688	48.86	1.0363	Clear
40	1.1547	39.09	1.0345	Clear
30	1.1239	29.32	1.0508	Clear
20	1.0897	19.54	1.0916	Clear
10	1.0867	9.77	1.1571	Clear
5	1.1669	4.89	1.2623	Clear
4	1.1991	3.91	1.2739	Clear
3	1.3011	2.93	1.3647	Clear
2	1.3285	1.95	1.4085	Clear
1	1.5043	0.98	1.6018	Clear
0.5	1.7206	0.49	1.6167	Clear

3.11 References for Chapter 3

1. Macri, R. V.; Karlovská, J.; Doncel, G. F.; Du, X.; Maisuria, B. B.; Williams, A. A.; Sugandhi, E. W.; Falkinham, J. O., III; Esker, A. R.; Gandour, R. D., Comparing anti-HIV, antibacterial, antifungal, micellar, and cytotoxic properties of tricarboxylato dendritic amphiphiles. *Bioorg. Med. Chem.* **2009,** *17* (8), 3162–3168.

2. Actis, M. L. Synthesis, Characterization, Critical Micelle Concentration and Biological Acitivity of two-Headed Amphiphiles: Master of Science Thesis. Virginia Tech, Blacksburg, VA, November 6, 2008.
3. Aguiar, J.; Carpena, P.; Molina-BolÌvar, J. A.; Carnero Ruiz, C., On the determination of the critical micelle concentration by the pyrene 1:3 ratio method. *J. Colloid Interface Sci.* **2003,** *258* (1), 116-122.
4. Kalyanasundaram, K.; Thomas, J. K., Environmental Effects on Vibronic Band Intensities in Pyrene Monomer Fluorescence and Their Application in Studies of Micellar Systems. *J. Am. Chem. Soc.* **1977,** *99*, 2039–2044.
5. Karpovich, D. S.; Blanchard, G. J., Relating the Polarity-Dependent Fluorescence Response of Pyrene to Vibronic Coupling. Achieving a Fundamental Understanding of the py Polarity Scale. *The Journal of Physical Chemistry* **1995,** *99* (12), 3951–3958.
6. Lin, S.-Y.; Lin, Y.-Y.; Chen, E.-M.; Hsu, C.-T.; Kwan, C.-C., A Study of the Equilibrium Surface Tension and the Critical Micelle Concentration of Mixed Surfactant Solutions. *Langmuir.* **1999,** *15* (13), 4370–4376.
7. Paleos, C. M.; Michas, J.; Malliaris, A., Alkyl derivatives of iminodiacetic acid: A novel class of compounds forming thermotropic liquid crystals and aqueous micelles. *Mol. Cryst. Liq. Cryst.* **1990,** *186*, 251–260.
8. Shinoda, K., The Critical Micelle Concentrations in Aqueous Solutions of Potassium Alkane Tricarboxylates. *J. Phys. Chem.* **1956,** *60* (10), 1439–1441.

Chapter 4: The Minimal Inhibitory Concentration (MIC) for the 2CCbn Series

4.1 Introduction to the MIC

The minimal inhibitory concentration (MIC) is the concentration at which inhibition of bacterial growth occurs. The MIC is an important measurement in drug design and discovery, where measurements are carried out in *in vitro* bioassays. The bacterial cultures are grown in appropriate broths and the ability of each drug to inhibit cell growth is observed. Our goal is to develop potent compounds for curing infections caused by *Staphylococcus aureus* and MRSA. Bacteria are becoming more resistant to current antibiotics like penicillin, methicillin, and vancomycin. Thus, it is necessary to keep developing new potent drugs for curing these infections.

The MICs of the **2CCbn** series were measured by using *in vitro* bioassay and these activities were compared to those of the **2CAmn**, **3CAmn**, **3CCbn**, and **3CUrn** series. Ms. Myra Williams and Professor Joseph O. Falkinham measured the MIC's of all the series in the Department of Biological Sciences at Virginia Tech.

4.2 Method of the MIC Measurements on the Growth of *S. aureus* and MRSA

The stock solutions for all homologues were prepared by vortexing each of the **2CCbn** series amphiphiles (25 mg) in (5% w/v) aqueous triethanolamine (TEA) solution (2 mL). The *S. aureus* and MRSA strains were grown in Brain Heart Infusion Broth containing 0.2% (w/v) sucrose (BHIB+S; final pH=7.4). During the growing process, the *S. aureus* and the MRSA strains were used to inoculate (introduce a cell or organism into a culture medium) in BHIB+S (5 mL) in sterile 16 × 125 mm screw cap tubes, which were incubated at 37 °C without shaking for 3–4 d. These 3–4 d cultures (5 mL) were used to inoculate in BHIB+S (45 mL) in sterile Nephalometry flasks that were incubated

at 37 °C in a rotary water bath (60 rpm) for aeration (introduce air into). Cultures were grown until they reached mid-log phase (mid-growing) and were incubated again till they reached there stationary phase. Turbidity was measured at mid-log phase and stationary phase every hour at 580 nm.

The MICs of the compounds dissolved in 5% (w/v) TEA were measured by broth microdilution in 96-well microtiter plates.[1] Preliminary experiments demonstrated that 5% (w/v) TEA/water did not inhibit the growth of cultures. The 2-fold dilution series of the compounds were prepared in 96-well microtiter plates in a 1/10-strength BHIB+S (50 μL). Each dilution series was inoculated with the test strains (*S. aureus* and MRSA) (50 μL). Plates were incubated at 37 °C and growth as turbidity was evaluated visually by using a microtiter plate reader (absorbance at 540 nm) on the fourth day.

4.3 The MIC against *S. aureus* and MRSA

Increasing the chain length (**n**) in each series improved the antibacterial activity against both the *S. aureus* strain ATCC 6358 and the MRSA strain ATCC 43330 (Figure 4.1 and 4.2). The antibacterial activity against *S. aureus* increased (MIC decreased) with increasing chain length up to **n** = 20 for the **3CCbn** and the **3CUrn** series, and then reached a plateau (Figure 4.1). For the **3CAmn** and the **2CAmn** series, the antibacterial activity against *S. aureus* increased (MIC decreased) with the increasing chain length (Figure 4.1).

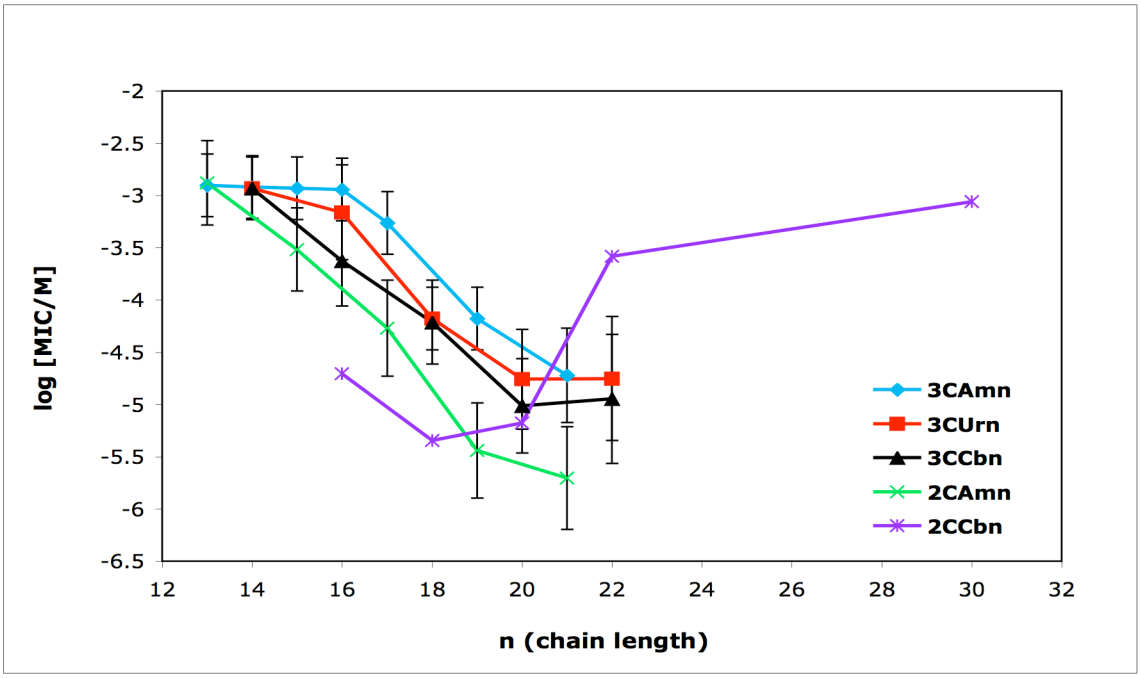

Figure 4.1 The MIC comparisons for *S. aureus*. Error bars (±0.3) represent a two-fold dilution where multiple determinations of the MIC gave the same value. In cases where different values were obtained the average is reported and ±(log standard of the mean) is added to ±0.3. Lines connecting symbols are eye guides.

The antibacterial activity against MRSA increased (MIC decreased) with increasing chain length up to **n** = 20 for the **3CCbn** and the **3CUrn** series and up to n = 19 for the **2CAmn** series and then reached a plateau (Figure 4.2). For the **3CAmn** series, the antibacterial activity against MRSA also increased (MIC decreased) with increasing chain length up to **n** = 21 (Figure 4.2). In general, the chain length is a good predictor for the activity.

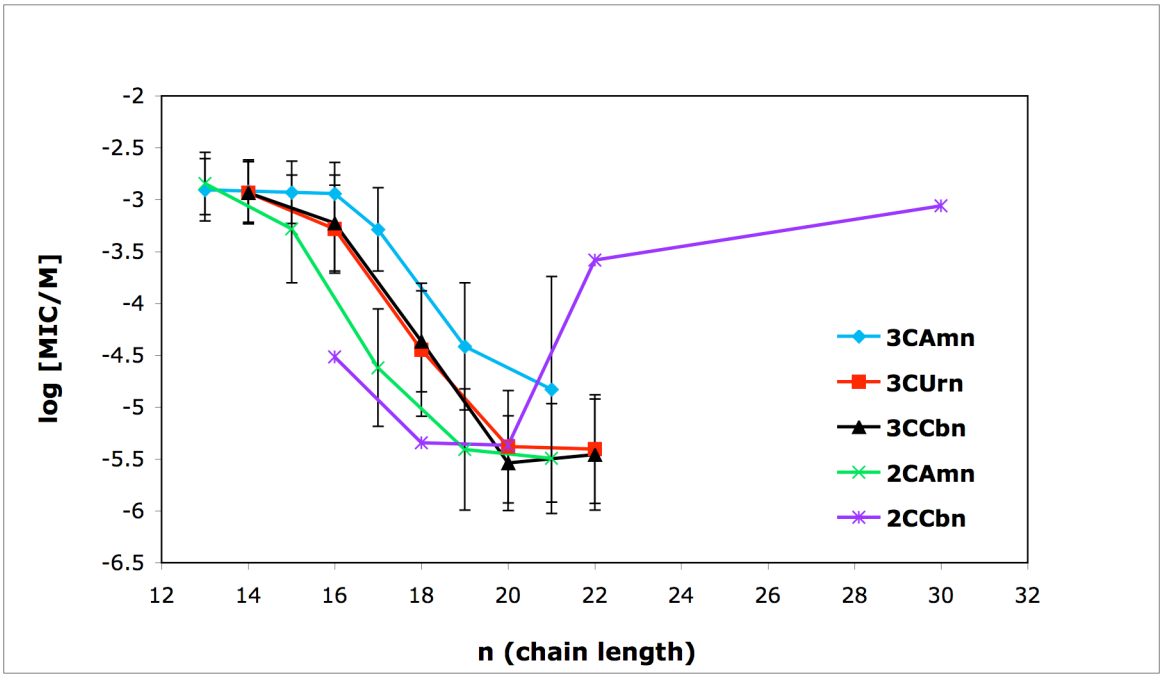

Figure 4.2 The MIC comparisons for MRSA. Error bars (±0.3) represent a two-fold dilution where multiple determinations of the MIC gave the same value. In cases where different values were obtained the average is reported and ± (log standard of the mean) is added to ±0.3. Lines connecting symbols are eye guides.

4.4 Lipophilicity and Related Activity

Lipophilicity is a key point for understanding the partition of a drug (amphiphile) between an organic phase (octan-1-ol) and water by using clog *P* and log *D* values, discussed in chapter 1 (Section 1.7.2). Figure 4.3 shows the ionization equilibria (K_a's) in water at pH 7.4 for **3CCb18** and **2CCb18;** the calculated K_a's are shown above the equilibrium arrows.[2] The clog *P*'s are given in parentheses for each ionization state (microspecies).[2] The more negative the number, the more likely the molecule will partition into water; the more positive the number, the more likely the molecule will partition into the hydrophobic layer.

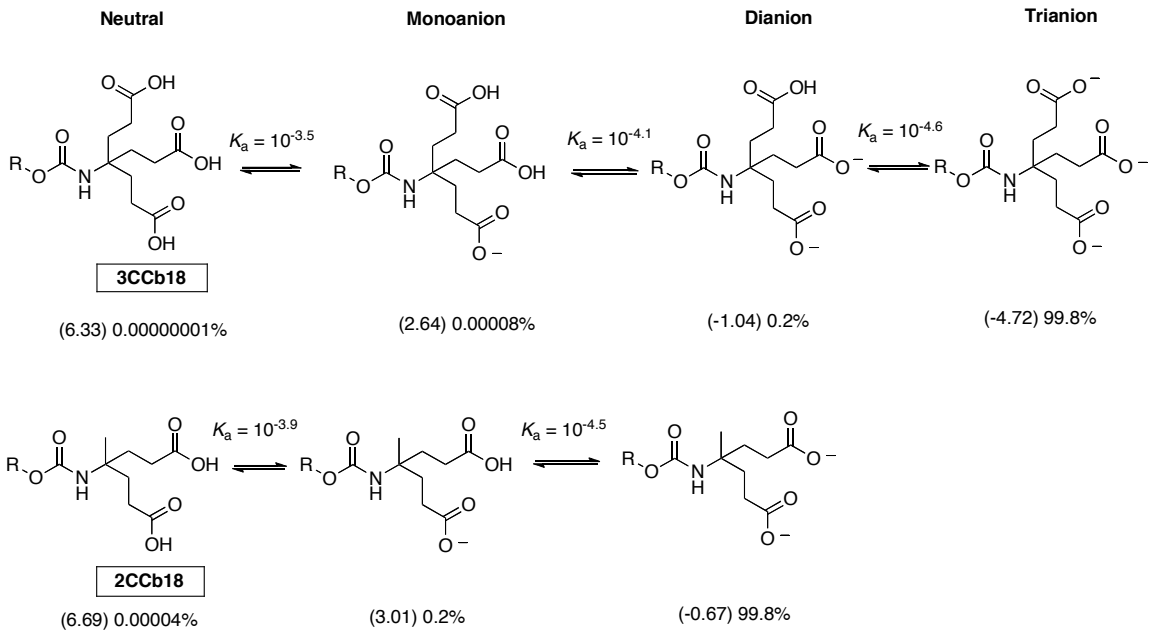

Figure 4.3 Ionization equilibrium for **3CCb18** and **2CCb18**. Values of K_a and % distribution of microspecies at pH 7.4 calculated on Marvin Sketch 5.2.0. (Ref. 2.)

The most hydrophilic microspecies for **3CCb18** is the trianion (clog *P*, -4.72) and for **2CCb18** is the dianion (clog *P*, -0.67). The dianion of **3CCb18** (clog *P*, -1.04) has a similar value to that of the dianion of **2CCb18**. Both monoanion and neutral microspecies of **3CCb18** and **2CCb18** have similar clog *P* values. Both monoanion and neutral microspecies of **3CCb18** and **2CCb18** are hydrophobic and expected to incorporate into cell membranes. The values of clog *P* are constant for each microspecies, but pH affects the distribution of the microspecies.

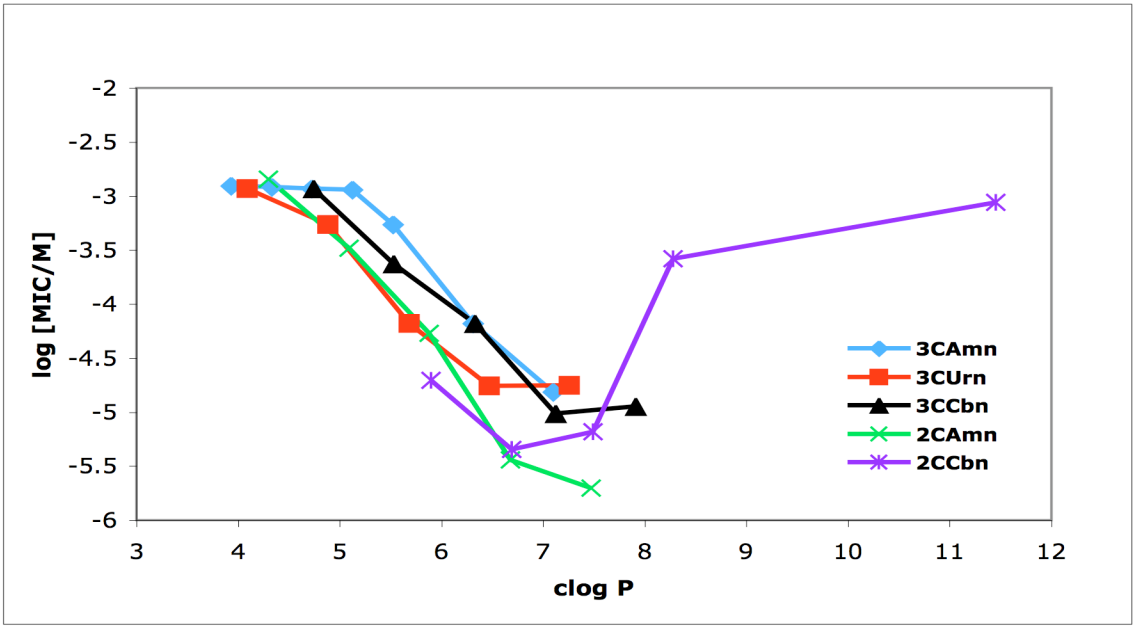

Figure 4.4 The log [MIC] against *S. aureus* versus clog *P* of neutral microspecies of the various amphiphiles.

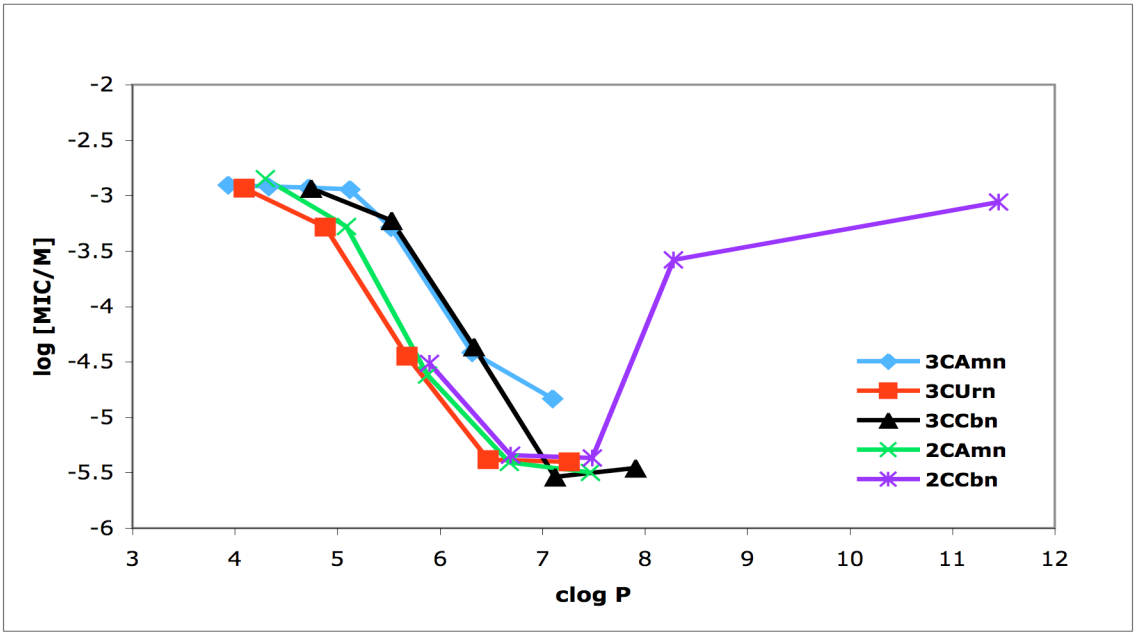

Figure 4.5 The log [MIC] against MRSA versus clog *P* of neutral microspecies of the various amphiphiles.

Plots of log [MIC] versus clog *P* of the neutral microspecies (Figure 4.4 and 4.5) show good agreement amongst the five species for both bacterial strains. The neutral

microspecies were chosen due to their most hydrophobic nature. The plots of log [MIC] versus clog *P* of the monoanions and dianions gave identical patterns to those in Figure 4.4 and 4.5.

The log *D* is a combination of pK_a and clog *P*. Unlike clog *P*, which is calculated for each microspecies, a single log *D* is calculated for a distribution of microspecies at a given pH. The calculated log *D*s for **3CCb18** and **2CCb18** at pH 7.4 are -3.11 and 0.55, respectively. According to calculations, the dominant microspecies (>99%) at pH 7.4 for **3CCb18** and **2CCb18** are the trianions and dianions, respectively.

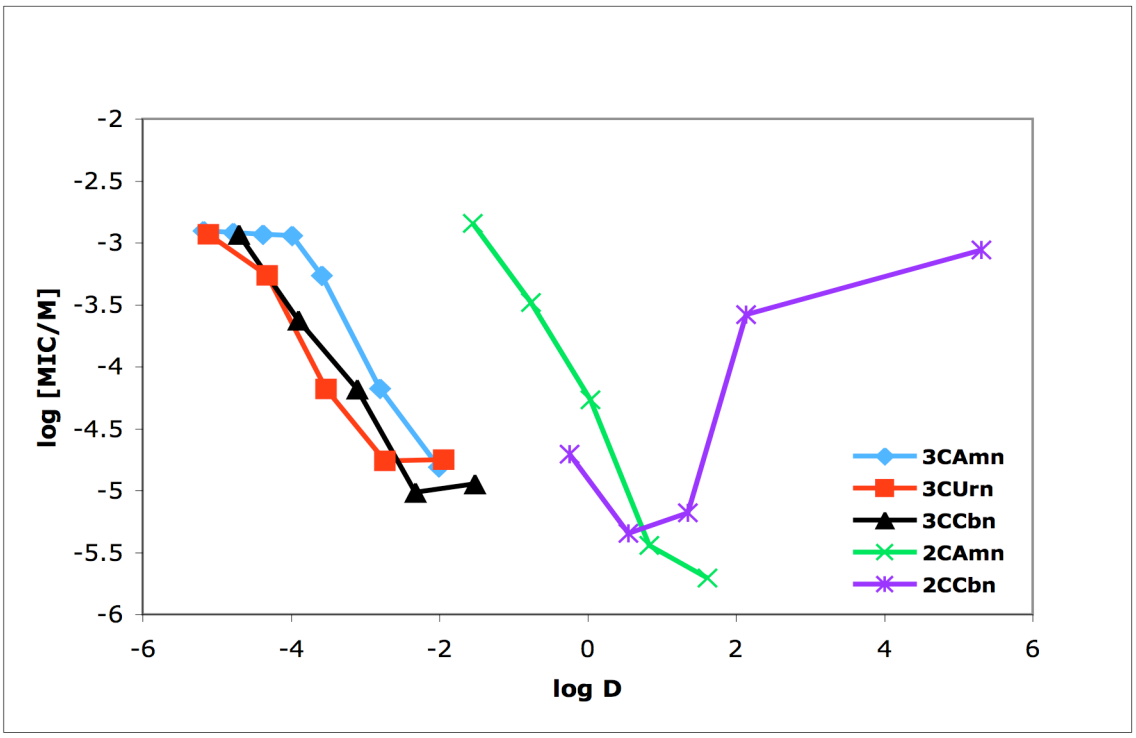

Figure 4.6 The log [MIC] against *S. aureus* versus log *D* at pH 7.4 for the various amphiphiles.

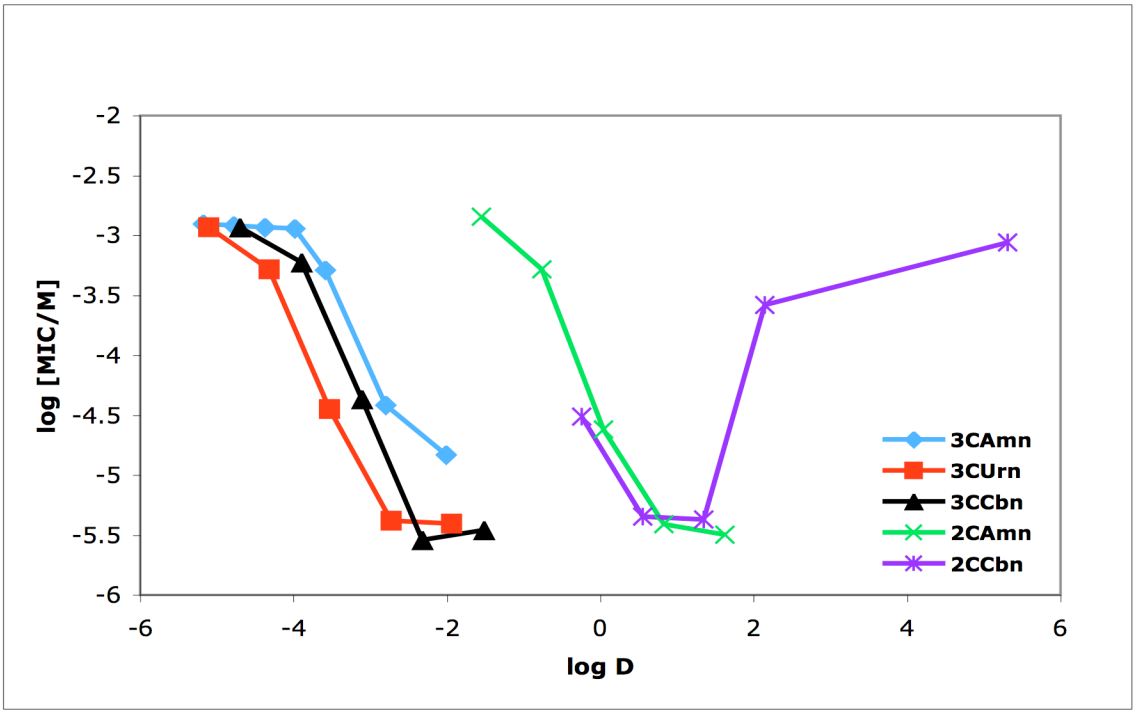

Figure 4.7 The log [MIC] against MRSA versus log *D* at pH 7.4 for the various amphiphiles.

Plots of log [MIC] versus log *D* (Figures 4.6 and 4.7) of the amphiphiles clearly show that log *D* is not the right tool to predict the antibacterial activity. The plot for the **2CCbn** series and the **2CAmn** series were distinct from those of the three-headed series for both strains (Figures 4.6 and 4.7). The activities of **3CCb18**, **3CCb20,** and **3CCb22** have similar ranges of values to that of **2CCb16**, **2CCb18,** and **2CCb20**, respectively. However, the log *D*'s of the **2CCbn** series are very different from those of the **3CCbn** series (Figures 4.6 and 4.7), and this is due to the dianions and trianions, which are the dominant species at pH 7.4.

4.5 The Antibacterial Activity of the 2CCbn Series and Vancomycin against *S. aureus* and Clinical Isolates of MRSA

The MICs of each of the longest homologues of the **2CCbn** series against *S. aureus* and MRSA were measured; the MIC value (Table 4.1) averaged a duplicate measurement of two separate cultures, in which **2CCb18** exhibited strong antibacterial activity. The antimicrobial activities of the **2CCb16** and **2CCb20** were not as effective as **2CCb18**, whereas the vancomycin was a stronger antibacterial agent in comparison to the **2CCbn** series.

Table 4.1 MICs of the 2CCbn series and Vancomycin against *S. aureus* strain ATCC 6358 and clinical isolates of MRSA

Amphiphiles	*S. aureus* (µg/mL)	MIC (µg/mL)					
		MRSA 43300	MRSA 34380	MRSA 523000	MRSA 36361	MRSA 34864	MRSA 53016
2CCb16	9	14	36	9	9	18	36
2CCb18	2.2	2.2	2.2	1.7	2.2	2.2	2.2
2CCb20	3.4	2.2	4.5	3.4	2.2	4.5	3.4
2CCb22	142	142	-	-	-	-	-
2CCb30	>570	>570	-	-	-	-	-
2CCb5α-cholestan-3ß-ol	750	375	-	-	-	-	-
Vancomycin	0.8	-	0.5	0.5	0.75	0.38	0.38

4.6 Comparison Between the CMC and the MIC

Detergency behavior of an agent causes toxicity. The detergency behaviors are observed around CMCs. For good antibacterial activity, the agents should have low MIC. Agents with high CMC and low MIC values are preferred for drug use.[3] The log [CMC] and log [MIC] versus chain length plot (Figure 4.8) against *S. aureus* and MRSA for the **2CCbn** series shows the safety of an amphiphile as a drug use. Having CMC/MIC ≥ 100 means that detergency is not the mechanism of the activity (Table 4.2). According to Table 4.2, **2CCb16**, **2CCb18**, **2CAm19**, and **2CCb5α-cholestan-3ß-ol** were the best amphiphile against *S. aureus*. Amphiphile **2CCb18** has good activity (MIC 4.5 μM) and the largest difference between CMC and MIC, which suggests that **2CCb18**, may be the least toxic in comparison to the others. Amphihiles **2CCb16**, **2CCb18**, **3CCb20**, **3CUr20**, **3CUr22**, **3CAm21**, and **2CAm19** were the best against MRSA. Amphiphile **3CUr20** has good activity (MIC 4.2 μM) and the largest difference between CMC and MIC, which suggests that **3CUr20**, may be the best compound against MRSA with a good balance of activity and CMC.

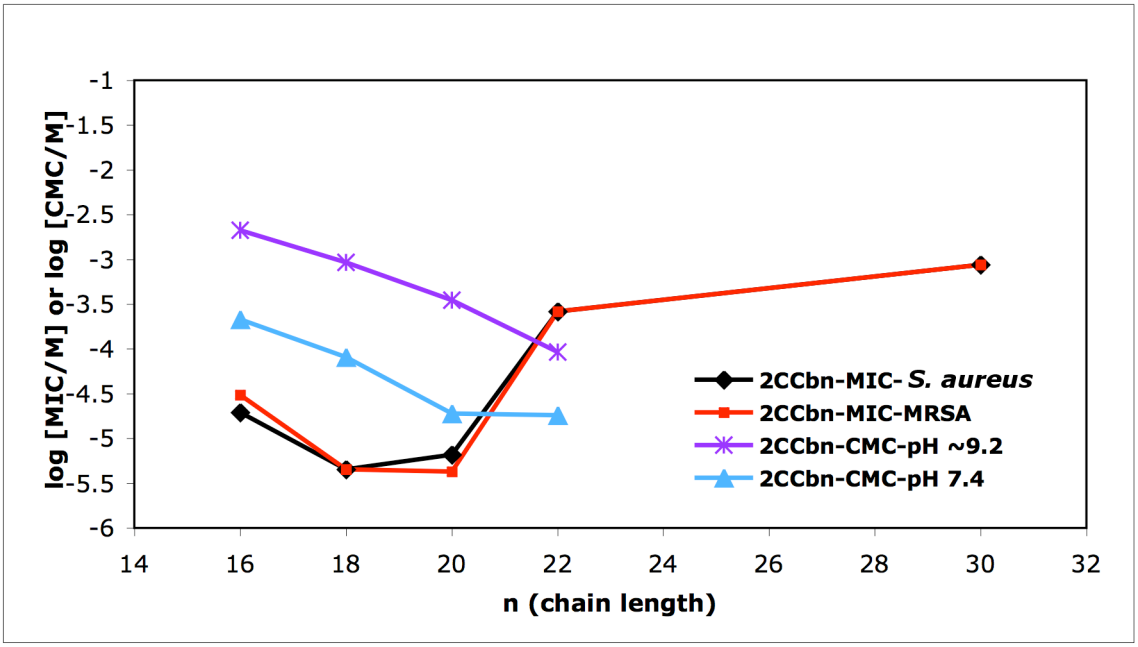

Figure 4.8 CMC and MIC comparison for the **2CCbn** series against *S. aureus* and MRSA.

Table 4.2 Concentration ratio (CMC/MIC) for *S. aureus* and MRSA

Amphiphile	pH ~9.2		pH 7.4	
	S. aureus	MRSA	*S. aureus*	MRSA
2CCb16	167	107	11	7
2CCb18	273	273	18	18
2CCb20	24	36	3	4
2CCb22	0.1	0.1	0.1	0.1
2CCb5α-cholestan-3ß-ol	101	92	-	-
3CCb20	54	183	-	-
3CCb22	22	72	-	-
3CUr20	81	339	-	-
3CUr22	57	256	-	-
3CAm19	45	76	-	-
3CAm21	94	120	-	-

2CAm19	205	190	-	-
2CAm21	84	52	-	-

4.7 Conclusion

Among the **2CCbn** series, amphiphile **2CCb18** completely inhibits the growth of *S. aureus* and MRSA. The CMC/MIC value for **2CCb18** is very high and it proves that detergency is not the mechanism of antibacterial activity. Table 4.2 shows that the **2CCb18** and **2CAm19** are the most active amphiphiles against *S. aureus*, while **3CUr20** is the most active amphiphile against MRSA.

4.8 References for Chapter 4

1. Willilam, A. A., Sugandhi, E. K., Macri, R. V., Falkinham III, J. O., Gandour, R. D., Antimicrobial activity of long-chain, water-soluble, dendritic tricarboxylato amphiphiles. *J. Antimicrob. Chemother.* **2007,** *59*, 451–458.
2. MarvinSketch 5.2.0. http://intro.bio.umb.edu/111-112/OLLM/111F98/newclogp.html (accessed April 25, 2009).
3. Vieria, O. V., Hartmann, D. O., Cardoso, C. M. P., Oberdoerfer, D., Baptista, M., Santos, M. A. S., Almeida, L., Ramalho-Santos, J., Vaz, W. L. C., , Surfactant as microbicides and contraceptive agents: a systematic in vitro study. *PLoS One* **2008,** *3* (8), e2913.

Chapter 5: Summary and Conclusion

5.1 Summary

In this project, nitrodiester, aminodiester, isocyanatediester, **2ECb16, 2ECb18, 2ECb20, 2ECb22, 2ECb30, 2ECb5α-cholestan-3ß-ol, 2CCb16, 2CCb18, 2CCb20, 2CCb22, 2CCb30,** and **2CCb5α-cholestan-3ß-ol** were successfully synthesized. Flash column chromatography was used to purify nitrodiester, isocyanatediester, and the **2ECbn** series. The aminodiester was purified through Celite® cake filtration, while the **2CCbn** series were purified by chase solvent system. The compounds were fully characterized by melting point, ^{1}H NMR, ^{13}C NMR, and IR spectroscopy. The isocyanatediester, the **2ECbn** series, and the **2CCbn** series were also fully characterized by high-resolution mass spectroscopy and elemental analysis.

The CMCs of the **2CCbn** series collected by the fluorescence method because the CMCs for the **2CAmn** series measured by the fluorescence method were similar to the surface tension method.[1] The fluorescence method requires less time and gave good break off compare to the surface tension method. The CMCs for the **2CAmn** series and the **2CCbn** series were measured at pH ~9.2 and 7.4. The CMCs measured at pH ~9.2 were higher than it measured at pH 7.4. The CMCs values were observed to decrease in a linear fashion at pH ~9.2 [log CMC = for the **2CAmn** series, the surface tension method: (–0.28 ± 0.01) × **n** + 2.2 ± 0.1; for the **2CAmn** series, the fluorescence method: (–0.25 ± 0.02) × **n** + 1.6 ± 0.3; for the **2CCbn** series, the fluorescence method: (–0.34 ± 0.03) × **n** + 3.0 ± 0.6] with increasing chain length. The CMCs values were observed to decrease in a linear fashion at pH 7.4 [log CMC = for the **2CAmn** series, the fluorescence method: (–0.35 ± 0.04) × **n** + 2.3 ± 0.8; for the **2CCbn** series, the fluorescence method: (–0.19 ±

0.04) × **n** + (–0.7 ± 0.8)]. The CMCs values of the **2CAmn** series and the **2CCbn** series were lower than those of three-headed amphiphiles but higher than those of fatty acids.

MIC studies were performed successfully against *S. aureus* and several strains of MRSA. The chain length and clog *P* values were found to be good predictors for the antimicrobial activity. The cutoff effect was observed for the **2CCbn** series. The most active amphiphile against *S. aureus* and MRSA was found to be **2CCb18** (MIC–2.2 μg/mL). The safety ratio (CMC/MIC) proved that the antimicrobial activity is due to the monomers and not micelles. The higher the ratio is, the less toxic an amphipile is. Among the **2CCbn** series, the **2CCb18** gave the largest safety ratio (CMC/MIC = 273 at pH ~9.2; CMC/MIC = 18 at pH 7.4) against *S. aureus* and MRSA. Between the two- and three-headed amphiphiles, the two-headed amphiphiles were the most active against *S. aureus*, while the three-headed amphiphiles were the most active against MRSA.

5.2 Conclusion

The growth of *S. aureus* and MRSA were inhibited completely by the amphiphile **2CCb18**. The CMC/MIC ratio was found to be high for the **2CCbn** series, which proves that they are not toxic, and the antimicrobial activity is due to the monomers not micelles. The chain length and clog *P* values can be used as predictors for the antimicrobial activity for future homologous series of amphiphiles. The CMC and MIC values were observed to decrease with increasing chain length. The **2CCbn** series is the homologues of the **2CAmn** series. **2CCb18** is the bioisostere of **2CAm19**, and both were found to be effective against *S. aureus* and MRSA.

To increase the antimicrobial activity for the three-headed amphiphiles against *S. aureus* and for the two-headed amphiphiles against MRSA, future work needs to make the headgroups less hydrophilic by changing the carboxyl groups.

5.3 References for Chapter 5

1. Actis, M. L. Synthesis, Characterization, Critical Micelle Concentration and Biological Acitivity of two-Headed Amphiphiles: Master of Science Thesis. Virginia Tech, Blacksburg, VA, November 6, 2008.